สำนักหอสมุดกลาง พระจอมเกล้าลาดกระบัง

A MECHANISM FOR IMPROVING PERFORMANCE OF DIRECT-SEQUENCE SPERAD-SLOTTED ALOHA UNDER IMPAIRED SATELLITE CHANNEL ENVIRONMENT

SERI ASVARUK

เลขหมู่.....
เลขทะเบียน 46631
วัน,เดือน,ปี 12 ก.ย. 2549

.b.....
.i.....

A THESIS SUBMITTED IN PARTIAL FULFILMENT

OF THE REQUIREMENTS FOR THE DEGREE OF

DOCTOR OF ENGINEERING IN ELECTRICAL ENGINEERING

SCHOOL OF GRADUATE STUDIES

KING MONGKUT'S INSTITUTE OF TECHNOLOGY LADKRABANG

2005

ISBN 974-15-1799-8

This material is reserved for educational use only, not allowed for commercial use.
Forbidden to modify the content, and cite the document when use.

COPYRIGHT 2005
SCHOOL OF GRADUATE STUDIES
KING MONGKUT'S INSTITUTE OF TECHNOLOGY LADKRABANG

This material is reserved for educational use only, not allowed for commercial use.
Forbidden to modify the content, and cite the document when use.

หัวข้อวิทยานิพนธ์	**วิธีการปรับปรุงประสิทธิภาพของ Direct-Sequence Spread-Slotted ALOHA ภายใต้สภาวะช่องสัญญาณคาวเทียมที่ถูกรบกวน**
นักศึกษา	**นายเสรี อัศวารักษ์**
รหัสประจำตัว	41060010
ปริญญา	**วิศวกรรมศาสตรดุษฎีบัณฑิต**
สาขาวิชา	**วิศวกรรมไฟฟ้า**
พ.ศ.	2548
อาจารย์ผู้ควบคุมวิทยานิพนธ์	**รองศาสตราจารย์ ดร. สุวิพล สิทธิชีวภาค** **รองศาสตราจารย์ ดร.รัตติกร วรากูลศิริพันธุ์**

บทคัดย่อ

ในวิทยานิพนธ์ฉบับนี้ได้ทำการศึกษาและนำเสนอโครงสร้างของระบบ Direct-Sequence Spread-Slotted ALOHA ที่มีองค์ประกอบและโปรโตคอลของสถานีภาคพื้นดินรวมทั้งช่องสัญญาณไร้สายที่สามารถควบคุมการเปลี่ยนแปลงปริมาณของแพ็คเกตทราฟฟิคโดยอิสระในแต่ละสถานีลูกข่าย และไม่ต้องพึ่งพาข้อมูลจากสถานีกลาง วัตถุประสงค์ของการสร้างองค์ประกอบและโปรโตคอลของสถานีลูกข่ายและช่องสัญญาณดังกล่าว เพื่อให้สามารถใช้งานได้สอดคล้องกับการให้บริการบนเครือข่ายไร้สายที่มีรูปแบบแตกต่างกันและมีการใช้งานอยู่ในปัจจุบัน รวมทั้งเครือข่ายที่ให้บริการผ่านทางดาวเทียมวงโคจรปานกลางหรือค้างฟ้า ปัจจัยหลักของโปรโตคอลที่ได้ทำการศึกษาคือ การพัฒนาและใช้คิวภายในของแต่ละสถานีลูกข่าย จัดการกับแพ็คเกตที่เกิดการชนและต้องมีการส่งใหม่ ในขณะเดียวกันจำนวนของแพ็คเกตที่รออยู่ในคิวดังกล่าวสามารถนำไปพัฒนาเป็นปัจจัยในการควบคุมปริมาณทราฟฟิคภายในสถานีลูกข่ายดังกล่าว โดยกระบวนการทั้งหมดต้องกระทำโดยอิสระในแต่ละสถานีลูกข่าย ในการวิจัยได้ใช้กระบวนการ Semi-Markov เป็นเครื่องมือในการอธิบายพฤติกรรมเชิงสถิติของระบบที่สภาวะเสถียร การตรวจสอบแบบจำลองทางคณิตศาสตร์ที่สร้างขึ้นจะใช้แบบจำลองทางโปรแกรมในการเปรียบเทียบความถูกต้องของผลลัพธ์ที่ได้ภายใต้สภาวะแวดล้อมที่แตกต่างกัน และผลลัพธ์ที่ได้สามารถนำไปใช้เป็นข้อมูลในการสร้างอัลกอริธึ่มสำหรับควบคุมปริมาณของแพ็คเกตในระบบขณะนั้นทันทีโดยไม่ต้องรอข้อมูลจากสถานีกลาง

This material is reserved for educational use only, not allowed for commercial use.
Forbidden to modify the content, and cite the document when use.

Thesis Title	A Mechanism for Improving Performance of Direct-Sequence Spread-Slotted ALOHA under Impaired Satellite Channel Environment.
Student	Mr. Seri Asvaruk
Student ID.	41060010
Degree	Doctor of Engineering
Programme	Electrical Engineering
Year	2005
Thesis Adv.	Assoc. Prof. Dr. Suvepol Sittichevapak
	Assoc. Prof. Dr. Ruttikorn Varakulsiripunth

ABSTRACT

This thesis has studied the architecture of the Direct-Sequence Spread-Slotted ALOHA (DS-SSA) system with modified node components and protocol in order to construct a load control structure in which the service rates of each node can be dynamically adapted without using feedback information. This architecture is intended to support various types of newly wireless applications. These include the application that is operated over low earth orbit and geo-stationary satellite system. In contrast to the traditional DS-SSA system which is widely represented with single queue, prior emphasis of the approach is laid on the usage of an additional queue which is applied to manage the collided packet traffic while its queue size is also used as a load control parameter. Semi-Markov process is applied to describe the protocol and statistic behavior of the system in steady state. Trade-offs between two major performance parameters, i.e. delay and throughput, are presented and compared with those of the traditional system in several different environments. The results obtained from the simulation and numerical analysis using queuing concept are compared. With these results, an advantage performance for group packets is shown, and we finally extend the concept based on the obtained results to describe a simple algorithm using one way control message as the tool to alleviate the stability problem.

This material is reserved for educational use only, not allowed for commercial use.
Forbidden to modify the content, and cite the document when use.

ACKNOWLEDGEMENT

The author would like to thank Dr. Suvepol Sittichevapak and Dr. Ruttikorn Varakulsiripunth for helpful supports and comments helped in improving the ideas described in this thesis. He would also like to thank for discussing and helping in designing the models. Special thanks also to all his colleagues for their many valuable help and comments.

Seri Asvaruk

King Mongkut's Institute of Technology Ladkrabang

This material is reserved for educational use only, not allowed for commercial use.
Forbidden to modify the content, and cite the document when use.

Table of contents

This material is reserved for educational use only, not allowed for commercial use.

Forbidden to modify the content, and cite the document when use.

Table of contents (cont.)

This material is reserved for educational use only, not allowed for commercial use.
Forbidden to modify the content, and cite the document when use.

List of Figures

This material is reserved for educational use only, not allowed for commercial use.
Forbidden to modify the content, and cite the document when use.

List of Figures (cont.)

This material is reserved for educational use only, not allowed for commercial use.
Forbidden to modify the content, and cite the document when use.

List of Tables

King Mongkut's Institute of Technology Ladkrabang

This material is reserved for educational use only, not allowed for commercial use.
Forbidden to modify the content, and cite the document when use.

Chapter 1

Introduction

1.1 Introduction

The advances in recent technology have resulted in the emergence of new application, especially real-time services, which require more system performance and complexity. Direct-Sequence Spread-Slotted ALOHA (DS-SSA) system is a type of multiple-access system which is expected to provide diverse services with more capacity. However, there are some issues needed to be resolved based on the requirement of upcoming application and services. Those are :

- Long round-trip propagation which is the major factor that causes the difficulty in supporting any specific protocols in which their messages are packetized before being presented to the satellite protocol layer.
- Back-off policy which is required to stabilize load capacity and also to keep the packets in the correct sequence when arriving at the receiver.
- Many system architectures which are based on the use of central HUB to provide distributed control messages for tuning the remote terminals' parameters.
- With DS-SSA features, the system can be rapidly changed from stable state to unstable state.

To reduce the effect of these issues, ground terminal and channel protocol needed to be developed to cope with above difficulties.

This thesis studies an approach of implementing DS-SSA system with modified node components in order to reduce the packet waiting time spent in each node and to construct a load control structure in which the service rates of each node can be dynamically adapted without using feedback information. To achieve this, two major components have to be dealt with:

1. Channel characteristic when operated under interference or fading environment.

This material is reserved for educational use only, not allowed for commercial use.
Forbidden to modify the content, and cite the document when use.

2. Suitable architecture which has to be designed according to performance and behavior of the certain application

The relation between above factors is needed to be evaluated as the major parameters for the system design.

1.1.1 Channel characteristic when operated in the impaired environment.

In multiple access architectures such as slotted or unslotted ALOHA and Spread-Spectrum random access, several classes of packet streams containing various traffic characteristics share channel resources and statistically perform traffic loads to system. This load results in unstable behavior in which low throughput and high delay may be experienced. Such undesirable condition also occurs in the Spread-Slotted ALOHA (SSA) system in which hybrid schemes of slotted ALOHA and Spread-Spectrum multiple access are exploited. By deriving the distribution of interference variance over all possible phase and delay, the root mean square values of noise plus interference can be obtained. This thesis studies the channel behavior when the system suffers in performance due to excessive multiple-access interference and impaired channel characteristics caused by long-term and short-term fading. The former fading effect is possibly reduced by adding margin into Line-of-Sight component or using diversity schemes, but the latter is more difficult since any restricted area in close vicinity may need vastly different margin. If improper adding power is used, the signal from that terminal will becomes significant interference to other users, especially, in the Spread-Slotted ALOHA system where all users operate in time-coordinate burst mode. Although hardware counteraction has been exploited, particular protocol having ability to adjust traffic loads in order to sustain system stability is necessary. The method of identifying point of state transition is considered by mean of the terminal queue which contains the number of packets more than that was bounded. When an alarm condition is detected, system can decide the process to protect or moderate the effect of degradation.

1.1.2 Performance behavior of the certain application

Spread-Spectrum multiple access techniques are increasingly being used or considered for commercial applications requiring high bandwidth efficiency. In

This material is reserved for educational purposes. Forbidden to modify the content, and cite the document when use.

particular, CDMA systems are being developed as potential candidates for using in digital cellular mobile and other applications [1]-[3]. The mobile and personal satellite communications environment is significantly different from cellular system in several aspects such as code sharing population, path delay, near-far problems, etc.

In certain application which is operated over wireless or satellite environments, traffic flow from an upper protocol layer into media-access layer is composed of variable-sized messages that need to be segmented into smaller packets. The length of the packet is usually assumed to be equal to the size of the channel time slot and sequentially sent out to the receiver.

When these packet segments are sent across the large propagation network such as satellite system, the delay incurred by satellite propagation, multiple access and delay time spent in the terminal queues may cause upper protocol layer (application layer) to assume them as lost packet events, despite correctly receiving them, and possibly retransmitted them needlessly. These disadvantages will significantly limit the performance and channel capacity. Main factor that also makes the system susceptible to the delay figures is the backlogged condition which is considered necessary for stabilizing channel reliability and also for keeping the packets in the correct sequence when arriving at the receiver. Though the corresponding results achieve the required performance when considering individual packet, the scheme has a potential problem of increasing the waiting time within the internal queue, resulting in throughput constraint and high message delay when input traffic is the messages carrying one or more packet(s). To mitigate this disadvantage, the concept of freely transmitting the packets in order to reduce time spent in the terminal's queues is applied.

When a terminal has the new packet(s) in its first buffer, it immediately sends those packets to the next time slot. The receiver responds to all transmitted packets via the outbound channel. In the proposed architecture, when a new packet is generated, the terminal does not join the backlogged state. Instead, the terminal can send the new packets up to the limited window size, and the terminal whose packet was collided can also send new packets at the original rate, and simultaneously manage retransmission.

This material is reserved for educational use only, not allowed for commercial use.
Forbidden to modify the content, and cite the document when use.

1.2 Objective of the Study

1. Study the behavior of the Spread-Slotted CDMA channel under the impaired environment. Numerical analysis and simulation program are used as the tools to create the channel model.

2. Study the system characteristic when certain applications are operated. By using the simple state flow diagram to represent channel characteristic and behavior at equilibrium point, the channel model can be created.

3. Modify the protocol to build the model whose architecture is possible to be implemented and operated according to the certain applications.

1.3 Organization of the Thesis

Chapter 1 Introduction

Chapter 2 Introduce the theory and concept of slotted ALOHA and Spread-Spectrum multiple access. Since the channel expressions obtained in this study are based on the characteristics of Direct-sequence Spread-Slotted-ALOHA in which hybrid schemes of both multiple access types are exploited.

Chapter 3 Explain the characteristic of DS-CDMA channel when operated on impaired environment. Simulation model is developed to verify the correctness of proposed numerical model. Both simulation and numerical models are required in Chapter 4

Chapter 4 Using the queuing concept and Semi-Markov model to develop a Slotted DS-CDMA system with the control structure. The new protocol concepts also provide to complete the system architecture. OPNET simulation program is used as the tool to verify the characteristic of the proposed approach.

Chapter 5 Conclusion

This material is reserved for educational use only, not allowed for commercial use.
Forbidden to modify the content, and cite the document when use.

Chapter 2

Theory of Multiple-Access

2.1 Introduction

Channel expressions obtained in this study are based on the characteristics of Direct-sequence Spread-Slotted-ALOHA in which hybrid schemes of slotted ALOHA and Spread-Spectrum multiple access are exploited.

2.2 Introduction to Slotted ALOHA

This section introduces a general model of multiple access satellite channel which has basic structure of slotted ALOHA. It is a very well-known system and has been implemented and used for more than two decades in both terrestrial and satellite network. The model of Slotted ALOHA channel can be concluded as 1) stations randomly generate the data, 2) the data are formatted into fixed-size packets. It is normally referred to "*slot*", 3) station immediately send out the packet if its internal queue is not empty, 4) Collision occurs whenever there are more than one stations transmit their packets in the same slot. Following subsections will briefly explain more aspects of this multiple access scheme.

2.2.1 Performance Analysis.

A familiar generalization of the described model for slotted ALOHA channel with multiple access scheme, had been summarized in [4]. The simple parameters that are used to characterize performance of the scheme can be defined with,

- maximum throughout at equilibrium point,

- average delay measured from the time that a packet is first transmitted from sender station until it was successfully received by receiver station, including time that spent for retransmission(s) and waiting in the buffers in case of collided packets,

- channel capacity and input load,

This material is reserved for educational use only, not allowed for commercial use.
Forbidden to modify the content, and cite the document when use.

- optimum and stability point of system performance.

2.2.2 Throughput Model

Behavior of satellite channel (or state) depends upon a number of factors such as the number of ***thinking***, ***idle*** and ***blocked*** stations, retransmission algorithm, the methodology of the particular algorithm intended to gain more efficiency of network parameters for different types of application, input rate of terminal, etc. However, our principle concern in this study is the number of *blocked* station (terminals in retransmission mode). This number can be used to describe the transition state of slotted ALOHA channel [5][6]. To reduce the complexity of computation, system behavior will be evaluated at the equilibrium point. Thus the first simple formula for slotted ALOHA based channel can be defined as:

$$Q_{in}(1 - P_n) = Q_{out} P_n \tag{2.1}$$

where Q_{in} and Q_{out} denote the number of packets arrived at the system and packets successfully transmitted in a period of time. P_n is the probability that a newly generated packet and retransmitted packet will be successfully transmitted. In the next section, "Q_{in}" will be used as a key parameter to contain the channel event occurred in each condition for those different types of satellite channel as previously mentioned.

2.2.3 Delay Model

In the case that the positive acknowledgement is not required, the expected average time when a packet is generated until it is successfully received can be simply expressed as the sum of average delay time occurred in each possible condition(assumed independent to each others) weighted by probability of the occurrence of event in that condition [7]. With this definition, the total delay time can be written as :

$$T_{tot} = p_1(T_{s1} + T_{r1}) + p_2(T_{s2} + T_{r2}) + \ldots + p_n(T_{sn} + T_{rn}) \tag{2.2}$$

where p_n is the probability of *n*-th conditioned even.

In writing this delay formula, it can take advantage from the fact that, in slotted ALOHA multiple access system, there are only two possible delay encountered by a

This material is available for educational use only, not allowed for commercial use.
Forbidden to modify the content, and cite the document when use.

terminal after it had transmitted a packet. One is the delay time occurred in case of successfully transmission, T_{sm}, and the other is delay time caused by collision, T_{rm}. Note that, the first part of the delay encountered by a message when it arrives at a station is the delay in queue before it is conformably divided into smaller packets. The evaluation of this delay is complicated by the factor of time spent in the queue which depends on the number of messages sending to the channel from other stations. Even the stations in the system have been defined to be independent among them. This corresponds to the behavior of the whole system and is important for the design of the integrated network. Thus, it will be left to be concerning topic and not include here.

2.3 Introduction to Code Division Multiple Access (CDMA)

In Code Division Multiple Access (CDMA) systems all users transmit in the same bandwidth simultaneously. This concept is known as "Spread Spectrum technique". *Spread Spectrum* is a communication technique that has been widely accepted in mobile and wireless communications. They have very beneficial features, like antijam, security, and multiple access. The emphasis of this thesis will be on the *Direct Sequence Spread Spectrum*(DS-SS) scheme. In this transmission scheme, the frequency spectrum of a data-signal is spread using different codes. As a result the bandwidth occupancy is much higher then required. The codes used for spreading are designed or selected to have low cross-correlation values and are unique to every user. This is the reason that a receiver which has knowledge about the code of the intended transmitter is capable of selecting the desired signal. Spread-spectrum communications can be defined by two functions:

- The signal occupies a bandwidth much greater than that which is necessary to send the information. This results in many benefits, such as immunity to interference and jamming and multi-user access.

- The bandwidth is spread by means of a code which is independent of the data. The independence of the code distinguishes this from standard modulation schemes in which the data modulation will always spread the spectrum.

In order to recover the data, the code used is pseudo-random. It appears random, but is actually deterministic, so that the receiver can reconstruct the code for synchronous detection. This pseudo-random code is also called pseudo-noise (PN). The

This material is reserved for educational use only, not allowed for commercial use.
Forbidden to modify the content, and cite the document when use.

receiver knows how to generate the same code, and correlates the received signal with that code to extract the data. The main parameter in spread spectrum systems is the processing gain: the ratio of transmission and information bandwidth which is basically called spreading factor. The processing gain determines the number of users that can be allowed in a system, the amount of multi-path effect reduction, the difficulty to jam or detect a signal etc. For spread spectrum systems it is advantageous to have a processing gain as high as possible. There exist different techniques to spread a signal: Direct-Sequence (DS), Frequency-Hopping (FH), Time-Hopping (TH) and Multi-Carrier CDMA

2.3.1 Direct-Sequence Code Division Multiple Access(DS-CDMA)

Direct Sequence is the well-known Spread Spectrum Technique. The data signal is multiplied by a Pseudo Random Noise Code before modulation. In general DS-CDMA system, each station has its own code (sequence) and all active stations transmit their carriers on the same allocated bandwidth but overlap in time. Signal and data separation is achieved at the receiving station by correlation with the matching code. The other carriers from other stations certainly become interference to this station.

In the mobile system, the base station generates a unique code that changes for every connection. The base station adds together all the coded transmissions for every subscriber. The subscriber unit correctly generates its own matching code and uses it to extract the appropriate signals. Note that each subscriber uses several independent channels.

2.3.2 Generating Pseudo-Random Codes

2.3.2.1 Pseudo-Noise Sequence [8],[9],[10]

A PN code is a binary sequence of chips valued -1 and 1 (polar) or 0 and 1 (non-polar) and has noise-like randomness properties. This results in low cross-correlation values among the codes and the difficulty to jam or detect a data message. Several families of binary PN codes exist. A usual way to create a PN code is by means of at least one shift-register. In order for all this to occur, the pseudo-random code must have the following properties:

This material is reserved for educational use only, not allowed for commercial use.
Forbidden to modify the content, and cite the document when use.

1. The destination must be able to independently generate the code that matches the source code.

2. It must appear random to a listener without prior knowledge of the code (i.e. it has the statistical properties of sampled white noise).

3. The cross-correlation between any two codes must be small.

4. The code must have a long period before repeating itself).

The definition of randomness was studied by Golomb and requires the three properties as described in [1]

R.1: Balance property: Relative frequencies of "0" and "1" are each 0.5.

R.2: Run-length property : Run lengths (of zeros or ones) are as expected in a coin-flipping experiment; half of all run lengths are unity; one-quarter of length two; one-eighth are of length three; a fraction $1/(2)^n$ of all runs are of length n for all finite n.

R.3: Shift-and-add property : If the random sequence is shifted by any nonzero number of element, the resulting sequence will have an equal number of agreements and disagreements with the original sequence.

The correlation properties of PN codes play a major part in the code design for CDMA systems, since they determine not only the level of multiple access interference, i. e. the interference arising from other users of the channel and self-interference due to multipath propagation, but also the code acquisition properties. The first one is affected by the cross-correlation properties between different codes of the family whereas the last two are affected by the auto-correlation properties, that is the correlation between time-shifted versions of the same code. There are several variants of correlation functions:

Definition Let $\{u(t)\}$and $\{v(t)\}$ be the complex valued sequences of length N. The aperiodic cross-correlation function of the these two sequences can be defined by :

$$\rho_{uv}(\tau)=\begin{cases}\sum_{t=0}^{N-1-\tau}u(t+\tau)v^{*}(t) & ;0\geq\tau\geq N-1,\\ \sum_{t=-\tau}^{N-1}u(t+\tau)v^{*}(t) & ;1-N\geq\tau<0.\end{cases} \tag{2.3}$$

This material is reserved for educational use only, not allowed for commercial use.
Forbidden to modify the content, and cite the document when use.

The periodic (or even) cross-correlation function of $\{u(t)\}$and $\{v(t)\}$ is defined by

$$\theta_{uv}(\tau)=\sum_{t=-\tau}^{N-1}u(t+\tau)v^{*}(t)=\rho_{uv}(\tau)+\rho_{uv}(\tau-N) \tag{2.4}$$

The odd cross-correlation function of $\{u(t)\}$and $\{v(t)\}$ is defined by

$$\hat{\theta}_{uv}(\tau)=\rho_{uv}(\tau)-\rho_{uv}(\tau-N) \tag{2.5}$$

The aperiodic correlations give more realistic estimates of the CDMA system performance as the periodic ones do. However, since the problem of designing sequence families with low aperiodic correlation is a difficult task, the conventional approach has been to design based on periodic correlation properties and to subsequently to analyze the aperiodic properties of the resulting design. Some examples of this class of sequences, there are m-sequences, Gold codes and Kasami sequences.

2.3.2.2 Maximal Length Sequences(m-sequences) [8],[9],[10]

Linear Feedback Shift Register (LFSR) sequences having the maximum possible period for an *r*-stage shift register are called *maximal length sequences* or *m-sequences*. Not only m-sequences, but other various pseudo random codes are generated using LFSR. The generator polynomial governs all the characteristics of the generator and all operations are linear. The length of the sequence before repetition occurs depends upon two things, the feedback taps and the initial state. An LFSR of any given size *m* (number of registers) is capable of producing every possible state during the period $N=2^m-1$, but will do so only if proper feedback taps, or terms, have been chosen. Any LFSR can be represented as a polynomial of variable *a*, referred to as the *generator polynomial*:

$$G(a)=g_m a^m+g_{m-1}a^{m-1}+g_{m-2}a^{m-2}+\ldots+g_2a^2+g_1a+g_0 \tag{2-6}$$

The coefficients g_i represent the tap weights which are 1 for the taps that are connected (fed back), and 0 otherwise. The order of the polynomial, *m*, represents the number of LFSR stages. All mathematical operations are performed in modulo-2(0+0=0, 1+1=0, 0+1=1, 1+0=1) which can be easily implemented with exclusive-OR(XOR) gates. This type of generator polynomial always yield an *m*-sequence which

This material is reserved for educational use only, not allowed for commercial use.
Forbidden to modify the content, and cite the document when use.

complying all three Golomb properties, and have two-valued periodic auto-correlation function given by

$$R_c(j) = \begin{cases} -1 & ;j \neq 0(\oplus 2^m - 1) \\ 2^m - 1 & ;j = 0(\oplus 2^m - 1) \end{cases} \tag{2.7}$$

This is for the {0,1}-valued sequence. This sequence is normally transformed and transmitted by a bipolar waveform *a(t)* of positive and negative amplitudes according to the equation below :

$$a(t) = \sum_{i=0}^{2^m-1} a^i g(t - iT_c) \tag{2.8}$$

where $g(t)$ is the rectangular pulse of chip duration T_c and has unit amplitude. The sequence $\{a_i\}$ is a {-1,1}-valued sequence with an autocorrelation identical to (2-4) :

$$R_c(j) = \sum_{i=1}^{2^m-1} a_i a_{i+j} = \begin{cases} 2^m - 1 & ;j = 0 \\ -1 & ;0 < j < 2^m - 1 \end{cases} \tag{2.9}$$

The normalized autocorrelation function of the periodic bipolar wave form *a(t)* representing an *m* sequence is

$$\begin{aligned} r(\tau) &= \frac{1}{(2^m - 1)T_c} \int_0^{(2^m-1)T_c} a(t)a(t+\tau)dt \\ &= -\frac{1}{(2^m - 1)} + \frac{2^m}{2^m - 1} \Lambda(\tau) \Theta \sum_{j=-\infty}^{\infty} \delta[\tau - j(2^m - 1)T_c] \end{aligned} \tag{2.10}$$

where

$$\Lambda(\tau) = \begin{cases} 1 - \dfrac{|\tau|}{T_c} & ;|\tau| \leq T_c \\ 0 & ;|\tau| > T_c \end{cases}$$

and

$$\delta(x) = \begin{cases} \infty & ;x = 0 \\ 0 & ;x \neq 0 \end{cases}$$

with $\int_{-\infty}^{\infty} \delta(x)dx = 1$.

This material is reserved for educational use only, not allowed for commercial use.
Forbidden to modify the content, and cite the document when use.

$\delta(x)$ is the dirac delta function and $\Lambda(\tau)$ is the triangular function whose spectrum is shown in appendix A. Figure 2.1 and 2.2 illustrates the plot of $r(\tau)$ and its power spectral density, respectively. As seen from the figures, the autocorrelation has a large peaked maximum only for perfect synchronization of two identical sequences. Since the PSD and autocorrelation function are Fourier transform pairs, the power spectral density of the m-sequence waveform *a(t)* is the Fourier transform of $r(\tau)$ and is given by

$$S(w)=\frac{1}{(2^m-1)^2}\delta(w)+\frac{2^m}{(2^m-1)^2}\left[\frac{\sin(wT_c/2)}{wT_c/2}\right]^2\sum_{\substack{j=-\infty\\ j\neq 0}}^{\infty}\delta(w-\frac{2\pi j}{(2^m-1)T_c}) \qquad (2.11)$$

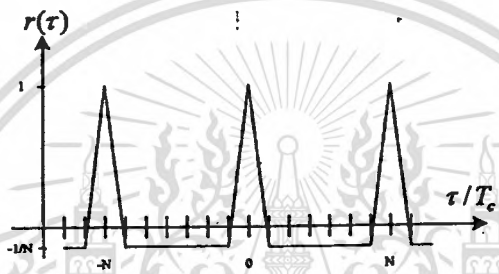

Figure 2.1 Normalized autocorrelation function of an m-sequence.

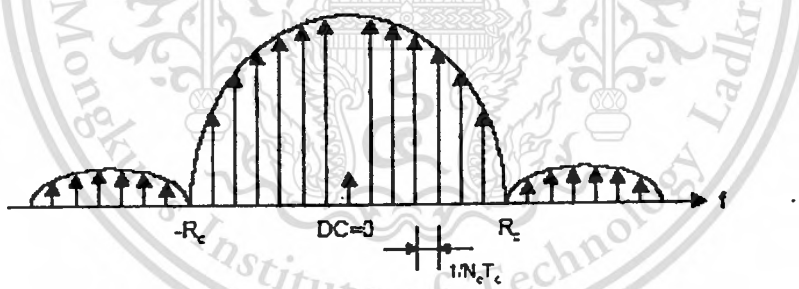

Figure 2.2 Power Spectral Density of m-sequence.

Each m-sequence generated by *G(a)* has 2^{m-1} ones and 2^{m-1}-1 zeros. M-sequences have good auto-correlation property, but its cross-correlation property is relatively poor compared to Gold codes. With these properties, the same sequences with different offset are used for different users in the same groups. The discrimination between different spreading codes only depends on partial autocorrelation property. There are two types of generator to build LFSR: Galois and Fibonacci feedback generator. Only Galois generator will be discussed here, the Galois generator structure consists of a shift register and feedback weights or tabs as shown in figure below.

This thesis is used for educational use only, not allowed for commercial use. Evaluation to study the content, and cite the document when use.

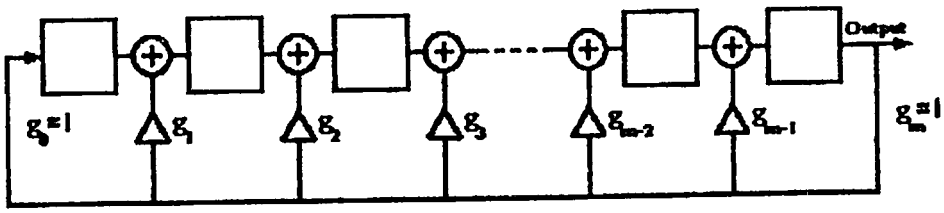

Figure 2.3 Galois LFSR Generator.

As an example, consider an LFSR of size $m = 8$ with feedback connections at g_8, g_6, g_5, g_4, and implied g_0, the feedback taps will be specified as (8, 6, 5, 4). Note that the taps are customarily arranged in a descending order. The sets of a LFSR generator are laid on the primitive factors of polynomial a^m+1. For example, in case of the maximal-length sequence, with $m=3$, its length will be $N=2^3-1=7$, and its sets can be found from the prime factor as

$$a^7+1=(a+1)(a^3+a^2+1)(a^3+a+1) \tag{2.12}$$

The primitive polynomials are those factors whose order is the same as the register size, $m = 3$. Of the three prime factors, only the last two meet this criterion. Thus it can be seen that there are exactly two sets of m-sequence feedback taps, (3, 1) and (3, 2).

2.3.2.3 Gold Codes [8],[9],[10],[11]

Gold codes are obtained by using a specified pair of PN sequences of period $N = 2^m - 1$, and modulo-2 adding or XORing the output together. All pairs of PN sequences do not yield Gold codes , but only some preferred pairs of m-sequences with the same degree can be used to generate Gold codes by linearly combining two m-sequences with different offsets. There do not exist preferred pairs for shift-registers with a length equal to $4n$ where n is an integer. This reference design uses a set of specific primitive polynimials over Galois Field. Gold codes have the property that the cross-correlation between any two, or between shifted versions of them, takes on one of three values: $-t(r)$, -1, or $t(r) - 2$, where

$$t(r)=\begin{cases}2^{(r+1)/2}+1 & ;odd \quad r\\ 2^{(r+2)/2}+1 & ;even \quad r\end{cases} \tag{2.13}$$

This material is reserved for educational use only, not allowed for commercial use.
Forbidden to modify the content, and cite the document when use.

By shifting one of the codes with respect to the other code, the different sequences can be obtained. The number of sequences that are available is 2^m+1 (the two M-sequences alone, and a combination with 2^m-1 different shift positions).

2.3.2.4 Kasami sequences [8],[11]

If a Gold-code is combined with a decimated version of one of the 2 m-sequences that form the Gold-code, a ``Kasami-code" can be obtained. For the m-sequences a, a^l is obtained by taking every qth bit of a and denoted by $a[q]$. a^l is called a decimated sequence of a. By choosing $q=2^{m/2}+1$, where m is the degree of sequence a, a^l is periodic with the period of $2^{m/2}-1$. By repeating a^l q times, a new sequence b is obtained. With a and b, a new set of sequences can be formed by adding a and $2^{m/2}-2$ cyclically shifted b. Including a and b, $2^{m/2}$ sequences can be obtained. These sequences are Kasami codes and can be formulated as follows:

$$R_r = uT^k vT^m w \tag{2.14}$$

here u and v are m-sequences of length: 2^m-1(m even) which form a preferred pair. w is a m-sequence resulting after decimation the v code with a value $2^{m/2}+1$. T denotes a delay of one chip, k is the offset of the v code with respect to the u code and m is the offset of the w code with respect to the u code. Offsets are relative to the all-ones state. There are two classes of Kasami sequences: the small set and the large set. The large set contains all the sequences in the small set. Kasami codes have the same correlation properties as Gold-codes, the difference lays in the number of codes that can be created. For the large set of Kasami codes this number is equal to $2^{n/2}(2^n+1)$. Choosing n equal to 6 gives us 520 possible codes.

2.3.2.5 Orthogonal Code [8],[14]

In the case of PN codes, they have non-zero cross-correlations. Orthogonal codes have "zero" cross-correlation. This cross-correlation value is "zero" only when there is no offset between the codes. Orthogonal Gold code shows reasonable cross-correlation and off-peak autocorrelation values while providing perfect orthogonality in zero-offset case. But they have much larger cross-correlation values with different offsets. Orthogonal codes are used in systems in which the receiver is perfectly synchronized

Forbidden to modify the content, and cite the document when use.

with the transmitter. For such systems, the despreading operation is ideal when orthogonal codes are used for the spreading. For example, they are used in the forward link of the standard IS-95 system [15], in which the base station transmits a pilot signal to help the receiver gain synchronization. There are several code building technique to generate orthogonal codes such as Hadamard code, Walsh code, Multi-rate orthogonal code and Orthogonal gold code.

2.3.2.6 Walsh-Hadamard Code [12],[13]

The Walsh-Hadamard codes are orthogonal on zero code delay where as the m-sequences, Gold-codes and Kasami-codes are non-orthogonal with varying cross-correlation properties. An important set of orthogonal code is the *Walsh* set. Walsh functions are generated using an iterative process of constructing a Hadamard matrix. starting with $H_1 = [0]$. The Hadamard matrix is built by:

$$H_N = \begin{bmatrix} H_{N/2} & H_{N/2} \\ H_{N/2} & -H_{N/2} \end{bmatrix} \quad \text{with} \quad H_0 = [1]$$

The rows of the matrix H_N are the Hadamard-Walsh codes. The rows of any H_N form a mutually orthogonal set of sequences. If $M>2$ is a power of 2, then

$$H_2 = \begin{bmatrix} 1 & 1 \\ 1 & -1 \end{bmatrix} \quad H_4 = \begin{bmatrix} 1 & 1 & 1 & 1 \\ 1 & -1 & 1 & -1 \\ 1 & 1 & -1 & -1 \\ 1 & -1 & -1 & 1 \end{bmatrix} \quad H_8 = \begin{bmatrix} 1 & 1 & 1 & 1 & 1 & 1 & 1 & 1 \\ 1 & -1 & 1 & -1 & 1 & -1 & 1 & -1 \\ 1 & 1 & -1 & -1 & 1 & 1 & -1 & -1 \\ 1 & -1 & -1 & 1 & 1 & -1 & -1 & 1 \\ 1 & 1 & 1 & 1 & -1 & -1 & -1 & -1 \\ 1 & -1 & 1 & -1 & -1 & 1 & -1 & 1 \\ 1 & 1 & -1 & -1 & -1 & -1 & 1 & 1 \\ 1 & -1 & -1 & 1 & -1 & 1 & 1 & -1 \end{bmatrix}$$

From the matrix, the Walsh-Hadamard codewords are given by the rows. In each case the first row of the matrix consist entirely of *1*'s and each of the other rows contains *N/2* of 0's and *N/2* of 1's. Row *N/2* starts with *N/2 1*'s and end with *N/2* 0's. The distance (number of different elements) between any pair of rows is exactly *N/2*. For H_8 the distance between any two rows is 4, so the Hamming distance of the Hadamard code is 4. Each sequence of n bits identifies one row of the matrix (there are $N=2^n$ possible rows). All rows are mutually orthogonal with $\sum_{k=0}^{N-1} h_{ik} h_{jk} = 0$ for all rows i

This material is reserved for educational use only, not allowed for commercial use.
Forbidden to modify the content, and cite the document when use.

and j. The cross-correlation between any two Hadamard-Walsh codes of the same matrix is zero, when perfectly synchronized. In a synchronous CDMA system this ensures that there is no interference among signals transmitted by the same station. Only when synchronized, these codes have good orthogonal properties. Note that it is usually map the binary data to polar form so the real numbers arithmetic can be used when computing the correlations. So 0's are mapped to 1's and 1's are mapped to -1.

As mentioned above these sequences have zero cross-correlation when the codes are synchronous, but when asynchronous, their cross-correlation is very much dependent on the particular pair of codes used, some will have cross-correlation zero while others will have a very high correlation. In addition, these codes have a number of drawbacks:

- The auto-correlation function of Walsh-Hadamard codewords does not have good characteristics. The codes do not have a single, narrow autocorrelation peak. It can have more than one peak and therefore, it is not possible for the receiver to detect the beginning of the codeword without an external synchronization scheme.

- The spreading is not over the whole bandwidth, but over a number of discrete frequency components.

- The cross-correlation can be non zero for a number of time shifts and un-synchronized users can interfere with each other. The partial cross-correlation is also not always identically zero. This is why Walsh-Hadamard code family is unsuitable for asynchronous application.

-Walsh-Hadamard codes do not have the best spreading behavior. They do not spread data as well as PN sequences does because their power spectral density is concentrated in a small number of discrete frequencies.

However, despite of the some drawbacks pointed out above, the Walsh-Hadamard sequences are used in IS-95 system for channel separation. Walsh-Hadamard codes are important because they form the basis for orthogonal codes with different spreading factors. This property becomes useful when the signals are needed with different Spreading Factors to share the same frequency channel.

This material is reserved for educational use only, not allowed for commercial use.
Forbidden to modify the content, and cite the document when use.

สำนักหอสมุดกลาง พระจอมเกล้าลาดกระบัง

2.3.2.7 Orthogonal Variable Spreading Factor Codes [16]

Two codes are said to be orthogonal when their inner product is zero. The inner product, in the case of codes with elements values *+1* and *-1*, is the sum of all the terms obtained by multiplying two codes element by element. For example, (*1, 1, 1, 1*) and (*1, 1, -1, -1*) are orthogonal when

$$(1 * 1) + (1 * 1) + (1 * -1) + (1 * -1) = 0 \tag{2.15}$$

The following diagram explains how to choose OVSF code family:

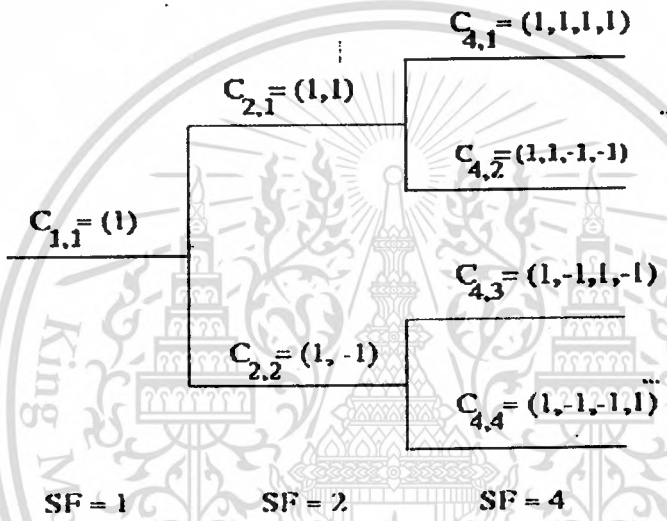

Figure 2.4 OVSF Diagram

Each stage of the tree has a different Spreading Factor. Each node in the OVSF tree is a code, denoted as $C_{SF,CN}$. SF is the spreading factor and CN is the code number or branch number. The top code $C_{1,1}$ of the tree is called the root code with a SF=1. Each code can generate two child codes and the SF values of child codes are doubled on the parent code. Codes on the same level have the same data rate. The bottom level codes of the tree are called leaf codes and have the minimum data rate. The data rate of codes on *m* level is double for the data rate of codes in *m+1* level. All codes at the same level are orthogonal to each other and a code is available if and only if all the codes on the path from the current code to the root call are empty. By the property of OVSF codes, when a new call requests a code with rate *R*, the system has to find an available code with *R* in the code tree and assign it to the new coming call. If the code tree has excess free capacity, but no available code, the new coming call will be blocked. In this case, it is

This material is reserved for educational use only, not allowed for commercial use.
Forbidden to modify the content and cite the document when use.
46631

called code block. The conditions of the codes on this particular tree can be summarized as follows:

- The first element in the tree is 1.

- For each element, there are two possible elements:

1. The first element is constructed by repeating the root of that element itself twice. So that the first element of (1) would be (1,1).

2. The second element is constructed by concatenating the root of that element with the inverse of itself. Thus, the second element of (1) would be (1, -1).

- At each level, all the codewords are the rows of the Hadamard matrix with the elements mapped to polar form. If [*C*] is a code length 2^r at depth r in the tree, where the root has depth 0, the two branches leading out of *C* are labeled by the sequences [*C C*] and [*C -C*], which have length 2^{r+1}. The codes at depth r in the tree are the rows of the matrix C_N, where $N = 2^r$.

Note that two OVSF codes are orthogonal if and only if neither code lies on the path from the other code to the root. Since codes assigned to different users in the same cell must be orthogonal, this restricts the number of available codes for a given cell. For example, if the code C_{41} in the tree is assigned to a user, the codes C_{10}, C_{20}, C_{82}, C_{83}, and so on, cannot be assigned to any other user in the same cell.

2.4 Characterization of DS-CDMA channel

Direct Sequence Code Division Multiple Access(DS-CDMA) is one of the most widely used *Spread Spectrum* techniques. As with all *Spread Spectrum* schemes, *DS-CDMA* uses a unique code to spread the Base-band signal, this allows it to have all the advantages of *Spread Spectrum* techniques mentioned in the previous chapter. After the spreading takes place, the spread signal is then modulated and transmitted through the specified medium. BPSK and QPSK are a widely used Digital Modulation scheme for *Spread Spectrum* systems. Since the results obtained from both schemes are similar, the analysis in this thesis will mainly concentrate on BPSK. Once the modulated data is received at the demodulator port, the signal is then demodulated using a BPSK demodulator that could be synchronized or un-synchronized to the transmitter's carrier

This material is reserved for educational use only, not allowed for commercial
Forbidden to modify the content, and cite the document when use.

frequency. Now, the spread signal will be at the output of the demodulator. This is then multiplied with the locally generated PN sequence. If the locally generated PN sequence is correlated with the one that was used in transmitter, the signal is dispread, yielding the original signal. Figure 2.5 illustrates a model of DS-CDMA system where k users are individually transmitting spread spectrum signals in the same frequency band.

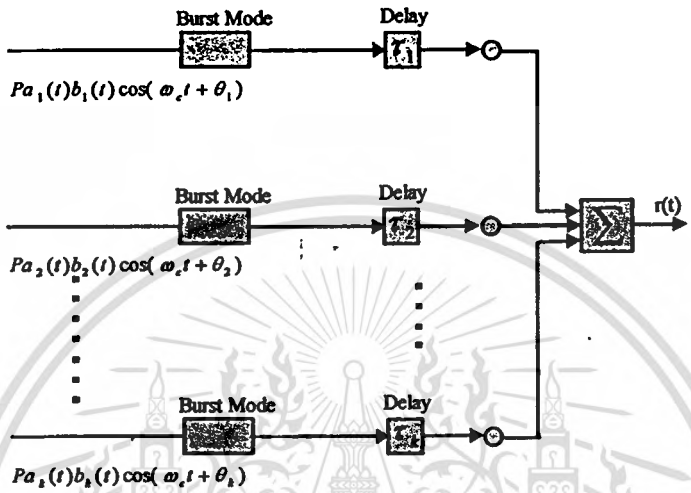

Figure 2.5 Model of a DS-CDMA system

Following Pursley[1], assume that K users occupy simultaneously a satellite timeslot and each transmits a signal:

$$s_k(t) = P_t b_k(t) a_k(t) \cos(w_c t + \phi_k) \tag{2.16}$$

where P_t is the transmitted signal amplitude, $b_k(t)$ is the sequence of independent and identically distributed random binary data denoted as:

$$b_k(t) = \sum_i b_k^i g(t - iT_b) \qquad ;0 \le t \le T_b,\ b_k^i \in \{+1,-1\}$$

and

$$a_k(t) = \sum_i a_k^i g(t - iT_c) \qquad ;0 \le t \le T_c,\ a_k^i \in \{+1,-1\}$$

is a spectral-spread PN sequence which is generated at a period of N chips. $g(t)$ is the rectangular pulse of unit height and θ_k is carrier phase. If T_c is the chip duration of PN sequence, NT_c represents one period of user data bit(T_b).

This material is reserved for educational use only, not allowed for commercial use.
Forbidden to modify the content, and cite the document when use.

In order to spread a signal spectrum in the transmitter of the k-th user, the data sequence $b_k(t)$ is directly multiplied by random sequence $a_k(t)$ which has much higher rate than $b_k(t)$. To simplify the analysis, tracking error results of signal and phase are assumed to be neglected. Each user generates the packets in burst mode and in constantly synchronous to satellite channel slot.

Each transmitter-receiver pair has been designed to encode and decode data using a particular code. The receiver has a local PN generator and carrier generator that generate replicas of those in the transmitter. In case of satellite system with given Doppler effect, it has to be determined the maximum chip rate of the system so that a station n can make a correction once per satellite roundtrip delay. One of the basic operations in the receiver is the removal of the "code" which was used by the transmitter to spread the data-message. This operation is known as dispreading. Dispreading is performed by combining the received signal with the same code which was used by the transmitter to code the data. To enable a low BER, the local code should be aligned with the received signal. An alignment error results is a loss of Signal-to-Noise Ratio (SNR). Obtaining this code-alignment is the code-synchronization process. The process of synchronizing the locally generated PN sequence with the received PN sequence can be accomplished in two steps. The first step, called acquisition, consists of bringing the transmitted and received spreading signals into coarse alignment with one another. Once the received PN sequence has been acquired, the second step, called tracking, takes over and continuously maintains the best possible waveform alignment by means of a feedback loop.

Acquisition Step

This step is the method to searching throughout an area of time and frequency in order to synchronize the received spread-spectrum signal with the locally generated PN sequence. The objective of this step is to resolve the code phase error to within certain bounds which can be further reduced by the tracking step. Since the dispreading process typically takes place before carrier synchronization, most acquisition schemes utilize non-coherent detection. A common feature of all acquisition methods is that the received signal and the locally generated PN sequence are first correlated with a coarse time step to produce a measure of similarity between the two signals. This measure is

This material is reserved for educational use only, not allowed for commercial use.
Forbidden to modify the content, and cite the document when use.

then compared to the threshold to decide if the two signals are in synchronism. If they are, the tracking algorithm is started.

Tracking step

The tracking maintains the PN code generator at the receiver in synchronism with the received signal. The remaining error after the acquisition step is likely too large to guarantee proper operation. The tracking step or fine tuning process is needed to achieve maximum processing gain. This process is a two-way search, meaning that the local reference clock can be shifted forward and backward. Tracking is performed continuously during data-detection and keeps the timing-error below an acceptable level.

2.4.1 Time-aynchronous DS-CDMA channel

In a time-asynchronous system, all the users' signals are added together asynchronously to the receiver input, with time delay τ_k and phase ϕ_k. τ_k is independent and uniformly distributed on $[0,T_c)$, and ϕ_k is a random variable uniformly distributed on $[0,2\pi)$. The different spreading waveforms of the interfering users are randomized by the variation in the propagation delays, and will be seen as pseudo random noise at the desired user. The signals transmitted from k users defined by (2.16) will be seen at the receiver as

$$s_k(t) = P_i b_k(t-\tau_k)a_k(t-\tau_k)\cos(w_c(t-\tau_k)+\phi_k) \tag{2.17}$$

If ignoring the effect of multipath and impair environment which will be explained in detail in the next section, and define the desired user to be user 1, equation (2.17) can be rewritten as

$$r_1(t) = b_1(t)T_b P_1 \cos\phi_{11}$$

$$+\sum_{k=2}^{K} P_k(b_k^{-1}R_{1k}(\tau_{1k}) + b_k^0\hat{R}_{1k}(\tau_{1k}))\cos\phi_{1k} + \eta_0 \tag{2.18}$$

Here τ_{mk} is the time delay for each user and path. P_k is the received signal amplitude, which is assumed to be constant and identical for all users. The vector

This thesis is in the King Mongkut's Institute of Technology Ladkrabang Library. It is for educational use only. Not allowed for commercial use.
Forbidden to modify the content, and cite the document when use.

(b_k^0, b_k^{-1}) represents a pair of consecutive data at previous and current time respectively. The carrier phase ϕ_{mk} is the Gaussian variable for the main path(m=1) of the desired user, but become the uniformly distributed random variable over $(0,2\pi)$ for other paths. k denotes the user who transmits this signal. Random variable η_o is Gaussian noise with two-sided spectral density(zero mean) and variance σ_0^2. $R_{1,k}$ and $\hat{R}_{1,k}$[17] are the continuous-time partial cross-correlation functions defined by:

$$R_{1,k}(\tau) = \int_0 a_1(t)a_k(t-\tau)dt \tag{2.19a}$$

$$\hat{R}_{1,k}(\tau) = \int_{\tau}^{T_c} a_1(t)a_k(t-\tau)dt \tag{2.19b}$$

for $0 \le \tau \le T_c$. Assume further that $0 \le lT_c \le \tau \le (l+1)T_c \le T_c$, where l is the integer number less than T_c. The above functions can be rewritten in the form of discrete partial cross-correlation functions, $C_{l,k}$ as

$$R_{1,k}(\tau) = C_{1,k}(l-N)T_c + [C_{1,k}(l+1-N) - C_{1,k}(l-N)](\tau - lT_c) \tag{2.20a}$$

$$\hat{R}_{1,k}(\tau) = C_{1,k}(l)T_c + [C_{1,k}(l+1) - C_{1,k}(l)](\tau - lT_c) \tag{2.21b}$$

where $C_{l,k}(.)$ is the discrete aperiodic cross-correlation function defined by

$$C_{l,k}(l) = \begin{cases} \sum_{j=0}^{N-1-l} a_j^l a_{j+l}^k & ;0 \le l \le N-1 \\ \sum_{j=0}^{N-1+l} a_{j-l}^l a_j^k & ;1-N \le l \le 0; \\ 0 & ;|l| \le N \end{cases} \tag{2.22}$$

The relation of equation (2-19) is computed with respect to the independent random variables $P, \tau, \phi, a(k)$ and $b(k)$.

With equation (2-19), Pursley[17] calculated the bit error rate using the standard Gaussian approximation with the Q-function of a signal-to-noise(SNR) ratio. Note that the results obtained from this method seems to be accurate only for the large number of users(>10-12), and becomes very optimistic as N grows. The alternative is to use the Improved Gaussian Approximation method proposed by [18]. R. K. Morrow uses the model in his paper similar to the previous paper [17]. Recall to the k-th user's input

This material is reserved for educational purposes. Forbidden to modify the content, and cite the document when use.

received signal defined by (2.16), Morrow built the similar model for the output of correlation-receiver with the different form of the discrete partial cross-correlation functions in the different form as:

$$R_{1,k}(\tau) = C_{1,k}(l-N)\hat{R}_{\psi}(\tau-\gamma T_c) + C_{1,k}(l+1-N)R_{\psi}(\tau-\gamma T_c) \tag{2.23a}$$

$$\hat{R}_{1,k}(\tau) = C_{1,k}(l)\hat{R}_{\psi}(\tau-\gamma T_c) + C_{1,k}(l+1)R_{\psi}(\tau-\gamma T_c) \tag{2.23b}$$

where $\gamma = \lfloor \tau / T_c \rfloor$. $R_{\psi}(s)$ and $\hat{R}_{\psi}(s)$ are the continuous-time partial autocorrelation functions of the code waveform defined by

$$R_{\psi}(s) = \int_0^{T_c} \psi(t)\psi(t-T_c-s)dt$$

$$\hat{R}_{\psi}(s) = \int_s^{T_c} \psi(t)\psi(t-s)dt$$

for $0 \le s \le T_c$, and

$$R_{\psi}(s) = \hat{R}_{\psi}(s) = 0 \text{ for } s > T_c \text{ or } s < 0$$

Let $b_k^{-1}R_{1k}(\tau_{1k}) + b_k^0\hat{R}_{1k}(\tau_{1k}) = B_{k,1}(b_k,\tau)$ and the fact that $(a_j^1)^2 = +1$, then it can be expanded and rearranged to be

$$B_{k,1}(b_k,\tau) = \sum_{j=0}^{N-2} Z_j(\hat{R}_{\psi}(S) + a_j^1 a_{j+1}^1 R_{\psi}(S)) + Z_{N-1}\hat{R}_{\psi}(S) + Z_N R_{\psi}(S) \tag{2.24}$$

where Z_j, $0 \le j \le N$ is a set of $N+1$ random variables defined by

$$Z_j = \begin{cases} b_{-1}a_{j-l+N}^k a_j^1, & ; j = 0,\ldots,l-1 \\ b_0 a_{j-l}^k a_j^1, & ; j = l,\ldots,N-2 \\ b_0 a_{N-l-1}^k a_{N-1}^1, & ; j = N-1 \\ b_{-1}a_{N-l-1}^k a_0^1, & ; j = N \end{cases} \tag{2.25}$$

where the random variable Z_j are mutually independent and satisfy

$$Pr\{Z_j = +1\} = Pr\{Z_j = -1\} = 1/2$$

For convenience, Morrow defines

$$f(s) = \hat{R}_{\psi}(s) + R_{\psi}(s)$$

This material is reserved for educational use only, not allowed for commercial use.
Forbidden to modify the content, and cite the document when use.

$$g(s) = \hat{R}_{\psi}(s) - R_{\psi}(s)$$

Set "A" be the set of all nonnegative integers i less than N-1 such that $a_j^1 a_{j+1}^1 = +1$

Set "B" be the set of all nonnegative integers i less than N-1 such that $a_j^1 a_{j+1}^1 = -1$

With the above definitions, the equation (2.24) can be rewritten as

$$B_{k,1}(b_k, \tau_k) = X_k f(S_k) + Y_k g(S_k) + P_k \hat{R}_{\psi}(S_k) + Q_k R_{\psi}(S_k) \tag{2.26}$$

where $X_k = \sum_{j \in A} Z_j$, $Y_k = \sum_{j \in B} Z_j$, $P_k = Z_{N-1}$, and $Q_k = Z_N$.

Now the decision statistic model for the output of correlation receiver can be expressed in the simplified form

$$r_1(t) = b_k^1 T_b P + P \sum_{k=2}^{K} W_k \tag{2.27}$$

where

$$W_k = (X_k f(S_k) + Y_k g(S_k) + P_k \hat{R}_{\psi}(S_k) + Q_k R_{\psi}(S_k)) \cos\phi_k \tag{2.28}$$

The quantities A and B are related to the discrete aperiodic autocorrelation of the signature sequence of receiver 1, offset by one chip, $C_{1,1}(1)$, and can be defined by

$$A = \frac{N-1+C}{2} \tag{2.29}$$

and

$$B = \frac{N-1-C}{2} \tag{2.30}$$

where $C_{1,1}(1) = \sum_{j=0}^{N-2} a_j^1 a_{j+1}^1$

2.4.2 Time-synchronous DS-CDMA channel

In a time-synchronous system, it is assumed [4] that the system is always synchronized and all K users are able to receive identical chip timing. This requires a common timing reference and compensation for transmission delays in various

This material is reserved for educational use only, not allowed for commercial use.
Forbidden to modify the content, and cite the document when use.

transmission paths. The carrier phase is $\phi_{11}=0$ while $\phi_{1k};k=2,...,K$ is the random variables uniformly distributed over $(0,2\pi)$. If the desired user is user 1, after sequence correlation and coherent demodulation, the signal at the receiver output is:

$$r_1(t)=P_1\int_0^{T_b} b_1(t)a_1^2(t)dt+\sum_{k=2}^{K}P_k\int_0^{T_b} b_k(t)a_k(t)a_1(t)\cos\phi_k dt+\eta_o \tag{2.31}$$

For notational convenience, let $a_{1k}=\frac{1}{T_b}\int_0^{T_b} a_1(t)a_k(t)dt$. Then, the statistic decision bases on the sign of data $b_1(t)$ is

$$P_b=\Pr\{1+\sum_{k=2}^{K}(\pm 1)a_{1k}\cos\phi_k<0\,|\,1\} \tag{2.32a}$$

and

$$P_b=\Pr\{-1+\sum_{k=2}^{K}(\pm 1)a_{1k}\cos\phi_k>0\,|\,-1\} \tag{2.32b}$$

2.4.3 System Performance (Probability of Bit Error)

A Gaussian approximation approach is widely used [4],[17],[19] to evaluate the error probability at the desired user's receiver output. For the large number of active users and the relative delays and phases between the desired and interference signals are fixed, the total multiple-access interference which results from the combination of the signals sent by other active users as a zero-mean Gaussian random variable can be modeled. In this method, the signal-to-noise ratio is computed by means of the expectations with respect to three prior parameters: phase shifts, time delays and data bits, which are all assumed to be mutually independent random variables. In the coherent BPSK under well-known Gaussian assumption, this signal-to-noise ratio can be used to calculate the probability of bit error with the Q function given by

$$Q[SNR_b]=\frac{1}{\sqrt{2\pi}}\int_{\sqrt{SNR_b}}^{\infty}\exp(\frac{-u^2}{2})du \tag{2.33}$$

Using the well-known concept of white noise which is stationary and strictly ergodic with zero mean($\langle n(t)\rangle=0$) and variance($\langle n^2(t)\rangle$) is σ^2, the ratio of mean signal power to mean noise power or instantaneous output SNR can be obtained from

This material is reserved for educational use only, not allowed for commercial use.
Forbidden to modify the content, and cite the document when use.

$$SNR = \frac{s^2(t)}{\langle n^2(t) \rangle} = \frac{s^2(t)}{2\sigma^2} \tag{2.34}$$

where $s(t)$ is desired signal amplitude.

2.4.4 Performance of Time-asynchronous DS-CDMA channel

To consider the average probability of bit error of time-asynchronous system, equation (2.18) which is the signal at the receiver output with respect to the chip duration(T_c) will be used. In this case, the received signal is the sum of an AWGN noise process $n(t)$ plus K spreading-spectrum signals each of which has different propagation delay and the lack of synchronism between the transmitter. Using the Gaussian approximation concept, the second and third term of the right-hand side of (2.19) can be considered as Gaussian random variables. This is true under the conditions that the number of K is large and all terms are independent and symmetrically distributed. Under these assumptions, it needs to evaluate only the mean and variance of (2.19) in order to obtain the bit error probability. One approach for evaluating the variance of the multiple-access noise is to find an expression for the cross and auto-correlation functions which model the multiple-access interference and to obtain the desired variance from that expression.

Assuming the data bits are equiprobable and following the concept of discrete aperiodic and continuous-time partial cross-correlation functions described in [17],[19], the total variance of the multiple-access interference and additional white noise as is :

$$\sigma^2 = \sum_{k=2}^{K} E[P_k^2]E[(b_k^{-1}R_{1k}(\tau_{1k}) + b_k^0\hat{R}_{1k}(\tau_{1k}))^2]E[(\cos\phi_{1k})^2] + E[(\eta_0)^2] \tag{2.35}$$

where $P_{1k} = \sqrt{\frac{P}{2}}$ for all transmitters. The main component in the summation are the cross-correlation value of the sequence codes $a_1(t)$ and $a_k(t)$. Note that the above equation is obtained based on the assumption that τ, ϕ and $b(k)$ are independent and symmetrically distributed. With the conditions that $\phi_{11} = 0$, $\tau_{11} = 0$ and P_k is normalized to 1, it obtains

$$SNR = \frac{1}{((K-1)/3N) + (N_o/2E_b)} \tag{2.36}$$

This material is reserved for educational use only, not allowed for commercial use.
Forbidden to modify the content, and cite the document when use.

This yields for the probability of bit error P_e:

$$P_e = Q\left[\left(\frac{1}{((K-1)/3N)+(N_o/2E_b)}\right)^{-1/2}\right] \tag{2.37}$$

Since the Gaussian approximation method seems to underestimate the value of P_e at low values of the number of simultaneous users and become optimistic when the values higher. R. K. Morrow[18] proposes a more accurate model called the Improved Gaussian Approximation method. An improved Gaussian approximation is based on the observation that the multiple-access is approximately Gaussian, conditioned on the delays and phases of all the interfering signals with the bit error probability

$$P_e = \int_0^\infty Q\left[\frac{N}{\sqrt{\psi}}\right] f_\Psi(\psi)d\psi \tag{2.38}$$

where

$$\Psi \equiv Var[MAI \mid S, \phi, B] \tag{2.39}$$

with the random vectors $S=(S_2,...,S_k);0 \le S_k \le T_c$ and $\Phi=(\Phi_2,...,\Phi_k);0<\Phi_k<2\pi$ are the delay and phases of the interfering signals. Note that the number of chips per bit, N, and the number of simultaneous users, K, are fixed. Ψ is given by

$$\Psi = \sum_{k=2}^{K} Z_k$$

where Z_k are identically distributed and conditionally independent given "B", with each Z_k specified by

$$Z_k = U_k V_K$$

$$U_k = 1+\cos(2\phi_k)$$

$$V_K = (2B+1)(S_k^2 - S_k)+N/2$$

where B is shown in (2.29). S_k and Φ_k are time and phase offsets relative to the signal for the desired user(user 1). The evaluation of bit error probability mainly involves in finding the densities of U_k and V_k conditioned on B which yields the conditional density

This material is reserved for educational use only, not allowed for commercial use.
Forbidden to modify the content, and cite the document when use.

of each Z_k $f_{z/B}(z)$; evaluating the $(k-2)$ convolution and taking the density of the total MAI variance with respect to B:

$$f_{\Psi}(z) = E[f_{z/B}(z) * \ldots * f_{z/B}(z)] \tag{2.40}$$

2.4.5 Performance of Time-synchronous DS-CDMA channel

The requirement at this point is to find the sequence for which the error probability $\Pr(r_i > 0 \mid b_k = -1)$ and $\Pr(r_i < 0 \mid b_k = +1)$ are small for all values of the parameter ϕ_k and (b_k^0, b_k^{-1}). Because of the time synchronous, the other users can no longer be treated as random processes, but rather as a sequence of binary random variables with random phase shift. Assume the maximum magnitude of the aperiodic cross-correlation, $\max\{|C_{l,k}(l)|\}; 1-N \le l \le N-1$ is $\psi_{\max}$, then the worst case or upper bound of bit error probability(BER) for any k-th receiver can be defined as

$$\Pr_{up} \le 1 - \Phi\left([1-(K-1)(2\psi_{\max}/N)]\sqrt{2E_b/N_o}\right) \tag{2.41}$$

where $\Phi(.)$ is the standard Guassian cumulative distribution function. This upper bound description is valid only when the period N of the code sequences is much larger than the number of users K. Otherwise the term $(K-1)2\psi_{\max}/N$ will be smaller than unity for only a few sequence delay, τ_k. In this case, the average value of the performance parameter is more appropriate.

In some system that number of K is not too large, it is possible to guarantee the system by setting the upper bound for the bit error probability with the maximum cross-correlation value $\psi_{\max}$. Then signal-to-interference plus noise ratio is :

$$SNR = \frac{1}{((K-1)\psi_{\max}^2/2) + (N_o/2E_b)} \tag{2.42}$$

In the system which K is large, it is more appropriate to use average error probability than guaranteed value. Apply the approximation of the cross-correlation of i.i.d PN sequence[4], equation (2.42) can be rewritten as

$$SNR = \frac{1}{((K-1)/2N) + (N_o/2E_b)} \tag{2.43}$$

This material is reserved for educational use only, not allowed for commercial use.
Forbidden to modify the content, and cite the document when use.

Another method to find the upper bound of bit error is by using Chernoff Bound(see Appendix B). This is the well-known bounding techniques for constant amplitude and phase signals, coherently demodulated in additive white Gaussian noise. From the appendix B, the Chernoff bound is in the form :

$$P_r(X > x) \le \exp(-\rho x) E[\exp(\rho X)] \tag{2.44}$$

For synchronous spread-spectrum CDMA with BPSK modulation, the output of the receiver is the summation of all signals defined as

$$Y = \sum_{n=1}^{N} y_n$$

Assume the system is completely synchronous and have identical chip timing, then,

$$y_n = \sqrt{P_1} b_1^l + \sum_{j=2}^{K} \sqrt{P_j} z_j^l + v_l \tag{2.45}$$

where z_j^l are the summation of the correlation of other-user spreading sequences. v_l is the background Gaussian noise. If the successive chips are independent and $b_1^l = -1$ for all i, the probability of bit error will be in the form;

$$P_e = P_r(Y > 0 \mid -1) < E\left[\exp\left(\rho \sum_{i=1}^{N} y_i\right)\right]$$

$$< \exp[-\rho N \sqrt{P_1}] \prod_{i=1}^{N} \left[E[\exp(\rho v_i)] \prod_{j=1}^{K} E[\exp(\rho \sqrt{P_j} z_j^i)] \right] \tag{2.46}$$

with $\rho > 0$. Assume further that each inferring user chip has amplitude $\pm\sqrt{P_j}$ and phase $\phi_i = \phi_j - \phi_1; j \neq 1$, which are binomial and uniform random variable, respectively. Thus,

$$E[\exp(\rho \sqrt{P_j} z_j^i) \mid \phi_i] = \frac{1}{2}[\exp(\rho \sqrt{P_j} \cos\phi_i) + \exp(-\rho \sqrt{P_j} \cos\phi_i)] \tag{2.47}$$

Since ϕ_i is a uniformly distributed random variable on $(0, 2\pi)$, thus

$$E[\exp(\rho \sqrt{P_j} z_j^i)] = I_o(\rho \sqrt{P_j})$$

$$< \exp(\frac{\rho^2 \sqrt{P_j}}{4}) \tag{2.49}$$

This material is reserved for educational use only, not allowed for commercial use.
Forbidden to modify the content, and cite the document when use.

where $I_o(\rho\sqrt{P_j}) \triangleq \frac{1}{2\pi}\int_0^{2\pi}\exp(x\cos\phi)d\phi$ is the zeroth-order modified Bessel function.

2.5 Simulation Model

Construction of the simulation model is completed by specifying all the system assumption presented in the previous section. However, the assumption concerning the real-time events can be relaxed. This can be obviously seen when trying to deal with short-term fading (Rayleigh fading) which will be described in detail in the next chapter. Figure 2.6 and Figure 2.7 illustrate the simulation model built by simulation program. The receiver is assumed to be able to lock onto the total phase of the desired user. No result of multipath or envelope fading is concerned until the next chapter. Results obtain from the model are shown in Figures 2.8-2.10. Figure 2.8 illustrates the simulation results and the comparison between Gaussian Approximation and Improved Gaussian method. The curves show bit error probability for ideal BPSK versus E_b/N_o in dB. It can be seen from the figure that the simulation results close to the curve of Improved Guassian method. Figure 2.9-2.10 illustrate the probability of bit error versus various number of users with *N=31* and *63*, respectively. The plots also show the comparison between two methods as a function of the number of users.

In the next chapter, this model will be modified and used to model the system operated in the impaired environment.

This material is reserved for educational use only, not allowed for commercial use.
Forbidden to modify the content, and cite the document when use.

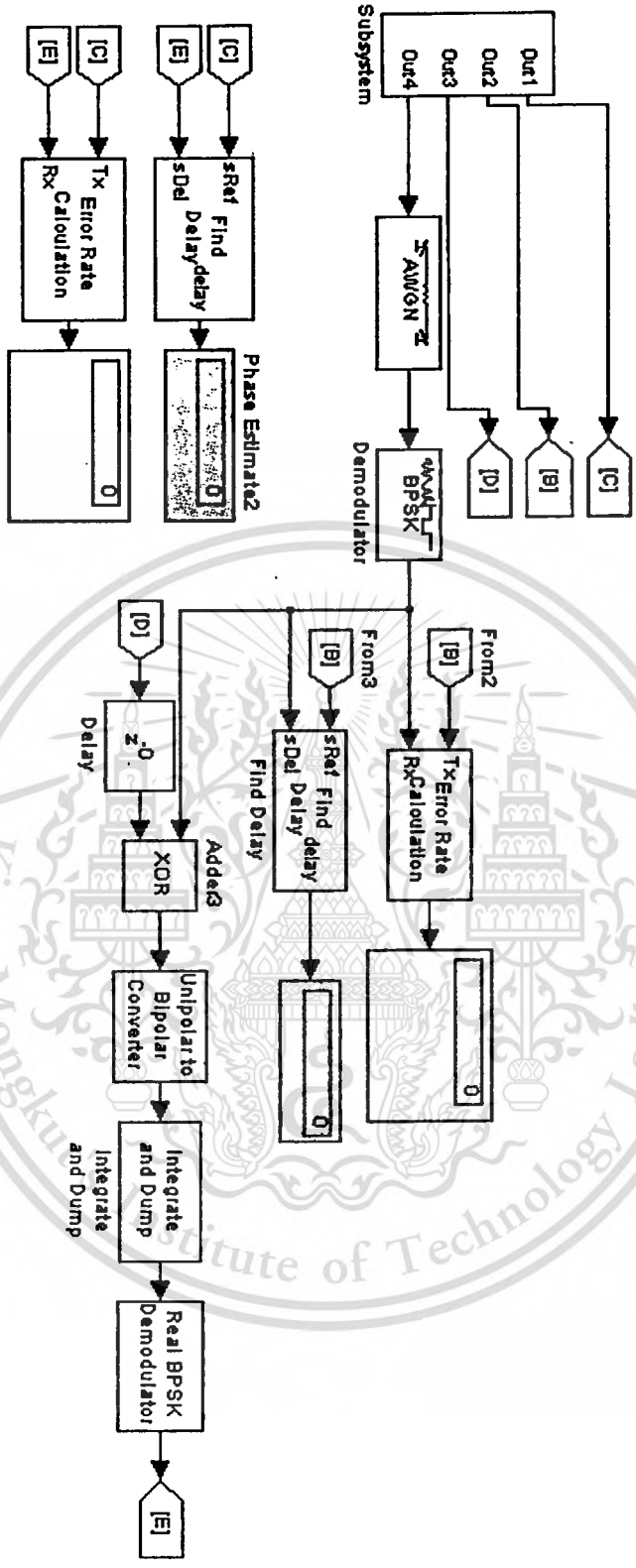

Figure 2.6 System Model(Ideal Channel)

This material is reserved for educational use only, not allowed for commercial use.
Forbidden to modify the content, and cite the document when use.

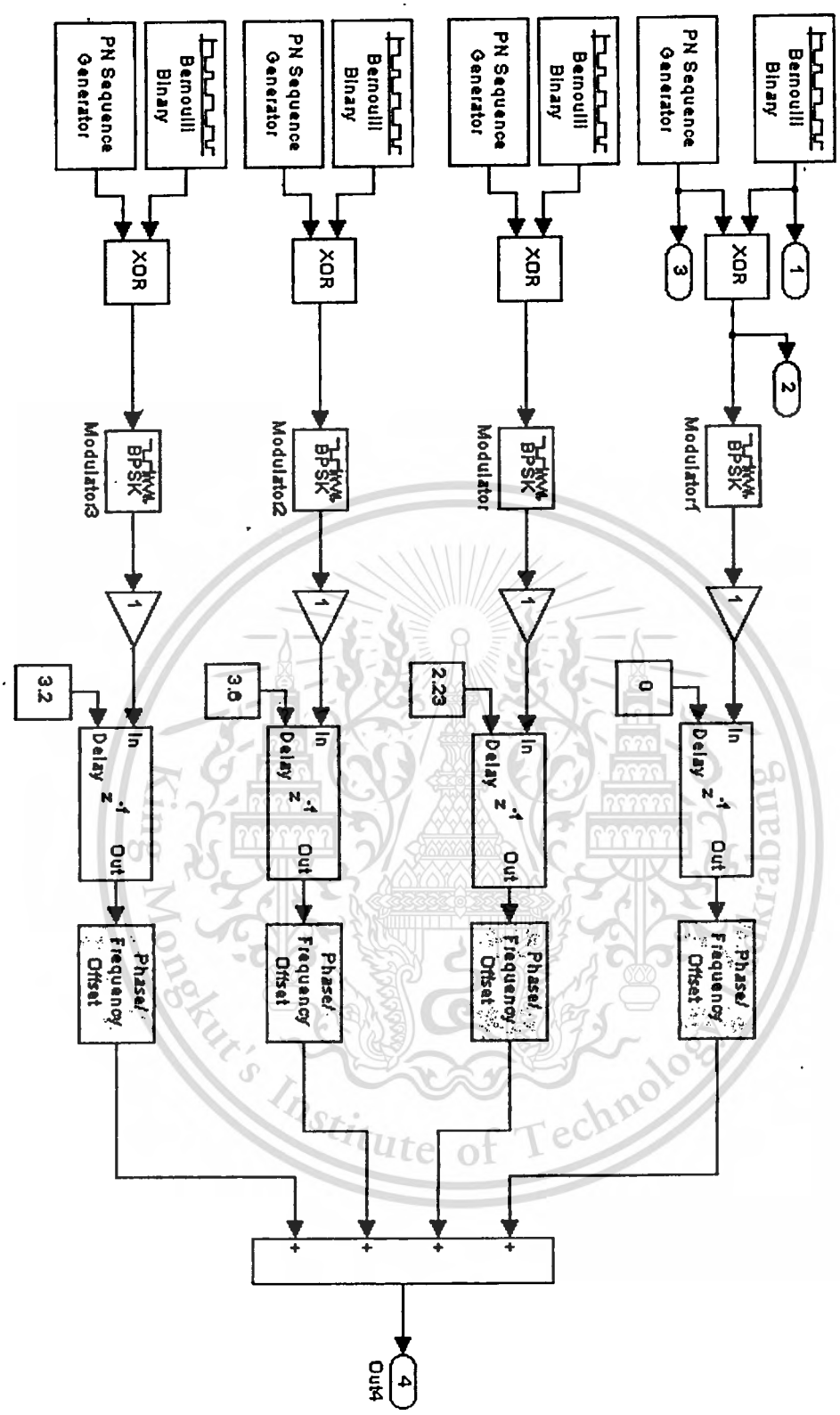

Figure 2.7 Subsystem

This material is reserved for educational use only, not allowed for commercial use.
Forbidden to modify the content, and cite the document when use.

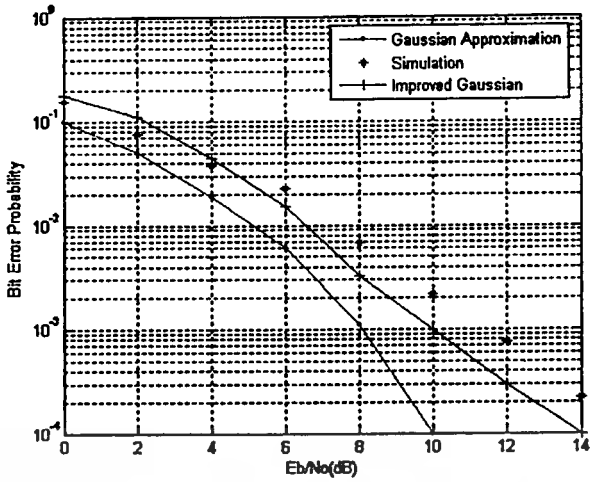

Figure 2.8 Ideal Channel

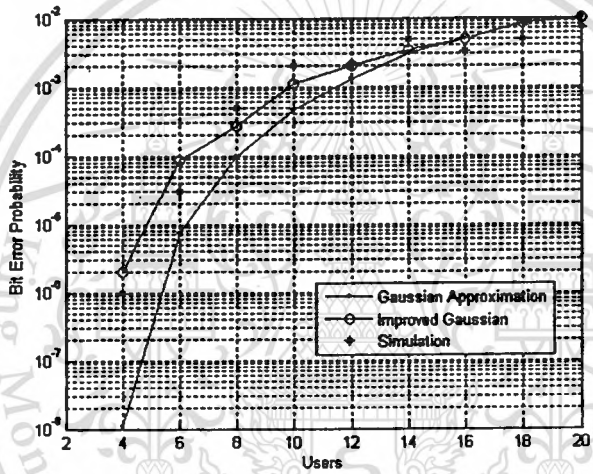

Figure 2.9 Bit error Probability versus #users with *N=31*

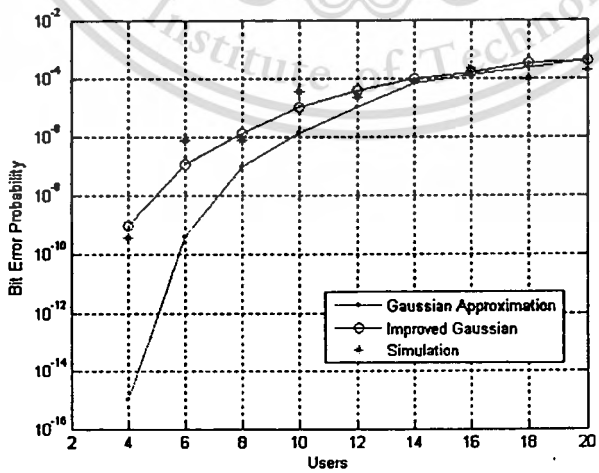

Figure 2.10 Bit error Probability versus #users with *N=63*

This material is reserved for educational use only, not allowed for commercial use.
Forbidden to modify the content, and cite the document when use.

Chapter 3

Land-Mobile Satellite Communication

3.1 Channel Characteristic

One usually infers that the signal attenuation versus distance behaves as if propagation takes place over ideal free space. The model of free space treats the region between the transmit and receive antennas as being free of all objects that might absorb or reflect radio frequency (RF) energy. It also assumes that, within this region, the atmosphere behaves as a perfectly uniform and nonabsorbing medium. Furthermore, the earth is treated as being infinitely far away from the propagating signal (or, equivalently, as having a reflection coefficient that is negligible). Basically, in this idealized free-space model, the attenuation of RF energy between the transmitter and receiver behaves according to an inverse-square law. The received power expressed in terms of transmitted power is attenuated by a factor, $L_s(d) = \left(\frac{4\pi d}{\lambda}\right)^2$, where d is the distance between the transmitter and the receiver, and λ is the wavelength of the propagating signal. This factor is called *path loss* or *free space loss.* For this case of idealized propagation, received signal power is very predictable. For most practical channels, where signal propagation takes place in the atmosphere and near the ground, the freespace propagation model is inadequate to describe the channel and predict system performance. In a wireless mobile communication system, a signal can travel from transmitter to receiver over multiple reflective paths; this phenomenon is referred to as *multipath* propagation. The effect can cause fluctuations in the received signal's amplitude, phase, and angle of arrival, giving rise to the terminology *multipath fading.* Multipath fading generally occurs when the transmitted signal is received not only via the direct path(LOS) component, but also after being reflected from objects during propagation.

It can be categorized into two types of fading effects that characterize mobile communications: large-scale and small-scale fading. Large-scale fading represents the average signal power attenuation or path loss due to motion over large areas. This phenomenon is affected by prominent terrain contours (hills, forests, billboards, clumps of buildings, etc.) between the transmitter and receiver. The receiver is often

This material is reserved for educational use only, not allowed for commercial use.
Forbidden to modify the content, and cite the document when use.

represented as being "*shadowed*" by such prominences. The statistics of large-scale fading provide a way of computing an estimate of path loss as a function of distance. This is described in terms of a log-normally distributed variation about the mean. Small-scale fading refers to the dramatic changes in signal amplitude and phase that can be experienced as a result of small changes (as small as a half-wavelength) in the spatial separation between a receiver and transmitter. Small-scale fading manifests itself in two mechanisms, namely, time-spreading of the signal (or signal dispersion) and time-variant behavior of the channel. For mobile radio applications, the channel is time-variant because motion between the transmitter and receiver results in propagation path changes. The rate of change of these propagation conditions accounts for the fading rapidity (rate of change of the fading impairments). Small-scale fading is also called Rayleigh fading because if the multiple reflective paths are large in number and there is no line-of-sight signal component, the envelope of the received signal is statistically described by a Rayleigh pdf. When there is a dominant nonfading signal component present, such as a line-of-sight propagation path, the small scale fading envelope is described by a Rician pdf. The nonfaded component is called the specular component. A mobile radio roaming over a large area must process signals that experience both types of fading: small-scale fading superimposed on large-scale fading. As the amplitude of the specular component approaches zero, the Rician pdf approaches a Rayleigh pdf, expressed as

$$p(r) = \begin{cases} \frac{r}{\sigma^2} \exp\left[-\frac{r^2}{2\sigma^2}\right] & ;r \geq 0 \\ 0 & otherwise \end{cases} \qquad (3.1)$$

where r is the envelope amplitude of the received signal, and $2\sigma^2$ is the predetection mean power of the multipath signal. The Rayleigh faded component is sometimes called the random or scatter or diffuse component. The Rayleigh pdf results from having no specular component of the signal; thus, for a single link it represents the pdf associated with the worst case of fading per mean received signal power. For the remainder of this article, it will be assumed that loss of signal-to-noise ratio (SNR) due to fading follows the Rayleigh model described.

The simple way to model the fading phenomenon was introduced by Bello [20] in 1963; he proposed the notion of wide-sense stationary uncorrelated scattering (WSSUS). The model treats signal variations arriving with different delays as

This material is reserved for educational use only, not allowed for commercial use.
Forbidden to modify the content, and cite the document when use.

uncorrelated. It can be shown [20] that such a channel is effectively WSS in both the time and frequency domains. With such a model of a fading channel, Bello was able to define functions that apply for all time and all frequencies. The term "time delay" is also used to refer to the excess delay. It represents the signal's propagation delay that exceeds the delay of the first signal arrival at the receiver. For a typical wireless channel, the received signal usually consists of several discrete multipath components. Note that, for making measurements of the multipath intensity profile, wideband signals (impulses or spread spectrum) need to be used. For a single transmitted impulse, the time T_m, between the first and last received component represents the maximum excess delay, during which the multipath signal power falls to some threshold level below that of the strongest component. The relationship between maximum excess delay time, T_m, and symbol time, T_s, can be viewed in terms of two different degradation categories, frequency-selective fading and frequency nonselective or flat fading. A channel is said to exhibit frequency-selective fading if $T_m > T_s$. This condition occurs whenever the received multipath components of a symbol extend beyond the symbol's time duration. Such multipath dispersion of the signal yields the same kind of intersymbol interference (ISI) distortion caused by an electronic-filter. In fact, another name for this category of fading degradation is channel-induced ISI. In the case of frequency-selective fading, mitigating the distortion is possible because many of the multipath components are resolvable by the receiver. A channel is said to exhibit frequency nonselective or flat fading if $T_m < T_s$ In this case, all the received multipath components of a symbol arrive within the symbol time duration; hence, the components are not resolvable. Here, there is no channel-induced IS1 distortion, since the signal time spreading does not result in significant overlap among neighboring received symbols. There is still performance degradation since the unresolvable phasor components can add up destructively to yield a substantial reduction in SNR. Also, signals that are classified as exhibiting flat fading can sometimes experience frequency-selective distortion. This will be explained later when viewing degradation in the frequency domain, where the phenomenon is more easily described. For loss in SNR due to flat fading, the mitigation technique called for is to improve the received SNR (or reduce the required SNR). For digital systems, introducing some form of signal diversity and using error-correction coding is the most efficient way to accomplish this.

Two major components needed to be considered are the coherence time and coherence bandwidth. Coherence time, T_o, is a measure of the expected time duration

This material is reserved for educational use only, not allowed for commercial use.
Forbidden to modify the content, and cite the document when use.

over which the channel's response is essentially invariant. Coherence bandwidth, f_o, is a statistical measure of the range of frequencies over which the channel passes all spectral components with approximately equal gain and linear phase. Thus, the coherence bandwidth represents a frequency range over which frequency components have a strong potential for amplitude correlation. That is, a signal's spectral components in that range are affected by the channel in a similar manner as, for example, exhibiting fading or no fading. Note that f_o and T_m, are reciprocally related (within a multiplicative constant). As an approximation, it is possible to write that $f_o \oplus T_m$. The maximum excess delay, T_m, is not necessarily the best indicator of how any given system will perform on a channel because different channels with the same value of T_m, can exhibit very different profiles of signal intensity over the delay span.

A channel is referred as frequency-selective if $f_o < 1/T_s$, where the symbol rate, $1/T_s$, is nominally taken to be equal to the signal bandwidth W. In practice, W may differ from $1/T_s$, due to system filtering or data modulation type (quaternary phase shift keying, QPSK, minimum shift keying, MSK, etc.) [21]. Frequency-selective fading distortion occurs whenever a signal's spectral components are not all affected equally by the channel. Some of the signal's spectral components, falling outside the coherence bandwidth, will be affected differently (independently) compared to those components contained within the coherence bandwidth. This occurs whenever $f_o < W$. Frequency-nonselective or flat fading degradation occurs whenever $f_o < W$. Hence, all of the signal's spectral components will be affected by the channel in a similar manner (e.g., fading or no fading). Flat-fading does not introduce channel-induced ISI distortion; but performance degradation can still be expected due to loss in SNR whenever the signal is fading. In order to avoid channel induced ISI distortion, the channel is required to exhibit flat fading by ensuring that $f_o < W = 1/T_s$. Hence, the channel coherence bandwidth f_o sets an upper limit on the transmission rate that can be used without incorporating an equalizer in the receiver.

For mobile applications, the channel is time-variant because motion between the transmitter and receiver results in propagation path changes. Thus, for a transmitted continuous wave (CW) signal, as a result of such motion, the receiver sees variations in the signal's amplitude and phase. Assuming that all scatterers making up the channel are stationary, whenever motion ceases, the amplitude and phase of the received signal remains constant; that is, the channel appears to be time invariant. Whenever the motion

This material is reserved for educational use only, not allowed for commercial use.
Forbidden to modify the content, and cite the document when use.

begins again, the channel once again appears time-variant. Since the channel characteristics are dependent on the positions of the transmitter and receiver, time variance in this case is equivalent to spatial variance.

The time-variant nature of the channel can be viewed in terms of two degradation categories, fast fading and slow fading. The terminology "fast fading" is used to describe channels in which $T_o < T_s$, where T_o is the channel coherence time and T_s, is the time duration of a transmission symbol. Fast fading describes a condition where the time duration in which the channel behaves in a correlated manner is short compared to the time duration of a symbol. Therefore, it can be expected that the fading character of the channel will change several times while a symbol is propagating, leading to distortion of the baseband pulse shape. Analogous to the distortion previously described as channel induced ISI, here distortion takes place because the received signal's components are not all highly correlated throughout time. Hence, fast fading can cause the baseband pulse to be distorted, resulting in a loss of SNR that often yields an irreducible error rate. Such distorted pulses cause synchronization problems (failure of phase-locked-loop receivers), in addition to difficulties in adequately defining a matched filter. A channel is generally referred to as introducing slow fading if $T_o > T_s$, Here, the time duration that the channel behaves in a correlated manner is long compared to the time duration of a transmission symbol. Thus, one can expect the channel state to virtually remain unchanged during the time in which a symbol is transmitted. The propagating symbols will likely not suffer from the pulse distortion described above. The primary degradation in a slow-fading channel, as with flat fading, is loss in SNR.

In satellite and land mobile communication, the systems always suffer from great variations of the received signal power due to multipath fading and signal shadowing. Due to the various different surroundings and propagation distance, multipath signals can results in deep fade and fluctuation. In case that the spread spectrum users implement pseudorandom sequences with duration T_c, each multipath signals can be distinguished if they are mutually separated by delays greater than T_c Shadowing occurs because the transmitted signal is reflected and refracted by buildings, bridges, trees or other different terrains, so that it is replicated at the receiver with several time delays, and results in attenuation over the total signal bandwidth. It is desirable for the mobiles or users to boost their transmitted power to compensate the shadow effect when

This material is reserved for educational use only, not allowed for commercial use.
Forbidden to modify the content, and cite the document when use.

they move into the shadowing terrain. In low earth orbiting satellite(LEOS) system, such a closed loop power control is not effective due to the large round trip time delay. This is instead required some degree of power margin in order to ensure that shadowed users do not experience an unacceptably large percentage of performance outages. This power margin can be applied so that shadowed users achieve the same average probability of error as the unshadowed users, or, with a smaller margin, that shadowed users realize some degraded, but still acceptable performance.

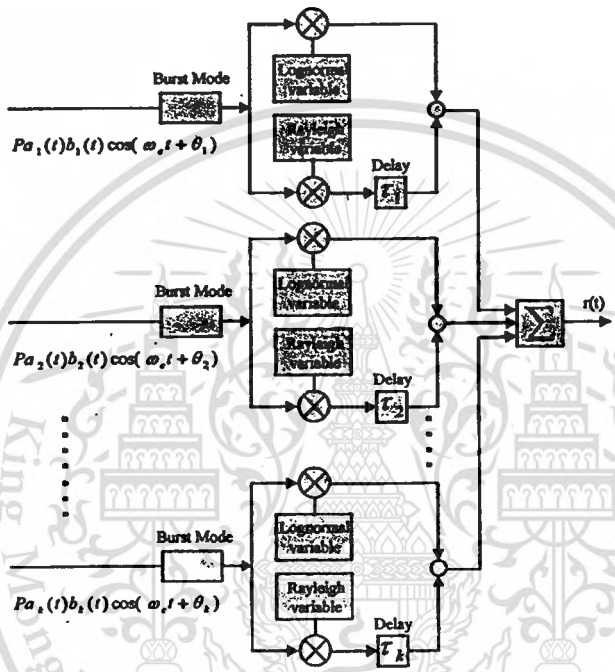

Figure 3.1 Model of Fading Channel

It is widely admitted that the received signal consists of a shadowed line-of-sight signal with a lognormal envelope distribution plus a sum of multipath signals with a Rayleigh distributed envelope as shown in Figure 3.1. These two random processes are assumed to be correlated and can be considered as the sum of two random phasors [22]

$$\mathrm{Re}^{j\theta} = ze^{j\phi_o} + \rho e^{j\phi} \tag{3.2}$$

where $ze^{j\phi_o}$ and $\rho e^{j\phi}$ represent the envelope distribution of shadowed signal and multipath signals, respectively. Note that the phase ϕ_o and ϕ must be uniformly distributed between $[0,2\pi]$. When no shadowing signal is present, the multipath signal is superimposed on the direct path signal, which simply forming a Rician vector [22],

This material is reserved for educational use only, not allowed for commercial use.
Forbidden to modify the content, and cite the document when use.

$$p(r/z)=\frac{2r}{\alpha}\exp(-(r^2+z^2)/\alpha)\mathrm{I}_o(\frac{2rz}{\alpha}) \tag{3.3}$$

where α is the variance of multipath components. $\mathrm{I}_o(.)$ is the modified Bessel function of zeroth order. Applying the total probability, the random amplitude envelope could be found by[22]

$$p(r)=\frac{2r}{\alpha}\int_0^\infty \exp(-(r^2+z^2)/\alpha)\mathrm{I}_o(\frac{2rz}{\alpha})p(z)dz \tag{3.4}$$

Since the z is assumed to be a lognormal distributed variable given by,

$$p(z)=\frac{1}{\sqrt{2\pi d}z}\exp[-(\ln z-\mu)^2/2d] \tag{3.5}$$

where d and μ are the variance and mean due to the lognormal component(shadowing).

The probability distribution of the total signal envelope(r) is [22],[23]

$$p(r)=\begin{cases}\dfrac{1}{\sqrt{2\pi d}}\exp[\dfrac{-(\ln r-\mu)^2}{2d}] & \text{for } r>>\sqrt{\alpha}\\ \dfrac{2r}{\alpha\sqrt{2\pi d}}\displaystyle\int_0^\infty\frac{1}{z}\exp[(-(\ln z-\mu)^2/2d)-(r^2+z^2)/\alpha]\mathrm{I}_o(\frac{2rz}{\alpha})dz & \text{for } r\approx\sqrt{\alpha}\\ \dfrac{2r}{\alpha}\exp(\dfrac{-r^2}{\alpha}) & \text{for } r<<\sqrt{\alpha}\end{cases} \tag{3.6}$$

This model is valid for a narrowband system which the spread-spectrum modulation is used with a chip duration less than the delay spread of the channel,

The probability density function of the received signal phase(ϕ) was found to be approximately Gaussian[23] :

$$P(\phi)=\frac{1}{\sqrt{2\pi\sigma_\phi^2}}\exp[\frac{-(\phi-\mu_\phi)^2}{2\sigma_\phi^2}] \tag{3.7}$$

where μ_ϕ and σ_ϕ^2 are the mean and variance of the received signal phase, respectively.

This material is reserved for educational use only, not allowed for commercial use.
Forbidden to modify the content, and cite the document when use.

3.2 Model of DS-CDMA over impaired channel

If the desired user is user 1, the model of received signal in term of the effect of multipath is given [18],[29] by

$$r_1(t) = b_1(t)T_b P_{11}\cos\phi_{11}$$

$$+\sum_{m=2}^{M} P_{m1}(b_1^{-1}R_{11}(\tau_{m1}) + b_1^0\hat{R}_{11}(\tau_{m1}))\cos\phi_{m1} + \sum_{k=2}^{K}\sum_{m=2}^{M} P_{mk}(b_k^{-1}R_{1k}(\tau_{mk}) + b_k^0\hat{R}_{mk}(\tau_{mk}))\cos\phi_{mk} + \eta_o \tag{3.8}$$

where m denotes the possible propagation paths. Assume that M is large and there are no predominant path except for $M=1$. P_{mk} has a shadowed Rician distribution for $m=1$, and a Rayleigh distribution otherwise. $b_k(t)$ is the sequence of independent and identically distributed random binary data. The carrier phase ϕ_{mk} is the Gaussian variable for the main path(m=1) of the desire user, but become the uniformly distributed random variable over $(0,2\pi)$ for other paths. k denotes the user who transmits this signal. Random variable η_o is Gaussian noise with two-sided spectral density (zero mean) and variance σ_0^2. $R_{1,k}$ and $\hat{R}_{1,k}$ are the continuous-time partial cross-correlation functions defined by:

$$R_{1,k}(\tau) = \int_0^{} a_1(t)a_k(t-\tau)dt \tag{3.9a}$$

$$\hat{R}_{1,k}(\tau) = \int_{\tau}^{T_b} a_1(t)a_k(t-\tau)dt \tag{3.9b}$$

for $0 \le \tau \le T_c$. $a_k(t)$ is a spectral-spread PN sequence which is generated at a period of N chips. θ_k is carrier phase. If T_c is the chip duration of PN sequence, NT_c represents one period of user data bit(T_b).

When $m=1$, it is the line-of-sight and its propagation statistics are described by (3.6) and (3.7). When $m>1$, they have a Rayleigh distribution and uniformly distributed phase. The parameters of the various path distributions can be found if power-delay profile is known. The power-delay profile can be described as

$$P(\tau) = \frac{c\alpha}{2}\exp(-c\tau) \tag{3.10}$$

This material is reserved for educational use only, not allowed for commercial use.
Forbidden to modify the content, and cite the document when use.

where 1/c is the delay spread and τ is the delay time. The correlation operation will be used to find the power of path *m*. Assuming the multipath power delay profile is exponential, then

$$b_m = \int_{m1}^{m2} \frac{c\alpha}{2} \exp(-c\tau) d\tau$$

$$b_m = -\frac{\alpha}{2}[\exp(-cmT_c) - \exp(-c(m-1)T_c]$$

$$b_m = -\frac{\alpha}{2}[1 - \exp(-cT_c)]\exp(-c(m-1)T_c) \quad (3.11)$$

3.2.1 Performance analysis : Bit error probability

Assume that the data bits -1 and 1 are equiprobable and the number of users(K) and multipath(M) are large, the bit error probability P_e can be approximated by Gaussian noise as

$$P_e = 0.5 \int_0^\infty erfc\left(\frac{xT_b}{\sigma\sqrt{2}}\right) p_t(x) dx \quad (3.12)$$

where erfc(.) is the complementary error function. $p_t(x)$ is the distribution of the signal envelope defined by

$$p_t(x) = 2\int_{x1}^{\infty} p(r)p(\phi)\left(\frac{\arccos(x/r)}{\sqrt{r^2 - x^2}}\right) dr \quad (3.13)$$

substituting $p(r)$ and $p(\phi)$, then

$$p_t(x) = \int_{x1}^{\infty}\int_0^{\infty} \frac{2r}{\alpha\sqrt{2\pi^2 d\sigma_\phi^2}} \exp\left(-\frac{(\ln z - \mu)^2}{2d} - \frac{(r^2 + z^2)}{\alpha} - \frac{\arccos^2(x/r)}{2\sigma_\phi^2}\right) \frac{I_o(2rz/\alpha)}{z\sqrt{r^2 - x^2}} dz dr \quad (3.14)$$

σ^2 is the total variance of the Gaussian noise defined by $\sigma^2 = \sigma_i^2 + E[(\eta_o)^2]$, where

$$\sigma_i^2 = \sum_{m=2}^{M} E[(b_1^{-1} R_{11}(\tau_{m1}) + b_1^0 \hat{R}_{11}(\tau_{m1}))^2] E[(P_{m1}\cos\phi_{m1})^2]$$

$$+ \sum_{k=2}^{K}\sum_{m=2}^{M} E[(b_k^{-1} R_{1k}(\tau_{mk}) + b_k^0 \hat{R}_{mk}(\tau_{mk}))^2] E[(P_{mk}\cos\phi_{mk})^2] + E[(\eta_o)]^2 \quad (3.15)$$

This material is reserved for educational use only, not allowed for commercial use.
Forbidden to modify the content, and cite the document when use.

If $m=1$, then P_{1k} has a shadowed Rician distribution, which can be viewed as a Rician distribution with a Rician parameter s^2/α. The product of this Rician variable with the cosine of a uniformly distributed variable gives a Gaussian variable with a mean of $s/\sqrt{2}$ and a variance of $\alpha/2$. The average value can be obtained as :

$$E[(P_{1k}\cos\phi_{1k})^2] = \int_0^\infty (b_1 + s^2/2)P(s)ds \tag{3.16}$$

Then the results obtained from the integration is:

$$E[(P_{1k}\cos\phi_{1k})^2] = b_1 + 0.5\exp(2d + 2\mu) \tag{3.17}$$

If m>1, then P_{mk} has a Rayleigh distribution which s=0 and

$$E[(P_{mk}\cos\phi_{mk})^2] = b_m \tag{3.18}$$

3.2.2 State Probability

As indicated in the last section, when the mobile or satellite moving into shadowed area where the multipath fading also exist, the multipath signal envelope which is a high-frequency process is superimposed on the low-frequency shadowing process(long-term fading). To moderate the effect of long-term fading, a margin is assigned to users when they are passing fading region. This can be achieved by recording the data related to satellite angle and the area of which the satellite passing through. This research concentrates on a comparable case when a signal x dBm oscillating by w dB around area median(m dBm) of fading, $x=m+w$. If assumed that w is the combined result of the short-term Rayleigh variation(y) in dB around its short-term median and the Gaussian variation from the short-term median around the long-term median, $w = y + \beta_w$. Refer to the general concepts that the cumulative distribution for the sum of random variables $z=a+b$ is given by[24],

$$P(z) = \int_{-\infty}^{\infty} P(z-b)p(b)db$$

then, the probability that the envelope level does not cross a specified level W dB below long-term margin is

$$P_w = \int_{-\infty}^{w} \frac{\exp(-w^2/2\sigma_L^2)\exp(10^{0.1\beta_w})dw}{\sigma_L\sqrt{2\pi}} \tag{3.19}$$

This material is reserved for educational use only, not allowed for commercial use.
Forbidden to modify the content, and cite the document when use.

while σ_L is the standard deviation of Gaussian distribution and β_w is the fade depth in dB from the short-term median(fade depth factor). Note that this equation is calculated based on the assumption that the short-term fluctuation and long-term fading variables are statistically independent [25].

3.2.3 Average Fade Duration(AFD)

According to Castro [26], AFD is defined by the equation

$$AFD = \frac{1}{N_w(w)} \int_0^w f_w(w)dw - \frac{P_w}{N_w(w)} \tag{3.20}$$

Where $N_w(W)$ is the level crossing rate defined as the expected rate at which the envelope crosses a specific signal envelope with the negative slope (downward LCR), and P_w is the cumulative distribution function given in (3.19).

3.3. Results

This section presents numerical and simulation results for channel performance under various conditions. Since β_w depend strongly on shadow characteristic as well as long-term margin, β_w will be treated as the key parameter. To evaluate channel behavior in different circumstance, four environmental conditions obtained from the experiment results recoded in [27] are rearranged in Table 3.1.

Figure 3.2 illustrates the guaranteed probability of error as a function of received signal variance under short-term fading. The results obtained from the figure are the upper bound probability of bit error in case of clear sky and impaired link. With the condition that each user has been assigned margin to compensate long-term fading, the mean signal gain (μ_L) is applied with 0 and -3 dB, the number of user K=10 and M=5 for each user. Since -3 dB signal gain below threshold causes small effect on channel performance, variance (σ_R^2) related to short-term variation can be viewed as a major factor. Figure 3.2 illustrates

This material is reserved for educational use only, not allowed for commercial use.
Forbidden to modify the content, and cite the document when use.

Table 3.1 Channel Parameters by Measurement

Parameters	μ_L (dB)	σ_L (dB)	σ_R (dB)
1	-12.9	5.0	11.9
2	-11.8	4.0	9.3
3	-8.8	3.8	11.7
4	-7.7	6.0	11.9

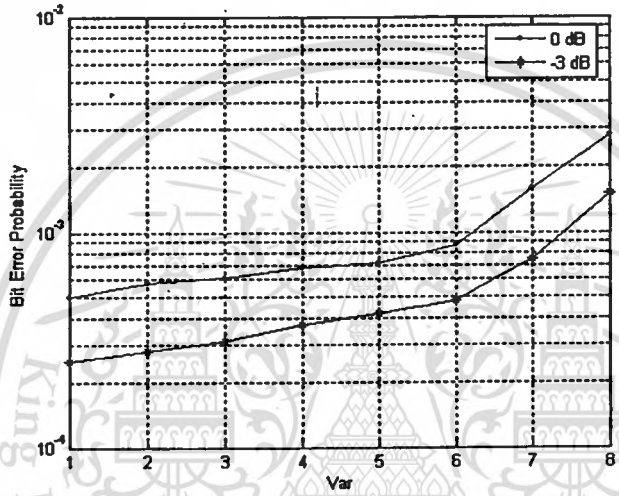

Figure 3.2 P_e versus received signal variance for μ_L=0 dB and μ_L=-3 dB

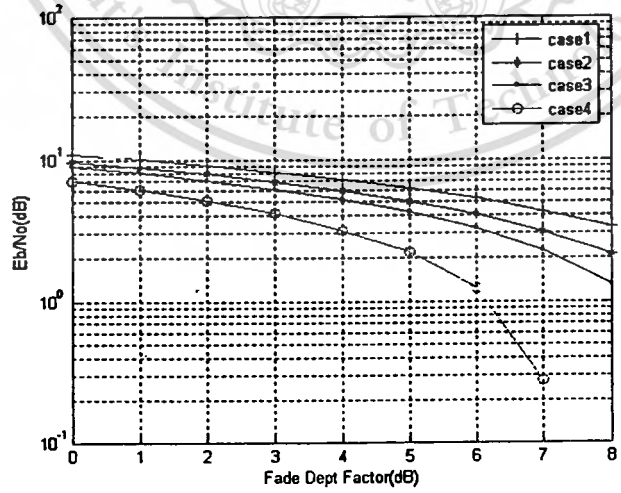

Figure 3.3 E_b/N_o versus β_w for channel parameter of case 1 - case 4

In Figure 3.3, results of E_b/N_o versus σ_R^2 for the channel parameter defined in Table 3.1 show the relation between signal gain due to fading E_b/N_o. Parameters use in the

This material is reserved for educational use only, not allowed for commercial use.
Forbidden to modify the content, and cite the document when use.

experiment are *K=10, M=5* and *N=127*. The curve indicated that σ_R^2 is likely to dominate the SNR while μ_L has the least effect. According to the results plotted in Figure 3.2, σ_R^2 may be used as an indicator of the channel behavior. If statistic information of each region was known, we would have important parameter such average fade duration (AFD) as a referent data in associate with the specified threshold envelope. This can be done when momentary fade duration is assumed to exceed two consecutive packets. To compare the simulation results with numerical ones, 4 different channel parameters shown in Table 3.2 are used. These values are firstly evaluated by [28] and reproduced by [29]. The diagram of simulation model is shown in Figure 3.4.

Using (3.14) with Guassian integration and Newton-Cotes techniques, the bit error probability is obtained and plotted in Figures 3.5-3.13. All numerical parameters are the same as that used in [28] with T_c=1e-6 sec, $1/T_b$=2400 b/s, N=4095 and k=1 for Figure 3.6,3.9 and 3.11. Numerical and simulation results show that the spread spectrum modulation yields better performance than narrow band modulation for light and average shadowing. For heavy shadowing, the performance is worst. The reason is that for light and average shadowing most of the signal power is received via the direct path, so if the multipath power is reduced by the use of spread spectrum feature, a less perturbed signal will be obtained. In the case of heavy shadowing, the direct path power is much smaller than the mutipath power, resulting in an approximately Rayleigh faded signal. The use of spread spectrum modulation now decreases the total signal power considerably, with the result that the bit error increases.

Table 3.2 Channel parameters by numerical method.

Parameters	Light	Average	Heavy
$\alpha/2$	0.158	0.126	0.0631
μ_L	0.155	-0.115	-3.91
$\sqrt{d}$	0.115	0.161	0.806
σ_R	0.36	0.45	0.52

In case that the transition threshold at lower of fade depth factor (higher value of E_b/N_o) is selected, the probability that signal fluctuation will be kept within threshold

Forbidden to modify the content, and cite the document when use.

level and probability of bit error(derived from Gaussian approximation method) increased, but duration of fade is also extended. Long fade duration tend to obscure the received information and higher order of FEC is required to improve system performance in this state. The results obtained from Figure 3.2 to Figure 3.13 can be concluded by following iteration route

$$.... \Rightarrow P_E \Rightarrow \beta_w \Rightarrow P_w \Rightarrow \frac{E_b}{N_0} \Rightarrow P_E \Rightarrow \beta_w \Rightarrow P_w \Rightarrow \frac{E_b}{N_0} \Rightarrow ....$$

which are bounded by P_E.

Table 3.3 Different phases by numerical method.

Parameters	Light	Average	Heavy
σ_ϕ(NB)	0.40	0.14	0.023
σ_ϕ(SS)	0.47	0.16	0.018
$\alpha/2$(SS)	1.55	1.42	0.009

When bit error probability(P_E) is known, the simplest method to derive packet error probability is by following equation

$$P_{pkt} = \sum_{i=0}^{x} [\frac{L}{i}](P_E)^i(1-P_E)^{L-i}$$

where L is the number of bit in a packet.

Based on above, designer can design point of alarm based on "x" error bit within a received packet in accordance with AFD. Range of both x and AFD are limited by means of upper-bounded P_E.

This material is reserved for educational use only, not allowed for commercial use.
Forbidden to modify the content, and cite the document when use.

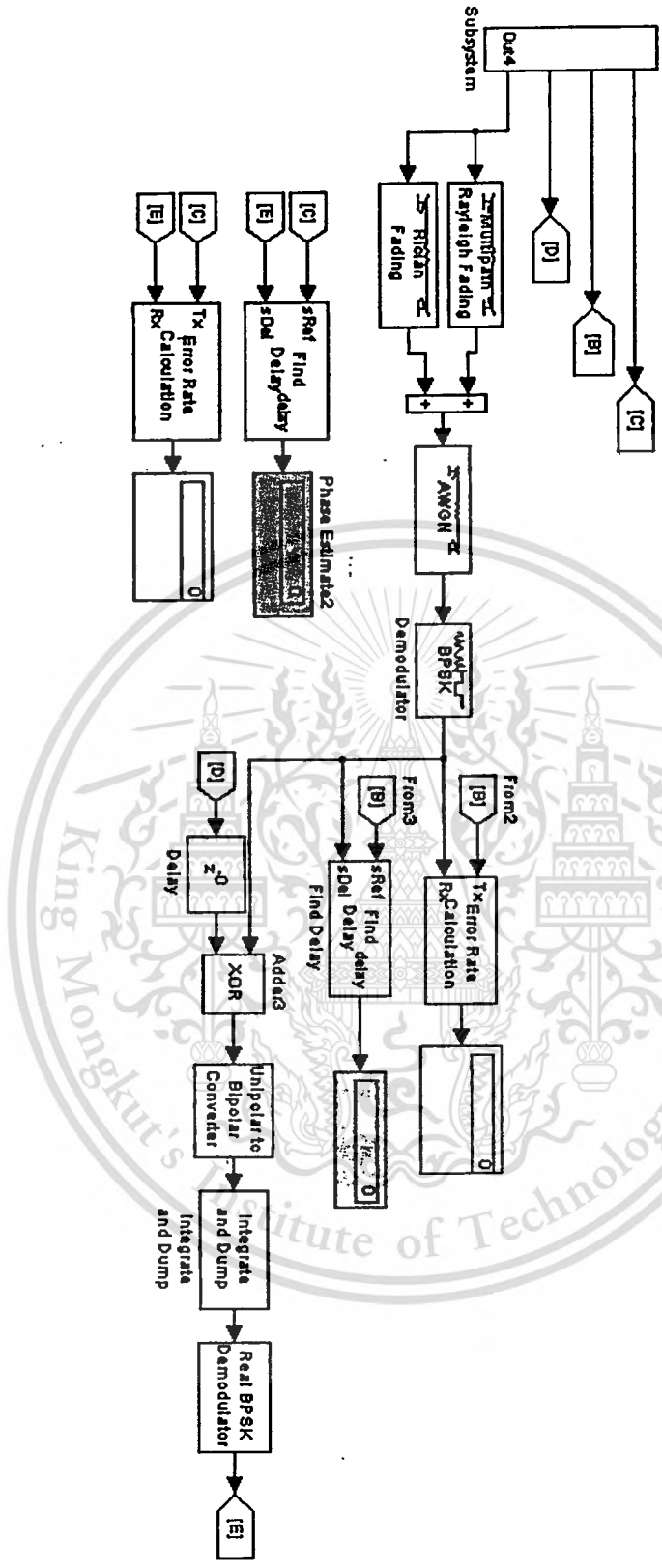

Figure 3.4 Simulation model for impair environment channel

This material is reserved for educational use only, not allowed for commercial use.
Forbidden to modify the content, and cite the document when use.

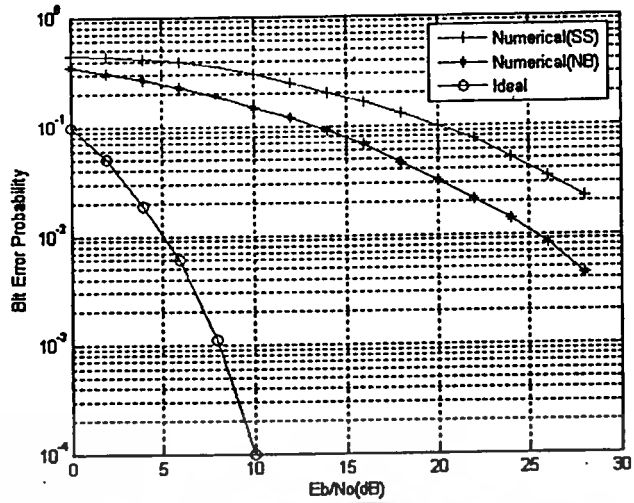

Figure 3.5 Performance on Heavy Shadowed area.

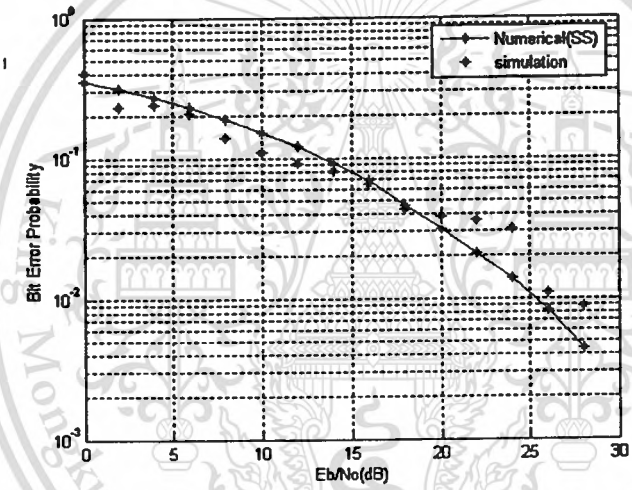

Figure 3.6 Comparison between numerical and simulation on Heavy Shadowed area

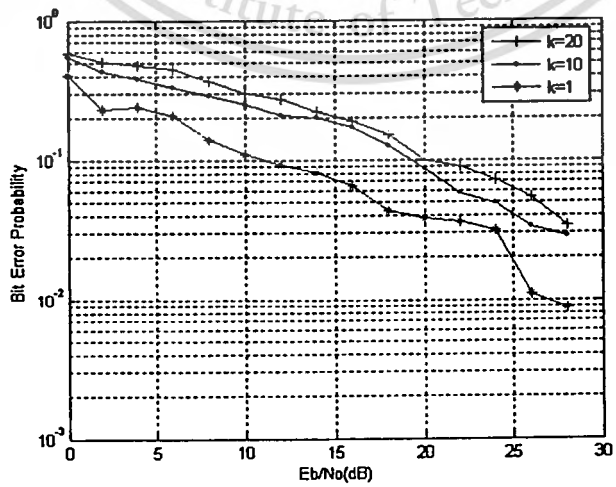

Figure 3.7 Simulation experiments witk k=1,10 and 20 on Heavy Shadowed area

This material is reserved for educational use only, not allowed for commercial use.
Forbidden to modify the content, and cite the document when use.

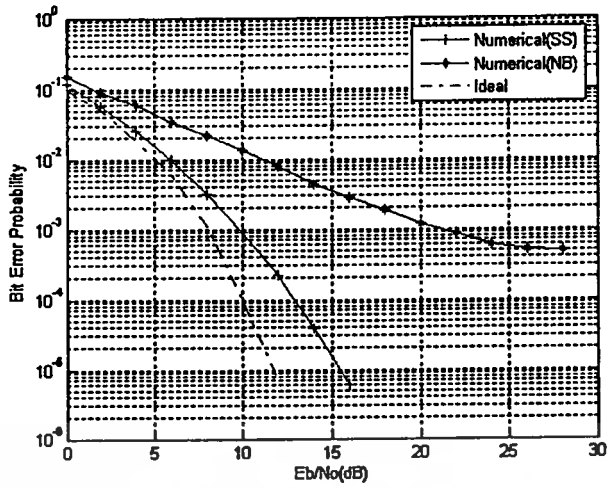

Figure 3.8 Performance on average Shadowed area.

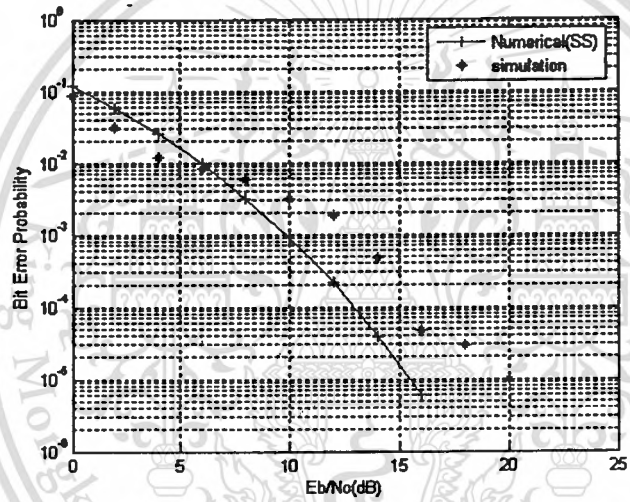

Figure 3.9 Comparison between numerical and simulation on average Shadowed area

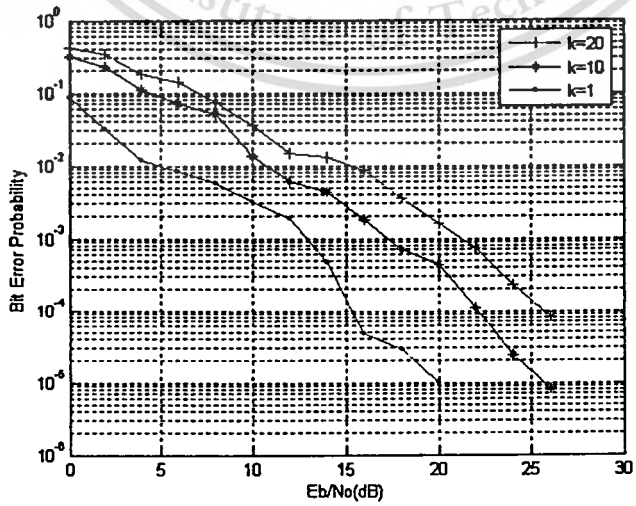

Figure 3.10 Simulation experiments witk k=1,10 and 20 on average Shadowed area

This material is reserved for educational use only, not allowed for commercial use.
Forbidden to modify the content, and cite the document when use.

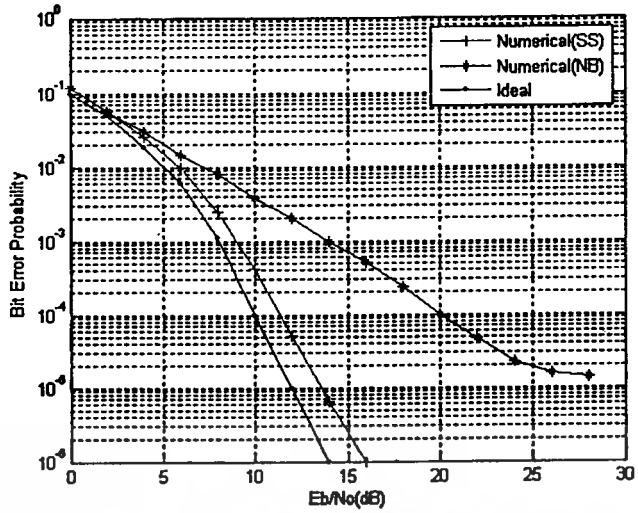

Figure 3.11 Performance on light Shadowed area.

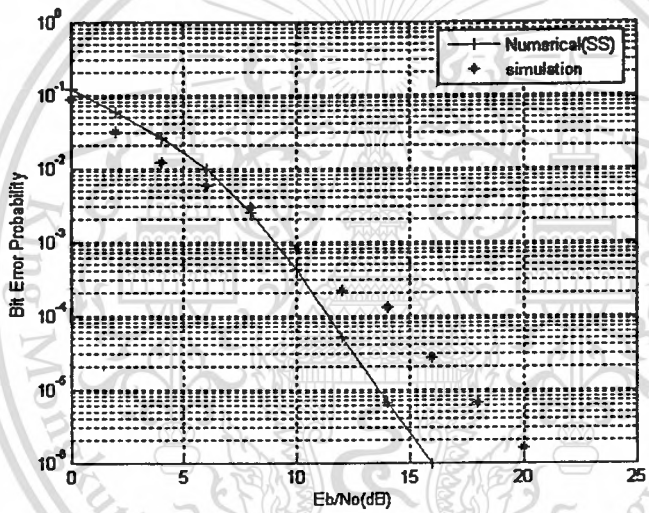

Figure 3.12 Comparison between numerical and simulation on light Shadowed area

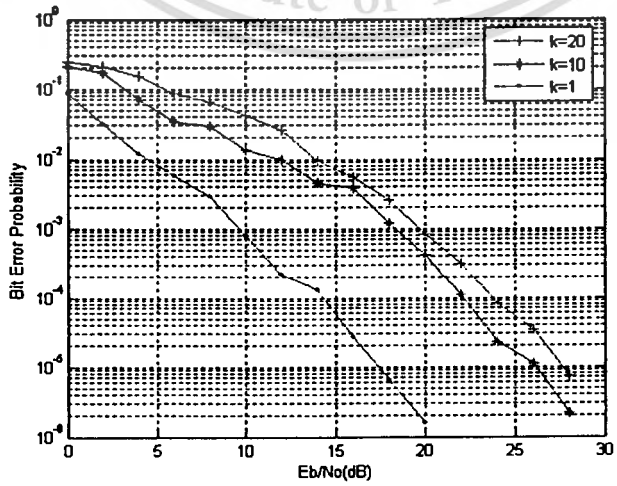

Figure 3.13 Simulation experiments witk k=1,10 and 20 on light Shadowed area

This material is reserved for educational use only, not allowed for commercial use.
Forbidden to modify the content, and cite the document when use.

Chapter 4

Controllable DS-SSA

4.1 Introduction

This section studies an approach of implementing DS-SSA system with modified node components in order to construct a load control structure in which the service rates of each node can be dynamically adapted without using feedback information. The modified protocol and architecture which are proposed in the next section are intended to support various types of newly wireless applications. These include the application that is operated over low earth orbit and geo-stationary satellite application [30]. When a station sends out a message segment across long propagation network, the delay incurred by the propagation plus multiple access and delay time spent in each terminal queues may cause upper protocol layer to assume them as lost packet events, despite correctly receiving them, and possibly retransmitted them needlessly. These disadvantages will significantly limit the performance and channel capacity. In contrast to the traditional DS-SSA which is widely represented with single queue, prior emphasis of the proposed approach is laid on the usage of an additional queue which is applied to manage the collided packet traffic while its queue size is also used as a load control parameter. Another factor which is intended to be modified is "the backlogged condition"[31] This parameter obviously makes the system susceptible to the delay figure, but it is considered necessary for stabilizing channel reliability and also for keeping the packets in the correct sequence when arriving at the receiver [32],[33]. New traffic that arrives at the main queue is assumed to be in the form of message carrying one or more packet(s)[34],[35]. When a terminal has packet(s) waiting in its queues, they will be unconditionally sent out in order to reduce the time spending in the queue. This condition includes the case of collided packet.

Semi-Markov process is used to describe the statistic behavior of the system in steady state. Trade-offs between two major performance parameters, i.e., delay and throughput, are studied and evaluated. The obtained results are compared with those of the traditional system [36],[37],[38]. Numerical models created based on queuing concepts are verified and compared with the simulation. With these results, an advantage performance for group packets can be explained, and the concept is finally

This material is reserved for educational use only, not allowed for commercial use.
Forbidden to modify the content, and cite the document when use.

extended based on the obtained results to describe a simple algorithm using one way control message as the tool to alleviate the problem of system stability.

4.2 System Model

The system illustrated in Figure 4.1 consists of N terminals, each of which is assigned a different spreading code. New traffic is assumed to be in the form of message carrying one or more packet(s), and will be unconditionally sent out in order to reduce the time spending in the queue. Each terminal is represented with three queues. The first queue (Q_1) deals with newly arrival packets, while the second queue (collision-resolved queue : Q_2) is used to store and manage the sequence of packets that are declared as collided traffic. The third queue (Q_3) is used to transmit a packet (new or retransmitted packet) to satellite channel in First-In-First-Out order. P_s and P_e are defined as unconditional successful and unsuccessful transmission probabilities, where $P_e = 1 - P_s$.

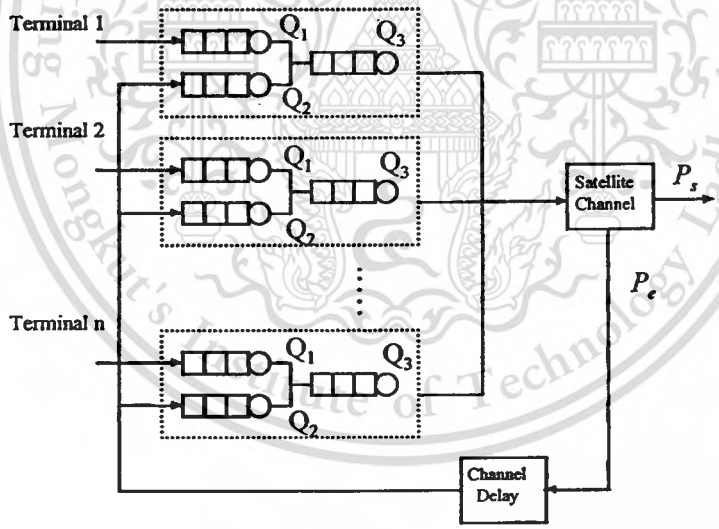

Figure 4.1 System model.

In traditional DS-SSA system, the collision is not declared unless the number of packets in a slot exceeds the limitation. The stations with unsuccessfully transmitted packets will be called backlog, and backlogged stations will attempt to retransmit their packets until they are successful as shown by timing diagram in Figure 4.2. Based on the concept of conventional slotted ALOHA which is applied to Slotted CDMA system, stations have only one queue which operates in FIFO discipline to hold the packets[34]-[36]. Compared to the controllable system whose timing diagram is illustrated in Figure

This material is reserved for educational use only, not allowed for commercial use.
Forbidden to modify the content, and cite the document when use.

4.3, it displays the delay conditions of the message segment after being sent out from Q_1. The shaded box represents the collided packet which will be acknowledged as a failure to the source.

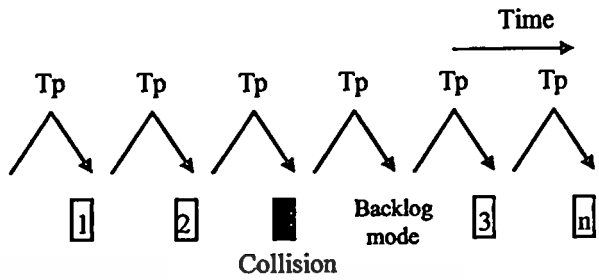

Figure 4. 2. Timing diagram of Traditional system

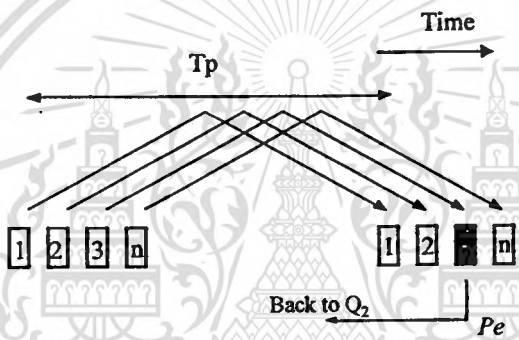

Figure 4.3 Timing diagram of Controllable system.

To denote the average number of packets arriving at the channel during one slot duration by "the offered load", it consists of new and retransmission traffic. New traffic arriving at the terminal is assumed to be the variable-sized messages which can be divided into one or more packets. These messages will be transferred to Q_1. When their first segments (packets) reach the head of queue and ready for service, they are orderly sent out with exponential rate of μ_1 packet per slot, without backlogged condition. After transmission, the terminal sends the replica of the transmitted packets to Q_2, and waiting for individual acknowledgements. When receiving the successful acknowledgements, the terminal discards the success packets out of Q_2. It will starts the retransmission process with Poisson parameter μ_2 (packet per slot) if collision acknowledgements are received. This collision-resolved process will be repeated until each collided packet is successfully received. Each terminal is assumed to be able to process the new transmissions and retransmissions individually and independently. Terminals are also assumed to operate in two states defined by the status of Q_2. It generates traffic with

Forbidden to modify the content, and cite the document when use.

rate μ_1 when Q_2 is idle and with rate $\mu_1 + \mu_2$ when Q_2 is busy.

With the concept of freely transmission, it frequently results in increasing the sending rate of terminals based on the active Q_2. This requires a simple control approach which can adjust the burstiness of the offered traffic to obtain overall system availability while maintaining individual user's performances.

4.3 System Analysis

4.3.1 Throughput Analysis

In this section, the channel throughput (*S*) is used as a measure to evaluate the system performance. Here, *S* is defined as the average number of successfully received packets per time slot, and is given [37] by

$$S = \sum_{k=1}^{N} kP_k P_s(k) \tag{4.1}$$

where N is the number of terminals, P_k is the probability that a packet is transmitted simultaneously with other *k-1* packets(from *k-1* terminals), $P_s(k)$ is the conditional successful transmission probability of a packet and given by $P_s(k) = [1 - Q_b(k)]^{L_b}$. Here, L_b is the number of data bit per packet, and $Q_b(k)$ is the bit error probability given in [17] as

$$Q_b(k) = Q\left(\left[\frac{k-1}{2n_c} + \frac{\eta_0}{2E_b}\right]^{-1/2}\right) \tag{4.2}$$

where $Q(\bullet)$ is the integral Gaussian function, E_b/η_0 is the energy per bit to spectral density of noise power ratio, k is the total number of simultaneously transmitted packet(s) in the slot, and n_c is the spreading sequence length. In this research, it is assumed that the long spreading code sequences and perfect power control are employed. An approximate expression for $Q_b(k)$ is derived based on the same manner of channel environment originally described in [17]. Systems are assumed to be ideal, and all imperfections such as multi-path fading is not considered. The dominant cause of unsuccessful transmission in a slot is the multiple access interference(MAI). Note that all spread interference appeared to the channel including MAI, is approximated as a Gaussian random variable (Gaussian approximation). Thus P_k is mainly based on the

This material is reserved for educational use only, not allowed for commercial use.
Forbidden to modify the content, and cite the document when use.

present number of terminals that have its second queue(Q_2) in busy condition (busy-Q_2).

Let define i and j ($0 \le i \le N, 0 \le j \le N$) be the number of terminals having busy-Q_2 at slot time t and $t+1$, respectively, p_{ij} be a state transition probability that the number of terminals which have busy-Q_2 change from i to j. Thus p_{ij} can be obtained in according to the following conditions.

Case 1: when $i < j$

$$p_{ij} \triangleq \sum_{a=0}^{\min(N-j,i)} C_{j-i+a}^{N-i} \tau_1^{\,j-i+a} (1-\tau_1)^{N-j-a} \, C_a^i \tau_0^{\,a} (1-\tau_0)^{i-a} \tag{4.3}$$

Case 2: when $i > j$

$$p_{ij} \triangleq \sum_{a=0}^{\min(N-i,j)} C_a^{N-i} \tau_1^{\,a} (1-\tau_1)^{N-i-a} \, C_{j-a}^{i} \tau_0^{\,i-j+a} (1-\tau_0)^{j-a} \tag{4.4}$$

Case 3: when $i = j$

$$p_{ij} \triangleq \sum_{a=0}^{\min(N-i,i)} C_a^{N-i} \tau_1^{\,a} (1-\tau_1)^{N-i-a} \, C_a^{i} \tau_0^{\,a} (1-\tau_0)^{i-a} \tag{4.5}$$

where $C_b^a = \frac{a!}{(a-b)!\,b!}$. τ_0 and τ_1 are the Busy-to-Idle and Idle-to-Busy transition probabilities of Q_2, respectively. Both events are assumed not to occur at the same given time slot. Let U_n be the steady state probability denoting that there are n terminals having busy-Q_2, and P be the state transition matrix of p_{ij} (i.e., $P = [p_{ij}]$, $(N+1)*(N+1)$ matrix) that can be obtained from equations (4.3), (4.4) and (4.5). Then, U_n can be derived by using the following $N+1$ equations [34].

$$U^T = U^T P \tag{4.6}$$

where, $U^T = [U_0, U_1, U_2, \ldots\ldots U_N]$, n = 0,1,2,……N, and $\sum_{n=0}^{N} U_n = 1$.

Thus, the average number of terminals having busy-Q_2, i.e., N_{av}, can be obtained as follows.

$$N_{av} = \sum_{n=0}^{N} n U_n \tag{4.7}$$

This material is reserved for educational use only, not allowed for commercial use.
Forbidden to modify the content, and cite the document when use.

In order to derive the value of τ_0 and τ_1, the queuing behavior of each terminal is needed to be considered, especially its Q_2. With the component shown in Figure 4.3, let us re-configure by folding all the components, except Q_2, into one box as illustrated in Figure 4.4.

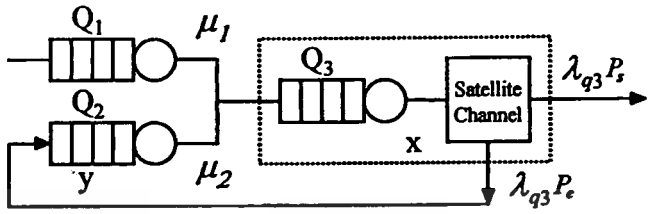

Figure 4.4 Functional diagram.

Here, μ_1 and μ_2 are the generate rates of new and retransmitted packets presented to the X box. λ_{q3} is the departure rate of packets from the X box and P_s is the unconditional packet success probability. Now, let x and y be the number of packet(s) in X box (including one being served) and in Q_2, respectively. By using the concept of birth-death process, the state-transition diagram for the system can be created as shown in Figure 4.5.

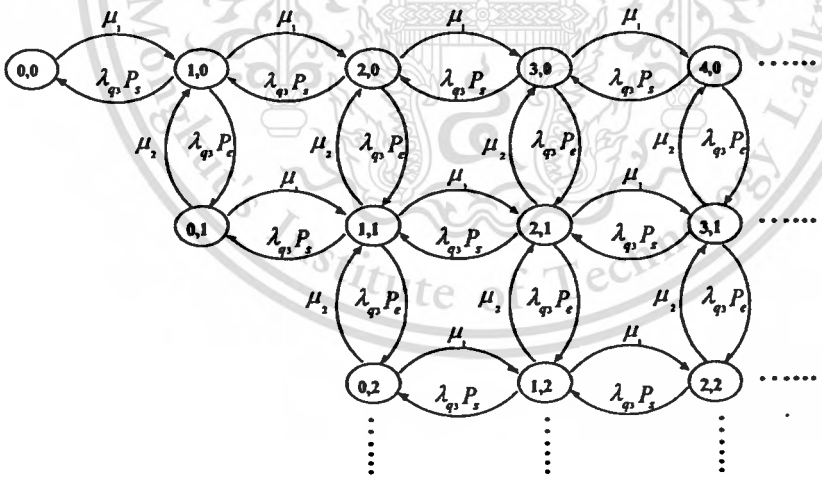

Figure 4.5 State-transition Diagram

Using the double z-transform and let $p_{x,y}$ be the equilibrium probability that the X box and Q_2 contains x and y packets respectively, a set of balance equations can be obtained as:

Case 1: when $x = 0, y = 0$

This material is reserved for educational use only, not allowed for commercial use.
Forbidden to modify the content, and cite the document when use.

$$\mu_1 p_{0,0} = \lambda_{q3} P_s p_{1,0} \tag{4.8}$$

Case 2: when $x > 0, y = 0$

$$\sum_{x=1}^{\infty} \mu_1 p_{x,0} z_1^x + \sum_{x=1}^{\infty} \lambda_{q3} p_{x,0} z_1^x$$

$$= \sum_{x=1}^{\infty} \mu_1 p_{x-1,0} z_1^x + \sum_{x=1}^{\infty} \lambda_{q3} P_s p_{x+1,0} z_1^x + \sum_{x=1}^{\infty} \mu_2 p_{x-1,1} z_1^x \tag{4.9}$$

Case 3: when $x = 0, y > 0$

$$\sum_{y=1}^{\infty} \mu_1 p_{0,y} z_2^y + \sum_{y=1}^{\infty} \mu_2 p_{0,y} z_2^y$$

$$= \sum_{y=1}^{\infty} \lambda_{q3} P_s p_{1,y} z_2^y + \sum_{y=1}^{\infty} \lambda_{q3} P_e p_{1,y-1} z_2^y \tag{4.10}$$

Case 4: when $x > 0, y > 0$

$$\sum_{x=1}^{\infty} \sum_{y=1}^{\infty} (\mu_1 + \lambda_{q3} + \mu_2) p_{x,y} z_1^x z_2^y$$

$$= \sum_{x=1}^{\infty} \sum_{y=1}^{\infty} \lambda_{q3} P_s p_{x+1,y} z_1^x z_2^y + \sum_{x=1}^{\infty} \sum_{y=1}^{\infty} \mu_1 p_{x-1,y} z_1^x z_2^y$$

$$+ \sum_{x=1}^{\infty} \sum_{y=1}^{\infty} \mu_2 p_{x-1,y+1} z_1^x z_2^y + \sum_{x=1}^{\infty} \sum_{y=1}^{\infty} \lambda_{q3} P_e p_{x+1,y-1} z_1^x z_2^y \tag{4.11}$$

Then, summing both sides of all cases and identifying,

$$P(z_1, z_2) = \sum_{x=0}^{\infty} \sum_{y=0}^{\infty} p_{x,y} z_1^x z_2^y$$

to obtain:

$$\mu_1 P(z_1, z_2) + \lambda_{q3} \left[P(z_1, z_2) - \sum_{y=0}^{\infty} p_{0,y} z_2^y \right] + \mu_2 \left[P(z_1, z_2) - \sum_{x=0}^{\infty} p_{x,0} z_1^x \right]$$

$$= \mu_1 z_1 P(z_1, z_2) + \frac{\lambda_{q3} P_s}{z_1} \left[P(z_1, z_2) - \sum_{y=0}^{\infty} p_{0,y} z_2^y \right] + \frac{\lambda_{q3} P_e z_2}{z_1} \left[P(z_1, z_2) - \sum_{y=0}^{\infty} p_{0,y} z_2^y \right]$$

$$+ \frac{\mu_2 z_1}{z_2} \left[P(z_1, z_2) - \sum_{x=0}^{\infty} p_{x,0} z_1^x \right] \tag{4.12}$$

This material is reserved for educational use only, not allowed for commercial use.
Forbidden to modify the content, and cite the document when use.

Define that $\sum_{i=0}^{\infty} p_{i,0} z_1^i = P(0,z_2)$ and $\sum_{j=0}^{\infty} p_{0,j} z_2^j = P(z_1,0)$, and substituting $z_1 = z_2 = z$ into (4.12), Then

$$\mu_1 P(z,z) + \lambda_{q3}[P(z,z) - P(0,z)] + \mu_2[P(z,z) - P(z,0)]$$

$$= \mu_1 z P(z,z) + \frac{\lambda_{q3} P_s}{z}[P(z,z) - P(0,z)]$$

$$+ \lambda_{q3} P_e[P(z,z) - P(0,z)] + \mu_2[P(z,z) - P(z,0)]$$

with some manipulations, then

$$z\mu_1 P(z,z) = \lambda_{q3} P_s[P(z,z) - P(0,z)] \tag{4.13}$$

Let $z=1$, then

$$P(0,1) = \frac{\lambda_{q3} P_s - \mu_1}{\lambda_{q3} P_s} \tag{4.14}$$

and

$$P(1,0) = 1 - \frac{\mu_1 P_e}{\mu_2 P_s} \tag{4.15}$$

Here, $P(0,1)$ and $P(1,0)$ represent the probability that there is no packet in the X box and in Q_2, respectively. With the description of τ_0 and τ_1 given earlier, they are $\tau_0 = \mu_2 P_s \sum_{x=0}^{\infty} p_{x,1}$ and $\tau_1 = \mu_1 P_e P(1,0)$. Let the ratio between the average number of terminals having busy-Q_2(N_{av}) and the number (N) of total terminals be ν_w, the total offered traffic appeared to the channel can be approximated by:

$$\mu_{w0} = (1 - \nu_w) N \mu_1 + \nu_w N(\mu_1 + \mu_2) \tag{4.16}$$

If the assumption of Poisson environment for μ_1 and μ_2 exists, then μ_{w0} can also be assumed as Poisson process. Let $G_{w0} = 1 - \exp(-\frac{\mu_{w0}}{N})$ be the probability of having at least one packet transmitted from a terminal. Thus the unconditional successful transmission probability for a packet at a given time slot can be formulated [38] as follows.

This material is reserved for educational use only, not allowed for commercial use.
Forbidden to modify the content, and cite the document when use.

$$P_s = \sum_{k=0}^{N} C_k^N G_{w0}{}^k (1 - G_{w0})^{N-k} P_s(k) \tag{4.17}$$

Now P_s can be computed iteratively based on ν_w and the condition $P(1,0) \le 1$ given μ_1 and μ_2.

In considering the equilibrium probability, the long-term unconditional value of P_s is needed. As seen in Figure 4.1, the queuing system of single terminal operates under the influence of the others. Therefore, the number of packets including the tagged one that simultaneously arrive at the channel can be vastly different from slot-to-slot. In this research, instead of evaluating the average, it selects P_s corresponding to the worst-case condition where the system is approaching unstable area. If the utilization factor of Q_2 (ρ_{q2}) is defined as the average arrival rate of packet per average service time, this area means $\rho_{q2} \approx 1$. By substituting $\nu_w = N_{av}/N$ in (4.16) and using $G_{w1} = 1 - \exp(-\frac{\mu_{w0}}{N})$, then

$$P_k = C_k^N G_{w1}{}^k (1 - G_{w1})^{N-k} \tag{4.18}$$

Table 4.1 Gap Size Effect

Gap size(sec)	Throughtput(%)	Packet error(%)	Delay(%)
0.10	19.63	14.27	9.58
0.12	18.82	13.52	9.12
0.14	18.62	13.11	8.54
0.16	18.21	12.78	8.28
0.18	17.94	11.59	6.23
0.20	17.21	10.83	5.11

Now the throughput S can be obtained from (4.1), (4.18) and $P_s(k)$. The accuracy of above analysis will be verified by comparing numerical results with the simulations running by simulation program (OPNET, see appendix B) as shown in Figure 4.6 and Figure 4.7. All curves illustrates the generated rates (μ_1) of the new traffic as a function of throughput (packet per time slot). Simulations are performed based on the same system configuration and environment previously defined for numerical analysis. Some parameters assigned in the program are shown in the Table 4.2. The simulation period is 3600 seconds for every experiment.

ducational use only, not allowed for commercial use.
Forbidden to modify the content, and cite the document when use.

Table 4.2 Simulation Parameters for Ground Terminals

Parameter	Define	Value	Unit
Packet size	IP_Packet_time	0.005	sec
Frame size	Sat_frame	0.311	sec
Propagation delay	pdelay	0.253	sec
Maximum Retx	Max_ReTx	3	times
Packet timeout	Pk_timeout	1.4	sec
Window Size	window_size	128	packets
Maximum nose	Max_node	50	uesrs

With the same condition for both experiments, Figure 4.6 are assigned with N=35 and μ_2= 0.3 while N=35 and μ_2= 0.5 for Figure 4.7, and define E_b/η_0= 15, n_c= 127, L_b= 1000 for CDMA channel. Simulation experiments are performed based on the same system configuration and environment defined for numerical analysis. During simulation, it is found that the effect of different gap size between channel slots have to be taken into account, since it is one of the main factor to the result of throughput. Several experiments are performed to record the effect of the gap size. The experiments are done at the 20% of maximum throughput with simulation period of 3600 sec. The obtained results are shown in Table 4.1. Packet error and delay are recorded in the ratio of the obtained results per results of 20% throughput.

Since this study concentrates on the results obtained from two systems (traditional and proposed one) at the same channel environment, the gap value that causes the lowest value of the packet error is selected. This results in losing about 7% in throughput, but gain the reduction in success probability and system delay by factor of 13%. As may be seen, the results obtained by numerical analysis show higher throughput than the simulation around the maximum area. This is under the condition that all relevant parameters are selected for the P_s at the area where the traffic generated to the channel almost reach the critical area, and the system may not turn to normal if moving further from this point. Although the numerical results are calculated based on the upper-bound condition of CDMA channel, the corresponding simulation results show trend agreement with the numerical ones.

This material is reserved for educational use only, not allowed for commercial use.
Forbidden to modify the content, and cite the document when use.

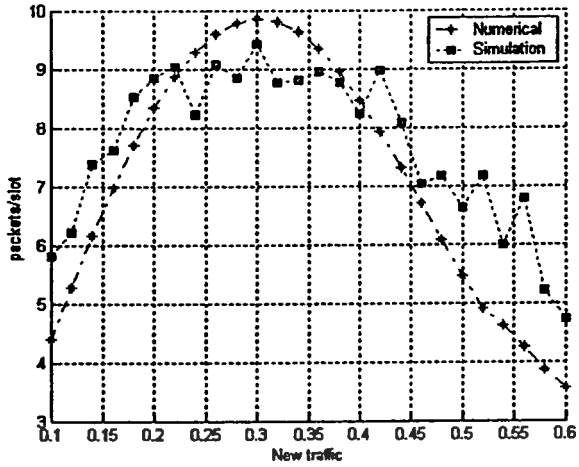

Figure 4.6 Throughput results, with $\mu_2 = 0.3$

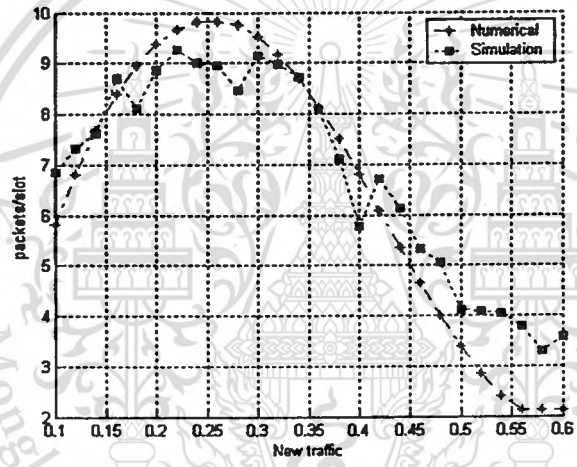

Figure. 4.7 Throughput results, with $\mu_2 = 0.5$

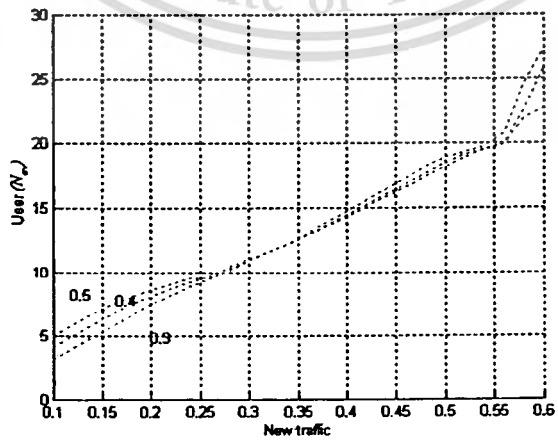

Figure 4.8 N_{av} versus μ_1, when $N = 35$.

This material is reserved for educational use only, not allowed for commercial use.
Forbidden to modify the content, and cite the document when use.

In Figure. 4.8, the average number of terminals having busy-Q_2 is plotted as a function of μ_1 with N=35. The results suggest that the critical area starts up at $\mu_1 \approx 0.52$. In solving the queuing behavior of each terminal, the channel is assumed to operate at this critical point for long period. Thus ν_v is assumed to be 65% of the total number of terminals. This research intends to have a control process performing individually within each terminal to keep the channel operating below this critical point. Under the control condition, ν_v should be kept lower than 60%-65% for N=35 in order to stabilize the channel.

4.3.2 Delay Analysis

In this section the message delay by means of numerical approximation is evaluated. As previously described, all queuing components are assumed to operate independently, and the waiting time plus service time in all queues is taken into account through the total message delay. Let us define the total message delay, W_{tot}, over the satellite link in terms of the sum of fixed transmission delay, processing time and average queuing delay as follows

$$W_{tot} = T_1 + T_3 + T_p + \bar{b}_{e,l} + (\bar{g}T_{pc}) \qquad (4.19)$$

where T_1 and T_3 are the expected delay time which a message spends in Q_1 and Q_3 respectively, $\bar{g}$ is the average message size(packets), T_{pc} is the processing time in central HUB, T_p is the propagation delay, and $\bar{b}_{e,l}$ is the mean delay of the retransmission process. When all message segments are successfully received, the total message delay is

$$W_{tot} = T_1 + T_3 + 2T_p + (\bar{g}T_{pc})$$

The analysis of W_{tot} can be carried out using the timing sequence shown in Figure 4.9

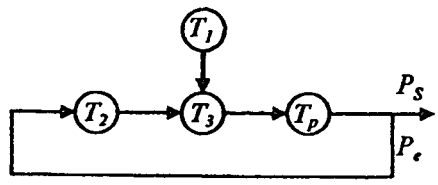

Figure 4.9 Timing sequence diagram

This material is reserved for educational use only, not allowed for commercial use.
Forbidden to modify the content, and cite the document when use.

4.3.2.1 Delay on Q_1

Each message arrives at the terminal's first buffer is assumed to follow Poisson arrival process with rate λ_g. Let the probability that a message carrying i packets is g_i, then the distribution of message size as $G(z) = \sum_{i=1}^{\infty} g_i z^i$ can be obtained. At the beginning of a given time slot, a terminal sends out a packet at the head of Q_1 with the departure rate μ_1 packet per slot. If the terminal has collided packet(s) waiting to be solved in Q_2, it transmits those packets with μ_2 packet per slot. Both departure processes are assumed to follow Poisson processes. Now the process of Q_1 with the Bulk arrival M/G/1 queuing system can be accomplished. The expected number of messages in Q_1 at any moment is given [39] as :

$$\overline{Q} = \frac{\lambda_g^2 t_m^{(2)}}{2(1-\lambda_g t_m^{(1)})} \tag{4.20}$$

where $t_m^{(1)}$ and $t_m^{(2)}$ are the first and second moment of service time of a message, respectively. Assume $T_m^*(s)$ is the Laplace transform of density function of service time of the message which is $T_m^*(s) = G(B_{q1}^*(s))$, where $G(z)$ and $B_{q1}^*(s)$ are the distribution of the message size and service time of each individual packet, respectively. Therefore,

$$T_m^{*(1)}(s) = G^{(1)}(B_{q1}^*(s)).B_{q1}^{*(1)}(s)$$

and

$$T_m^{*(2)}(s) = G^{(1)}(B_{q1}^*(s)).B_{q1}^{*(2)}(s) \quad + (B_{q1}^{*(1)}(s))^2 G^{(2)}(B_{q1}^*(s)) \tag{4.21}$$

where $T_m^{*(1)}(s)$ and $T_m^{*(2)}(s)$ are the first and second derivative of $T_m^*(s)$. Letting $s=0$ in (4.21) and applying Little's result, a delay measure of Q_1 which is the average waiting time for a message denoted by W_{q1} [34] can be obtained from :

$$W_{q1} = \frac{\lambda_g(\overline{g}t_m^{(1)})^2}{2(1-\rho_{q1})}\left[1 + C_g^2 + \frac{C_t^2}{\overline{g}}\right] \tag{4.22}$$

where C_g^2 and C_t^2 are the squared coefficient of variation for message size and message service time, respectively. Thus the average time spent in Q_1 is:

$$T_1 = (\frac{\overline{g}}{\mu_1}) + W_{q1} \tag{4.23}$$

This material is reserved for educational use only, not allowed for commercial use.
Forbidden to modify the content, and cite the document when use.

where $\bar{g}$ is the average message size.

4.3.2.2 Extended Delay on Collision-Resolved Queue (Q_2)

To evaluate the waiting time for Q_2, it is necessary to determine the virtual traffic of the packets that have problem. They are calculated based on the traffic generated by Q_2 and unconditional successful transmission probability (P_s). Q_3 represents an output port that processes the packet transmission according to the slot time of satellite channel. As described in the previous section, Q_1 and Q_2 are assumed to generate inter-departure traffic based on Poisson processes. With the well-known Poisson property, it can be assumed that the combined result of both traffic also in the form of Poisson process, and the expression of M/D/1 will be used to evaluate the average waiting time on this queue. Since its constant service time is equal to the satellite time slot, the average waiting time for Q_3 is given [39] by

$$W_{q3} = \frac{\lambda_{q3} t_{slot}^2}{2(1-\rho_{q3})} \tag{4.24}$$

Applying this individual waiting time with an average message segments and service time, then

$$T_3 = \bar{g}.(W_{q3} + t_{slot}) \tag{4.25}$$

where t_{slot} is the slot time of satellite channel, and ρ_{q3} is the utilization factor of Q_3. Note that the calculation of the delay in this queue is done based on the worst-case condition, since a message segment that arrives at Q_3 could reach the head of the queue and get service before the complete arriving of the whole message segments. This traffic becomes the arrival to Q_2 with the interarrival time distribution: $A^*(s) = \frac{\lambda_{q3}}{s+\lambda_{q3}}$; $\lambda_{q3} = \mu_1 + \rho_{q2}\mu_2$, where ρ_{q2} is the utilization factor of Q_2. When this queue sends out a packet, it is possibly still in busy state, or becomes empty. Given ρ_{q3}, the distribution of the interdeparture time is obtained as :

$$B_{q3}^*(s) = (1-\rho_{q3})A_{q3}^*(s)D_{q3}^*(S) + \rho_{q3}D_{q3}^*(s) \tag{4.26}$$

where $A_{q3}^*(s) = \lambda_{q3}/(s+\lambda_{q3})$ is the interarrival time distribution of Q_3, $\lambda_{q3} = \mu_1 + \rho_{q2}\mu_2$. ρ_{q2} is the utilization factor of Q_2. Since service time of Q_3, $d_{q3}(x)$, is deterministic with

This material is reserved for educational use only, not allowed for commercial use. Forbidden to modify the content, and cite the document when use.

value t_{slot}, the service functions of this queue will be in the form of $d_{q3}(x) = U_0(x - t_{slot})$ and $D^*_{q3}(s) = \exp(-st_{slot})$. Applying these parameters to (4.26) and taking out the Laplace transform, the departure time density is finally obtained from :

$$b_{q3}(t) = (1-\rho_{q3})\lambda_{q3}\exp(-\lambda_{q3}(t-t_{slot}))\delta(t-t_{slot}) + \rho_{q3}U_0(t-t_{slot}) \tag{4.27}$$

where $U_0(t)$ is the unit impulse function. Then

$$\bar{b}_{q3} = \frac{1-\rho_{q3}}{\lambda_{q3}} \tag{4.28}$$

If $\rho_{q3} \ll 1$(the service time is very short compared to the arrival rate), it can be assumed that the effect of Q_3 is insignificant, and its interdeparture traffic is close to λ_{q3}. When the packets arrive at the central HUB, they must spend some time in the HUB to be considered a success or failure before leaving to the higher protocol layer or returning to the source. In practice, each system is implemented with various different types of the acknowledgement process and architecture, and its direct analysis is not mathematically tractable. For simplicity, $P_e\lambda_{q3}$ will be defined as the average input rate for the return path to Q_2. This definition is the key factor to model Q_2 as a discrete time queue with general arrival process and Poisson distributed service rate with parameter $P_e\lambda_{q3}$ and μ_2, respectively. Given the upper bound on average waiting time of G/M/1 by [34], then

$$W_{q2} = \frac{(1+C_b^2)\rho_{q2}^2}{1+C_b^2\rho_{q2}^2}\left[\frac{(\sigma_t^2+\sigma_b^2)P_e\lambda_{q3}}{2(1-\rho_{q2}^2)}\right] \tag{4.29}$$

where C_b^2 is the squared coefficient of variation for service time. σ_t^2 and σ_b^2 are the variance of interarrival and service time, respectively. Since a packet may circulate more than one time, the remaining priority factor is the mean delay of the retransmission process, $\bar{b}_{e,f}$.

Let $B^*_{e,f}(s)$ be the Laplace transform of the total service time of Q_2, $B^*_{e,s}(s)$ be the Laplace transform for the delay time of unsuccessful transmission, and $B^*_{e,s}(s)$ be the Laplace transform for the delay time of successful attempt after retransmitting *n* times. Total delay in the form of Laplace can be written in the form :

This material is reserved for educational use only, not allowed for commercial use.
Forbidden to modify the content, and cite the document when use.

$$B^*_{e,1}(s) = \sum_{n=0}^{\infty} [(P_e B^*_{e,e}(s))^n (P_s B^*_{e,s}(s))]$$

$$= \frac{P_s B^*_{e,s}(s)}{1 - P_e B^*_{e,e}(s)} \tag{4.30}$$

Differentiate and let s=0, then

$$\bar{b}_{e,1} = \frac{P_s B^{(1)}_{e,s}(0) - P_s P_e (B^{(1)}_{e,s}(0) - B^{(1)}_{e,e}(0))}{(1 - P_e)^2} \tag{4.31}$$

where P_s is the unconditional packet success probability obtained from (4.17), $P_e = 1 - P_s$, and

$$B^{(1)}_{e,e}(0) = \bar{b}_{e,e} = 2T_p + \bar{g}P_e(W_{q2} + W_{q3} + t_{slot})$$

$$B^{(1)}_{e,s}(0) = \bar{b}_{e,s} = \bar{b}_{e,e} + T_{pc}$$

The total message delay, W_{tot} can now be derived by using (4.23), (4.25) and (4.31). The correctness of the mathematical model is verified by comparing with simulation results given in Figure 10 and Figure 11. Based on the message segments presented at Q_1, assume that $\lambda_g = 1$, $\bar{g} = 8$ and $\sigma_g^2 = 144.2$. With the same environment as in the last section, curves show analytic and simulation results obtained for average delay of an individual message with fixed values of $\mu_2 = 0.3$ and $\mu_2 = 0.5$.

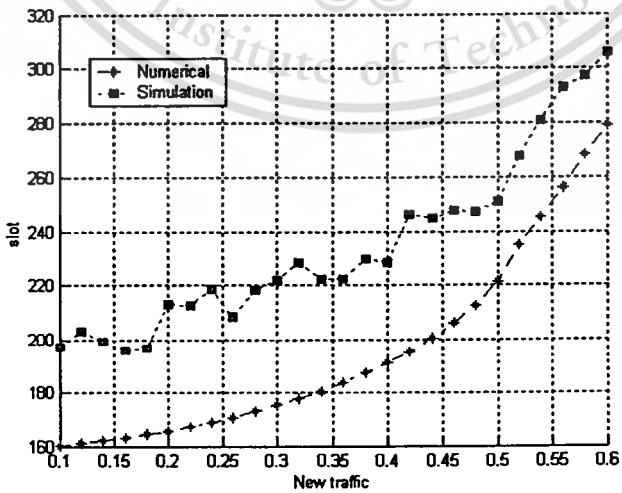

Figure 4.10 Delay results, with $\mu_2 = 0.3$.

This material is reserved for educational use only, not allowed for commercial use.
Forbidden to modify the content, and cite the document when use.

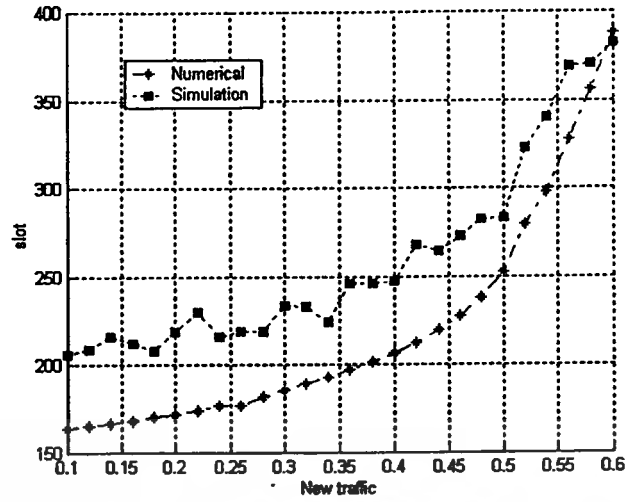

Figure 4.11 Delay results, with $\mu_2 = 0.5$.

One of the main impacts that makes the difference between the results obtained from both methods is the gap size between channel slots. This gap size helps the simulation program to identify 2 slots in a roll. If this value is too high, it will results in losing throughput, but gain more success probability and lower delay. Since this thesis concentrate on the results obtained from two systems (traditional and proposed one) at the same channel environments, we select the gap size will be selected at the value that causes the lowest value of the packet error. This results in losing around 7 percent in throughput, but gain the reduction in success probability and system delay by factor of 13 percent. More details of this gap size effect has been described in the previous section

4.4 System Comparison

In this section, the performance of the controllable scheme by means of numerical results is evaluated, and compared them with that of traditional scheme. Assume that both techniques are equivalent for which the offered loads are generated with the same manner and have the same pattern of throughput. Thus, μ_2 of the controllable system and average retransmission rate of traditional system can be considered as a common parameter.

This material is reserved for educational use only, not allowed for commercial use.
Forbidden to modify the content, and cite the document when use.

4.4.1 Throughput Comparison

Computing the throughput S as a function of μ_1 using (4.1) and (4.18) results in the plots of Figures 4.12 – 4.17. In the figures, the throughput is plotted against the offered load for various values of μ_1 with μ_2 equal to 0.3, 0.4 and 0.5. The curves of the results obtained from controllable and traditional DS-CDMA are shown for N=25, N=30 and N=35. The new traffic generated with rate μ_1 is assumed to be an average departure rate of Q_1 of all terminals. Compared with the traditional scheme, μ_1 can be defined as the transmission rate for the terminal in ready mode, while μ_2 is compared with retransmission rate for the terminal in backlogged mode.

Figures 4.14 – 4.17 depict the throughput and offered loads obtained from controllable and traditional system.

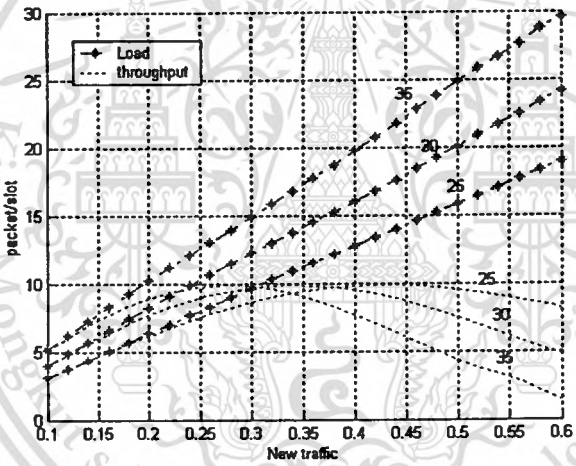

Figure 4.12 Throughput-Load curve for controllable system, with μ_2=0.4 .

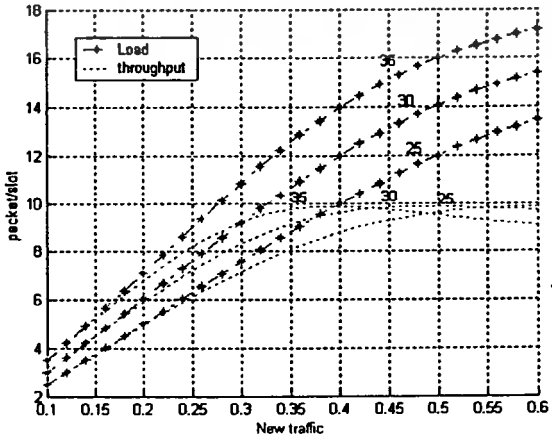

This material is reserved for educational use only, not allowed for commercial use.
Forbidden to modify the content, and cite the document when use.

Figure 4.13 Throughput-Load curve for the traditional system, with μ_2 = 0.4

The plots are made with transmission rate μ_1 for the new packet as a parameter while retransmission rate is kept constant. With these figures, a comparison is given between controllable and traditional DS-SSA system.

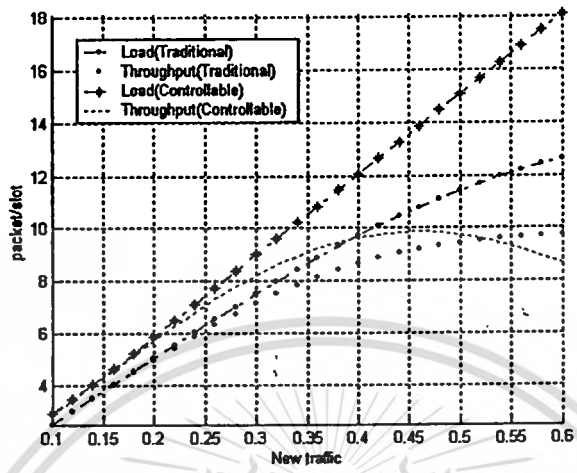

Figure 4.14 Throughput-Load comparison, with $\mu_2 = 0.3$ and $N = 25$.

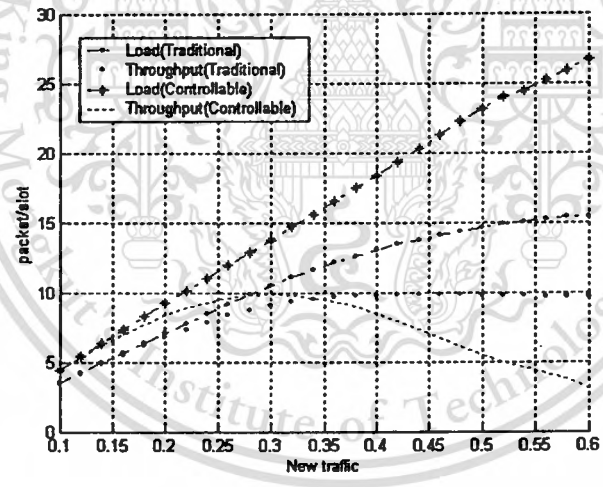

Figure 4.15 Throughput-Load comparison, with $\mu_2 = 0.3$ and $N = 35$.

Based on the infinite node assumption, the transmission rate more than 0.6 can not be applied. This is because it may be too large for the Markov chain to provide the correct values of the steady state distribution. When the control method is applied, each terminal will try to adjust its resources to keep the channel operate below this point.

By simulation, it can be seen that varying μ_2 doesn't result much in adjusting the performance(see Figure 8). A parameter that is more appropriate for this purpose is μ_1.

This material is reserved for educational use only, not allowed for commercial use.
Forbidden to modify the content, and cite the document when use.

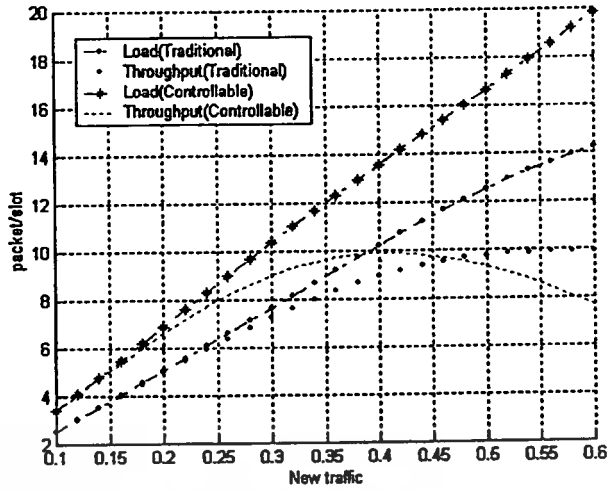

Figure 4.16 Throughput-Load comparison, with $\mu_2 = 0.5$ and $N = 25$.

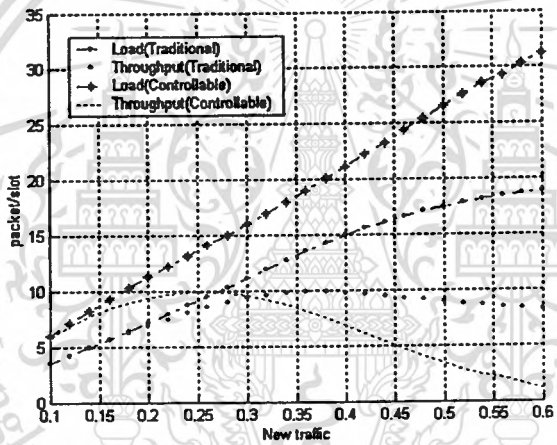

Figure 17 Throughput-Load comparison, with $\mu_2 = 0.5$ and $N = 35$.

4.4.2 Delay Comparison

In this subsection the results of mean message delay are presented by assuming infinite terminal's queue size. Equation (4.19) can be reconfigured to be two components as $T_1 + T_{ctr}$. T_1 is the message waiting time which occur on the terminal's first queue, while T_{ctr} is the delay since the first segment of the message was sent out from the terminal's first queue (input queue) until all the message segments is successfully received. Since the service time of Q_3 (output queue) is assumed to be very short compared to the arrival time, T_1 is considered as a constant for the DS-CDMA channel of both techniques. Figures 4.18 – 4.20 illustrate the results of delay comparison, with the parameters of N=25, 30 and 35, and $\bar{g} = 4$. Since both schemes are operated based on time interval of channel slot, the results are shown in the unit of slot.

This material is reserved for educational use only, not allowed for commercial use.
Forbidden to modify the content, and cite the document when use.

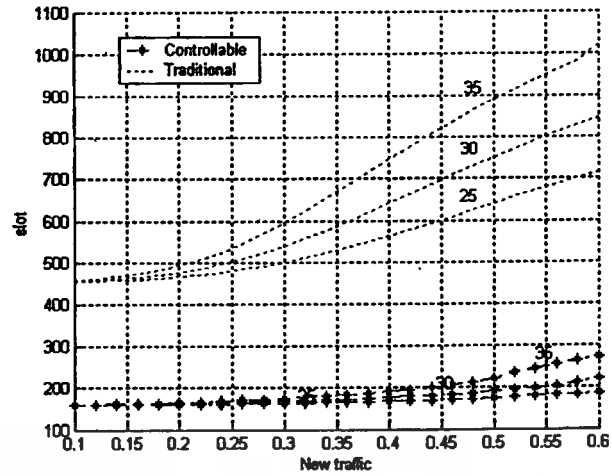

Figure 4.18 Delay comparison, with $\mu_2 = 0.3$.

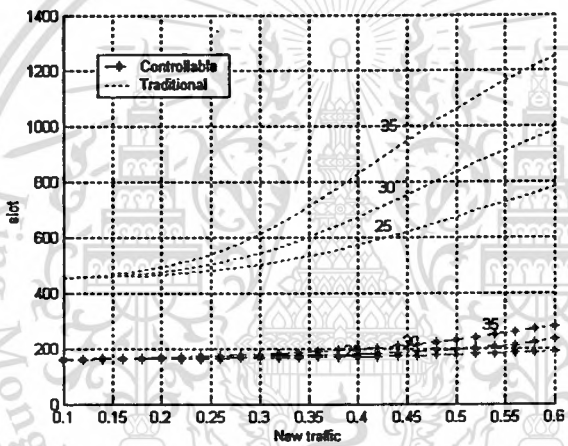

Figure 4.19 Delay comparison, with $\mu_2 = 0.4$

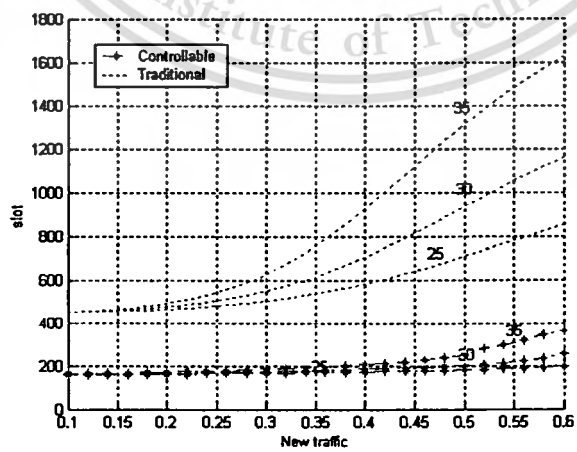

Figure 4.20 Delay comparison, with $\mu_2 = 0.5$.

This material is reserved for educational use only, not allowed for commercial use.
Forbidden to modify the content, and cite the document when use.

4.5 Control Architecture

The flowchart representation of the control approach is given in Figure 4.21. Since Q_2 is used to store and manage the sequence of packets that are declared as collision, its queue size associated with ACK messages can be considered as the parameters for determining the current status of the system and also for specifying the sending rate at which Q_1 should be performed.

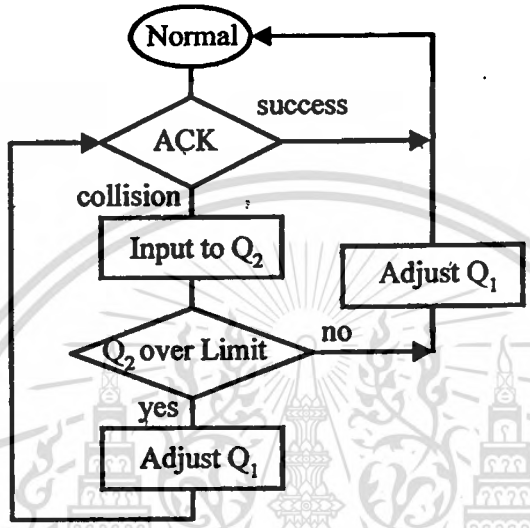

Figure 4.21 Flow chart of control approach

The cycle of the control process starts when stations receive the acknowledgement (ACK). In case ACK is negative, terminal stores the packet at the tail of Q_2, and checks whether its queue size reach the threshold. By adjusting the output rate of Q_1 based on pre-assigned threshold of Q_2, the total offer loads presented to the satellite channel can be controlled. For simplicity of the simulation, the single control step will be assigned to each terminal. For example, given the fixed value of $\mu_2 = 0.4$, N=25, 30 and 35, the service time of Q_1 is $\frac{1}{\mu_1}$ when its queue size ≤ 8, and is $\frac{2}{\mu_1}$ or $\frac{4}{\mu_1}$ when its queue size ≥ 8 (including the one being serviced). Figure 4.22-4.24 provides the results of message delay in unit of second under normal condition.

It can be noticed that the results obtained from the system with and without control conditions become close to each others, since the channel is stable and the queue size of Q_2 is always lower than threshold. Figure 4.25-4.27 shows the results when the channel suffer with degradations(E_b/N_o lower than 5 dBm). In this range, the lower μ_1 becomes, the better the total message delay is. This is because the packets are kept within Q_2

This material is reserved for educational use only, not allowed for commercial use.
Forbidden to modify the content, and cite the document when use.

instead of letting the terminal attempt to transmit packets over the acceptable traffic level. This event is not last if the arrival messages rate of Q_1 keep increasing. It is confirmed by the results illustrated in Figure 4.28. The plots show the average time duration of turning the terminal state from stable to unstable (start) and from unstable to stable (stop).

4.5.1 Experimental Results

As an illustration of the results, the controllable technique is more sensitive to the offered loads than the traditional ones. This is because a terminal sending out the traffic from two individual queues contained in it. When the channel status becomes worse by the result of heavy traffic, the number of terminals that have Q_2-active rapidly increases, and the throughput reaches the saturated point faster than that of traditional one. On the contrary, it can be seen that the total message delay obtained from the controllable system is far better, since the terminal is allowed to freely send out the packets in their input queues and let Q_2 take care all the collided packets. This makes a message deal with only one propagation delay plus the waiting time in queue, multiplied by the number of segments contained in that message in case of no collision occurring. Packets are also kept waiting in the buffer for a shorter duration in the Q_1 and Q_2. In Figure 4.14 - 4.20, It can be seen that the controllable scheme drives the system into saturation point faster, but gives the better delay results.

For a particular load offered to the channel, we wish to determine if the throughput at this point is still below the saturation point and the delay can be accepted by the application. In considering these questions, a power factor (i.e., throughput/message delay) is used as a parameter to justify the performance of our system, and the results shown in Figure 4.29. As seen form the plots, it is evident that the controllable scheme still works well if the offered load presented in the area mask of 30% below the saturation point, although the performance of the controllable technique degrades very rapidly as the offered traffic increases. To keep the system in the workable area, a control policy is needed for each remote terminal. Since the propagation delay is high not only in the satellite environment, but possibly also in other wireless media, it is not appropriate for the remote terminal to depend strictly on the response messages sent form the centralized or main HUB to control the output traffic.

This material is reserved for educational use only, not allowed for commercial use.
Forbidden to modify the content, and cite the document when use.

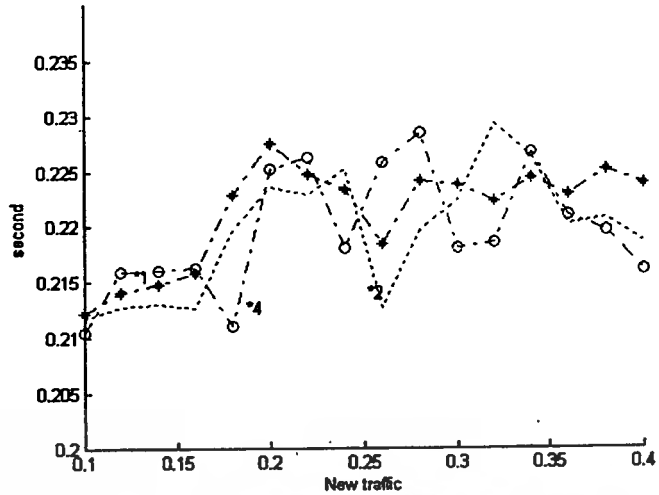

Figure 4.22 System with control approach under normal condition, N=25

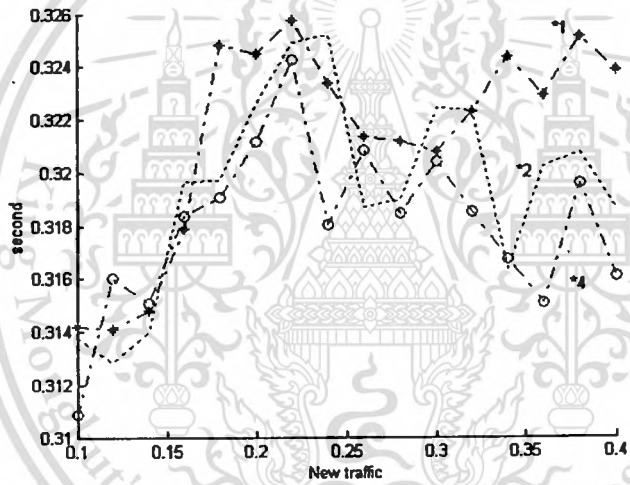

Figure 4.23 System with control approach under normal condition, N=30

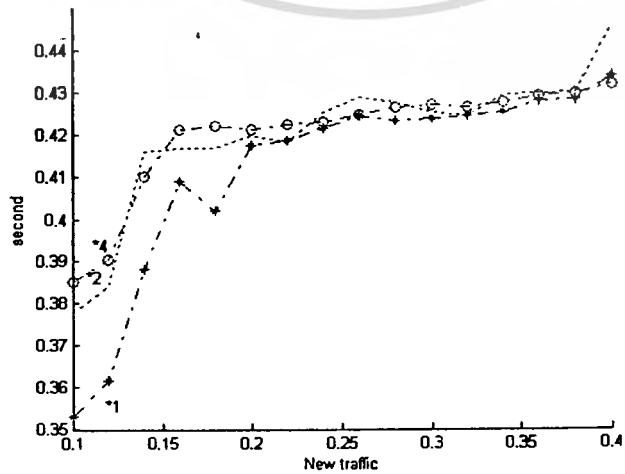

Figure 4.24 System with control approach under normal condition, N=35

This document is reserved for educational use only, not allowed for commercial use.
Forbidden to modify the content, and cite the document when use.

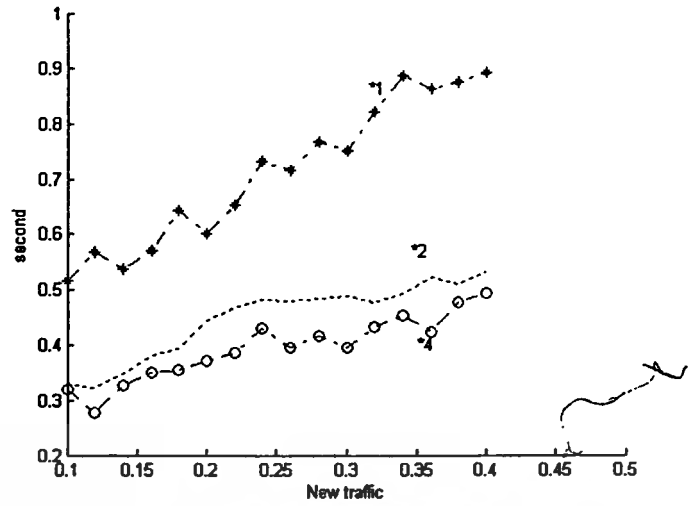

Figure 4.25 System with control approach under impaired condition, N=25.

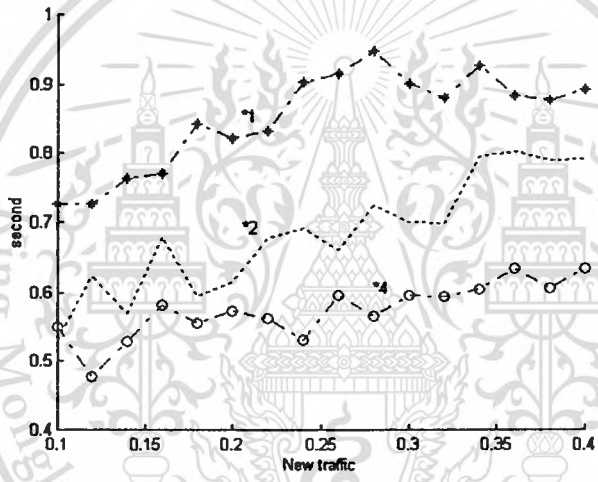

Figure 4.26 System with control approach under impaired condition, N=30

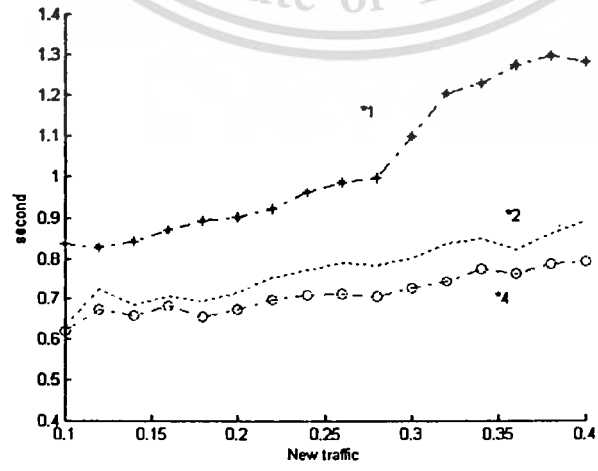

Figure 4.27 System with control approach under impaired condition, N=35

This material is reserved for educational use only, not allowed for commercial use.
Forbidden to modify the content, and cite the document when use.

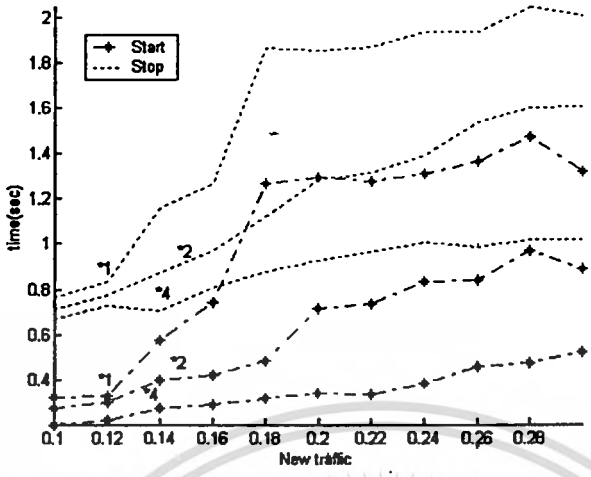

Figure 4.28 System stability.

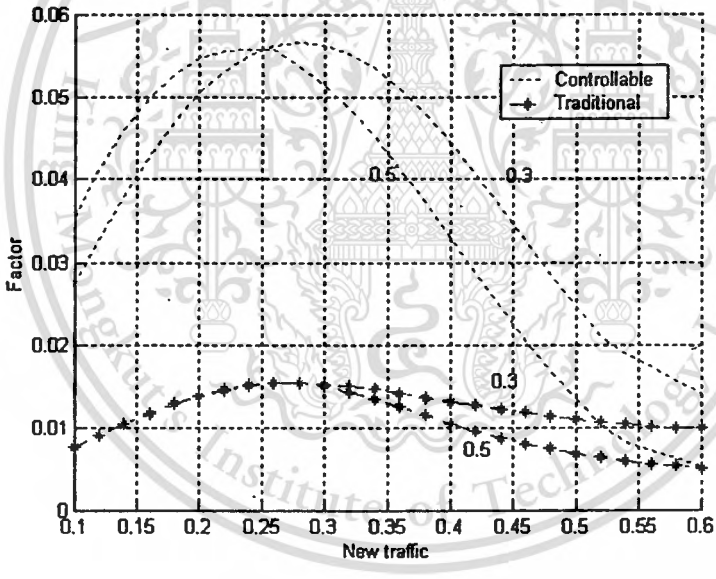

Figure 4.29 Power Factor (throughput/message delay) versus new traffic,

with $\mu_2 = 0.3$

This material is reserved for educational use only, not allowed for commercial use.
Forbidden to modify the content, and cite the document when use.

Chapter 5

Conclusion

Direct-Sequence Spread-Slotted ALOHA (DS-SSA) system has been developed for higher usage of channel capacity. However, with the characteristics of new applications and services, satisfactory performance is increasingly difficult to perform due to the difficulties described in chapter1. Moreover, in the fading or impaired environment of Land-mobile satellite, the features of DS-SSA itself are not enough to provide satisfactory solution for the long-term channel performance. To reduce the effect of these issues, this thesis proposes the architecture of DS-SSA system with modified node components and channel protocol in order to reduce the packet waiting time spent in each node and to construct a load control structure in which the service rates of each node can be dynamically adapted without using feedback information.

5.1 DS-SSA System with Modified Node Components

The modified node model which has been described in Chapter 4 comprises 3 queues. The first queue (Q_1) deals with newly arrival packets, while the second queue (Q_2) is used to store and manage the sequence of packets that are declared as collided traffic. The third queue (Q_3) is used to transmit a packet (new or retransmitted packet) to satellite channel in First-In-First-Out order. These are different from the traditional system model which is normally represented with single queue. By allocating an additional buffer as Q_2 for resolving problem packets, the concept of freely transmitting the packet in order to reduce time spent in the terminal's queues can be applied. Moreover, it can avoid the backlogged condition which is the main factor that makes the system susceptible to the delay figures. The results show that this model is more sensitive to the offered loads than the traditional ones. This is because we assume two individual queues contained in a terminal. When the channel status becomes worse by the result of heavy traffic, the number of terminals that have active-Q_2 rapidly increases, and the throughput reaches the saturated point faster than that of traditional one. On the contrary, it can be seen that the total message delay obtained from the controllable system is far better, since the terminal is allowed to freely send out the packets in their input queues and let Q_2 take care all the collided packets. This makes a message deal

This material is reserved for educational use only, not allowed for commercial use.
Forbidden to modify the content, and cite the document when use.

with only one propagation delay plus the waiting time in queue, multiplied by the number of segments contained in that message in case of no collision occurring. Packets are also kept waiting in the buffer for a shorter duration in Q_1 and Q_2. The conditions of the model and channel protocol can be concluded as follow :

- New traffic arriving at the terminal is assumed to be the variable-sized messages which can be divided into one or more packets.
- The average number of packets arriving at the channel during one slot duration is the offered load which consists of new and retransmission traffic.
- When a terminal has packet(s) waiting in its queues, they will be unconditionally sent out in order to reduce the time spending in the queue. This condition includes the case of collided packet.
- Assume that a terminal can process the new transmissions and retransmissions individually and independently.
- Require a simple control approach which can adjust the burstiness of the offered traffic to obtain overall system availability while maintaining individual user's performances.

5.2 Control Structure

As previously described, Q_2 is used to store and manage the sequence of packets that are declared as collision, its queue size associated with ACK messages can be considered as the parameters for determining the current status of the system and also for specifying the sending rate at which Q_1 should be performed. The total offer loads present to the satellite channel will be controlled by adjusting the output rate of Q_1 based on pre-assigned threshold. It can be seen from the results of power factor (Fig.23) that, under the disturbed environment, the controllable scheme still works well if the offered load presented within the mask of 30 percent below the saturation point. The area mask can be adjusted based on the control policy of the system.

This material is reserved for educational use only, not allowed for commercial use.
Forbidden to modify the content, and cite the document when use.

5.3 Discussion

By allocating an additional buffer as Q_2 for resolving problem packets, the terminal can manage two types of traffic independently. Furthermore, the terminal can sense the channel status by evaluating the size of this queue. Each terminal has been installed with load control structure in which its service rate can be dynamically adjusted based on the channel status and without using feedback information from the central HUB. When the number of terminals who have their second queue active is considered as the parameter of system status, it can be seen from the experiment results that the number of active terminal does not change much when varying the average departure rate assumed to be used in all terminals. Thus, to stabilize the whole system status, each terminal should be able to control its output traffic by adjusting the transmission rate of its first queue based on the behavior of its second queue.

King Mongkut's Institute of Technology Ladkrabang

This material is reserved for educational use only, not allowed for commercial use.
Forbidden to modify the content, and cite the document when use.

Reference

[1] W.C.Y. Lee, "Overview of cellular CDMA," *IEEE Trans. Vehic. Technol.*, vol. 40 no.2, May 1991.

[2] K. S. Gilhousen, I. M Jacobs, R. Padovani, A. J. Viterbi, L. A. Weaver, Jr., and E. Wheatley, " On the capacity of Cellular CDMA system," *IEEE Trans. Vehic. Technol.*, vol. 40 no.2, May 1991.

[3] R. L. Pickholtz, L. B. Milstein, and D. L. Shilling, "Spread Spectrum for mobile communications, "*IEEE Trans. Vehic. Technol.*, vol. 40 no.2, May 1991.

[4] T. T. Ha, "Digital Satellite Communication," McGraw-Hill, 1990.

[5] L. Kleinrock and S.S. Lam, "Packet Switching in a Slotted Satellite Channel," *NCC'73*, pp.703-710, 1973.

[6] Y. Onozato, "Performance Analysis of a Combined Random Reservation Access Scheme, " *IEEE Trans. Commun.*, April 1991.

[7] Fuji and Matsumoto, "AA/TDMA adaptive satellite access method for mini-earth station network," *Conf. Rec. Proc. Globecom'86.* pp. 1464-1499, December 1986.

[8] J. G. Proakis, "Digital Communications," Third edition, New York, McGraw Hill, 1995.

[9] R. Gold, "Maximal Recursive Sequences with 3-valued Recursive Cross-Correlation Functions," *IEEE Trans. Infor. Theory*, Jan., 1968, pp. 154-156.

[10] R. Gold, "Optimal Binary Sequences for Spread Spectrum Multiplexing, *IEEE Trans. Infor. Theory,* Oct., 1967, pp. 619-621.

[11] D.V. Sarwate, and M. B. Pursley, "Crosscorrelation Properties of Pseudorandom and Related Sequences," *Proc. IEEE,* Vol. 68, No. 5, May, 1980, pp. 583-619.

[12] R. Neil Braithwaite, "Using Walsh Code Selection to Reduce the Power Variance of Bandlimited Forward link CDMA Waveforms," *Electronic Systems Laboratory*
HP Laboratories Palo Alto, HPL-1999-87, July, 1999.

[13] B. J. Wysocki, T. A. Wysocki, "Modified Walsh-Hadamard Sequences for DS CDMA Wireless System," University of Wollongong, Northfields Avenue, Wollongong, NSW 2522, Australia.

[14] B. J. Wysocki, T. A. Wysocki, "Orthogonal Binary Sequences with Wide Range of Correlation Properties," School of Electrical, Computer and Telecom Engineering, University of Wollongong, NSW 2522, Australia.

This thesis is protected by copyright. Forbidden to modify the content, and cite the document when use.

[15] R. G. Cheng, "An Introduction to CDMA Air Interface: TIA/EIA/IS-95A," Advanced Technology Center, Computer & Communications Research Laboratories, Industrial Technology Research Institute, Taiwan.

[16] Y. Yang, T. P. Yum, "Maximally Flexible Assignment of Orthogonal Variable Spreading Factor Codes for Multi-Rate Traffic," Department of Information Engineering, The Chinese University of Hong Kong, Shatin, Hong Kong.

[17] M.B. Pursley, "Performance Evaluation for Phase-Coded Spread-Spectrum multiple-access communication –Part I: System Analysis," *IEEE Trans. Commun.*, vol. Com 25, Aug 1977.

[18] R. K. Morrow and J. S. Lehnert, "Bit-to-bit error dependence in slotted DS/SSMA acket systems with random signature sequences," *IEEE Trans. Commun.*,vol. COM-37, Oct. 1989.

[19] M. B. Pursley, "Performance Evaluation for Phase-Coded Spread-Spectrum multiple-access communication –Part II: Code Sequence ," *IEEE Trans. Commun.*, vol. Com 25, Aug 1977.

[20] P. A. Bello, "Characterization of Randomly Time-Variant Linear Channels," *IEEE Trans. Commun. Sys.*, vol. CS-I 1, no. 4, Dec. 1963, pp. 360-93.

[21] F. Amoroso, "The Bandwidth of Digital Data Signals," *IEEE Commun.Mag.*, vol. 18, no. 6, Nov. 1980, pp. 13-24.

[22] Petr. Beckmann, "Probability in Communication Engineering," *Hartcourt, Brace&World 1967.*

[23] C. Loo, "Measurements and models of a land-mobile satellite channel and their applicaiotn to MSK signals," *IEEE Trans. Vehic. Technol.*, vol. VT-36, Aug 1987.

[24] A. Papoulis, "Probability, random variables and stochastic processes," McGraw-Hill Inc. Third edition, 1991.

[25] M.K.Simon, J.K.Omura, R.A.Scholtz and B.K.Levitt, *Spread Spectrum Communications Handbook.* McGraw Hill, 1994.

[26] J. P. Castro, " Statistic Observation of data transmission over Land Mobile Satellite Channels," *IEEE J. Select Area Comm.*, October 1992.

[27] E. Lutz , D. Cygan, M. Dippold, F. Dolainsky and W. Papke, "The land mobile satellite communication channel-recording, Statistics and channel model," *IEEE Trans. On Vehicular,* vol.40, May 1991.

[28] C. Loo, "Digital transmissiont through a land-mobile satellite channel," *IEEE Trans. Commun. Sys.*, vol.38, no. 5, May 1990.

This material is reserved for educational use only, not allowed for commercial use.

Forbidden to modify the content, and cite the document when use.

[29] R. D. J. Van nee, H.S. Misser, "Direct-Sequence spread spectrum in a shadowed Rician fading land-mobile satellite channel," *IEEE J. Select Area Comm.,* vol. 10, no.2, Feb. 1995.

[30] R. L Peterson, R. E. Ziemer, and D. E. Borth, "Introduction to Spread Spectrum Communications," Prentice Hall International Editions, 1995.

[31] X. Cai, Y. Sun, Ali N. Akansu, " Performance of CDMA random access system with packet combining in fading channels," *IEEE Trans Commun.*, Vol. 2, No.3, May 2003.

[32] F. A. Tobagi, "Multiple access Protocols in Packet Communication systems", *IEEE Trans Commun.*, Vol. COM-28, No.4, April 1980.

[33] T. Saadawi, A. Ephremides, "Analysis, Stability and Optimization of Slotted ALOHA with a Finite Number of Buffered Users", *IEEE Trans on Automated Control*, June 1981.

[34] R. Al-Naami, "Queuing analysis of slotted ALOHA with finite buffer capacity, "IEEE Globecom'93, pp.1139-43, 1993.

[35] X. X. Yao, O. W. Yang, "A queuing analysis of slotted ALOHA system, "IEEE CCECE'93, pp.1234-38, 1993.

[36] D. Makrakis, K. M. Sundara Murthy, "Spread Slotted ALOHA Techniques for Mobile and Personal Satellite Communication Systems," *IEEE J. Select. Areas Commun.*, vol. 10, no.6, Aug. 1992.

[37] R. D. J. van Nee, R.N. van Wolfswinkel, "Slotted ALOHA and Code Division Multiple Access Techniques for Land-Mobile Satellite Personal Communications", *IEEE Trans Commun.*, Vol. COM-13, No.2, Feb 1995.

[38] P. W. de Graaf, J. S. Lehnert, "Performance Comparison of a Slotted ALOHA DS/SSMA network and a Multichannel Narrow-Band Slotted ALOHA Network", *IEEE Trans Commun.*, Vol. COM-46, No.4, April 1998.

[39] L. Kleinrock, Queuing Systems, Vol.1. John Wiley & Sons, New York, 1975.

This material is reserved for educational use only, not allowed for commercial use.

Forbidden to modify the content, and cite the document when use.

Appendix A

Spectrum of Triangular Pulse

Assume that the function of triangular pulse is defined by

$$w(t) = \Lambda(t/T) \triangleq \begin{cases} 1 - \dfrac{|t|}{T} & ;|t| \le T \\ 0 & ;|t| \ge T \end{cases} \tag{A.1}$$

Using the integral property, then

$$\frac{dw(t)}{dt} = \frac{1}{T}u(t+T) - \frac{2}{T}u(t) + \frac{1}{T}u(t-T) \tag{A.2}$$

and

$$\frac{d^2w(t)}{dt} = \frac{1}{T}\delta(t+T) - \frac{2}{T}\delta(t) + \frac{1}{T}\delta(t-T) \tag{A.3}$$

where $\delta(t)$ is the Dirac Delta function. Using the Fourier transform, we have

$$\frac{d^2w(t)}{dt} \leftrightarrow \frac{1}{T}e^{j\omega t} - \frac{2}{T} + \frac{1}{T}e^{-j\omega t} \leftrightarrow \frac{1}{T}(e^{j\omega T/2} - e^{-j\omega T/2})^2 = \frac{-4}{T}(\sin \pi f T)^2$$

Integrating twice, then

$$w(t) \leftrightarrow \frac{-4}{T}\frac{(\sin \pi f T)^2}{(j2\pi f)^2} \tag{A.4}$$

Another method to obtain the spectrum of the Triangular pulse is by using the convolution theorem. If the rectangular pulse is convolved with itself and then scaled by the constant *1/T*, the resulting time waveform is the triangular pulse. Applying the convolution theorem, the spectrum for the triangular pulse can be obtained by multiplying the spectrum of the rectangular pulse with itself and scaling with a constant *1/T*.

This material is reserved for educational use only, not allowed for commercial use.
Forbidden to modify the content, and cite the document when use.

Appendix B

Chernoff Bound

Let $x_1, x_2, ..., x_n$ be independent random variables where $x_i \in \{0,1\}$ for all $i \le n$. Then if X is the sum of the $\{x_i\}$ and if μ is the expected value of X, we have

$$\mu = \sum_i E[x_i] \quad \text{(independent of } X_i\text{)} \tag{B.1}$$

Thus, the probability that X deviates from μ is

$$P_r[X > \delta\mu] \le \exp(-\rho\delta\mu)E[\exp(\rho X)] \tag{B.2}$$

When the tighter upper bound can be obtained with the minimum value of ρ.

Proof: To establish the bound, we first write the density function $f_x(w)$ in the form of inequality

$$P_r[X > x] = \int_{-\infty}^{\infty} u(X - x) f_X(w) dw \tag{B.3}$$

where $u(.)$ is the unit step function.

Using the inequality $u(w - x) \le \exp(\rho(w - x)); \rho > 0$, to establish the bound

$$P_r(X > x) \le \int_{-\infty}^{\infty} \exp(\rho(X - x)) f_X(w) dx \tag{B.4}$$

Recall that the integral on the right hand side of this equation is in the form of the first moment generating function, then we have

$$P_r(X > x) \le \exp(-\rho x) E[\exp(\rho X)] \tag{B.5}$$

which is the required bounding formula.

This material is reserved for educational use only, not allowed for commercial use.
Forbidden to modify the content, and cite the document when use.

Appendix C

Simulation Tool

In this thesis, OPNET software is used to model and simulate the system and channel behavior. The model can be categorized into three levels,

1. Network Level
2. Node level
3. Process level(Finite-state diagram)

Network Level

Network level shows all the relevant components which, in this study, comprises the ground stations (node) and satellite channel(Satellite) as shown in Figure C.1.

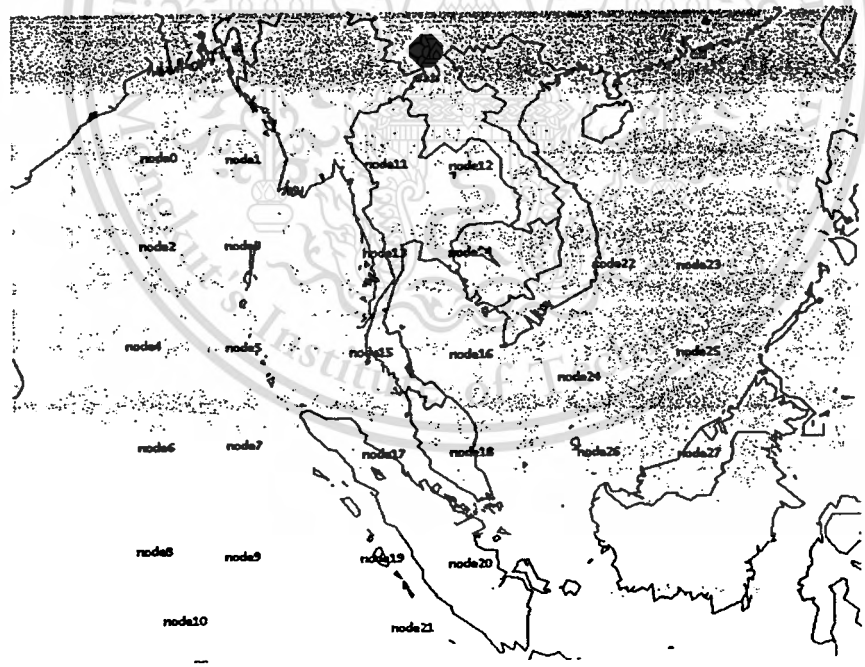

Figure C.1 Network Model

This material is reserved for educational use only, not allowed for commercial use.
Forbidden to modify the content, and cite the document when use.

Node level

As seen from the figure, there are only two types of nodes, ground station and satellite. They are shown in Figure C.2 and C.3, respectively.

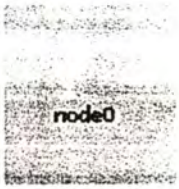

Figure C.2 Symbol of ground station

Figure C.3 Symbol of satellite channel station

When we select the symbol of station and satellite, it will go into the second level. This level can be called "Protocol" function of the ground station.

Figure C.4 Protocol components of ground station.

Figure C.5 Protocol components of satellite node.

Process level

If either "src" or "mac" node is selected, it will go into the third level which is called "Process" level which contains finite state diagram as shown in Figure C.6-C.8.

This material is reserved for educational use only, not allowed for commercial use.
Forbidden to modify the content, and cite the document when use.

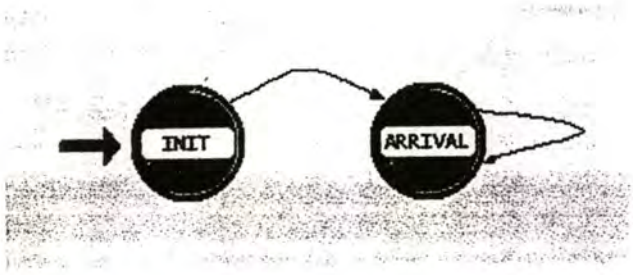

Figure C.6 Finite State diagram of "src".

Each state symbol contains the OPNET-based program structure inside. All link symbols between each state have particular meanings, and are the major components that make the model workable. Interruption between states is defined over these link symbols. With this structure, we can perform the experiments based on the model that has been designed.

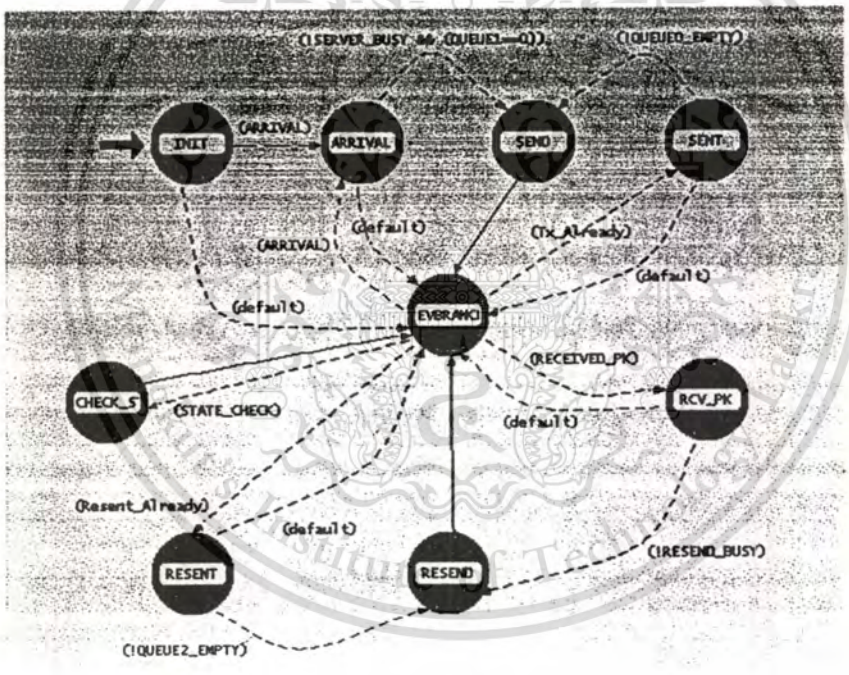

Figure C.7 Finite State diagram of "mac".

This material is reserved for educational use only, not allowed for commercial use.
Forbidden to modify the content, and cite the document when use.

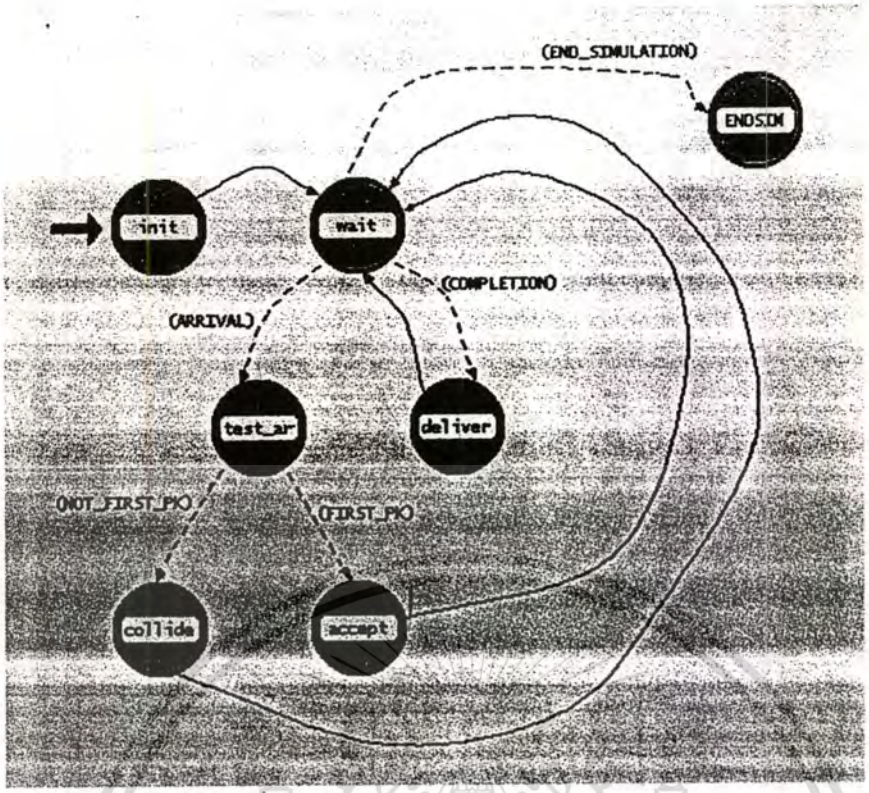

Figure C.8 Finite State diagram of "channel"

This material is reserved for educational use only, not allowed for commercial use.
Forbidden to modify the content, and cite the document when use.

Appendix D

Published Work

[1] S. Asvaruk, S. Sittichevapak, R. Varakulsiripunth, "Some General Approaches for Performance analysis of the ALOHA-Based Satellite Channel," IEEE Asia-Pacific Conference on Circuits and Systems, Nov 1998, Thailand, pp. 487-490

[2] S. Asvaruk, S. Sittichevapak, R. Varakulsiripunth, "Alarm Measure for Impaired Mobile Satellite Channel Using Direct-Sequence Spread-Slotted ALOHA Scheme," IEEE International Symposium on Intelligent Signal Processing and Communication system, Dec 1999, Thailand, pp. 1-4.

[3] S. Asvaruk, S. Sittichevapak, R. Varakulsiripunth, Y. Kato, N. Shiratori, "Performance Analysis on the Controllable Slotted DS-CDMA with an Allocating Buffer for Collided Traffic" IEICE Trans. on Communication, June 2005.

King Mongkut's Institute of Technology Ladkrabang

This material is reserved for educational use only, not allowed for commercial use.

Forbidden to modify the content, and cite the document when use.

PROCEEDINGS

IEEE

ISPACS'99

1999 IEEE International Symposium on Intelligent Signal Processing and Communication Systems

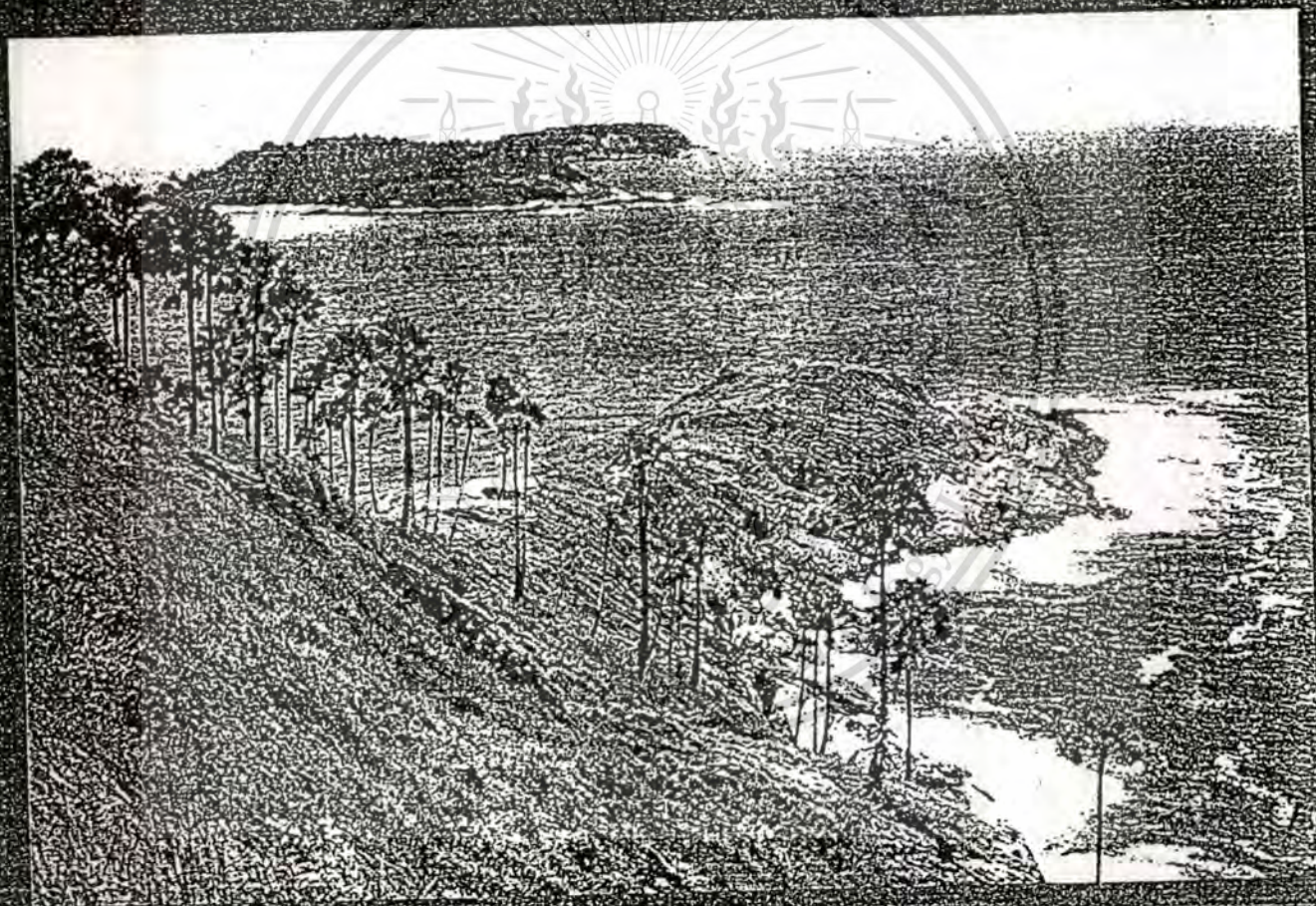

Signal Processing and Communications Beyond 2000

December 8-10, 1999

This material is reserved for educational use only, not allowed for commercial use.
Forbidden to modify this document, and cite the document when use.

EIC JICA NSTDA

Alarm Measure for Impaired Mobile Satellite Channel Using Direct-Sequence Spread Slotted ALOHA Scheme

Seri Asvaruk, Suvepol Sittichevapak and Ruttikorn Varakulsiripunth
Faculty of Engineering and Research Center for Communication and Information Technology,
King Mongkut's Institute of Technology Ladkrabang, Bangkok 10520, Thailand
Phone: (662)7372500 Ext.5028, Email: kusuvepo@kmitl.ac.th

Abstract

This paper study the method for identifying alarm measure when system channel is going to suffers in performance due to the excess multiple-access interference and impaired channel characteristics caused by long-term and short-term fading. Channel expressions obtained in this analysis are based on the characteristics of Direct-sequence spread slotted ALOHA system under fading and shadowing effect. To achieve this, we compare SNR of DS-SSA to threshold probability which is relative to common level of fade depth. Numerical and simulation results of decision are presented in case of the bad state assumed to be when the user who has been assigned margin encounters undesired random variability of signal amplitude in which a short-term variation is superimposed on a long-term variation.

1. Introduction

In multiple access architectures such as slotted or unslotted ALOHA and Spread-spectrum random access, several classes of packet streams containing various traffic characteristics share channel resources and statistically perform traffic loads to the system. This load results in unstable behavior in which low throughput and high delay may be experienced. Such undesirable condition also occurs in the spread-slotted ALOHA(SSA) system in which hybrid schemes of slotted ALOHA and spread-spectrum multiple access are exploited. By deriving the distribution of interference variance over all possible phase and delay, we obtain root mean square(r.m.s) value of noise plus interference. This paper study the method of using user packets as an alarm measure when system channel is going to suffers in performance due to the excess multiple-access interference and impaired channel characteristics caused by long-term and short-term fading. The former fading effect is possibly reduced by adding margin into LOS component or using diversity schemes, but the latter is more difficult since any restricted areas in close vicinity may need vastly different margin. If improper adding power is used, the signal from that terminal will becomes significant interference to other users, especially, in the spread-slotted ALOHA system where all users operate in time-coordinate burst mode. Although hardware counteraction have been exploited, particular protocol having ability to adjust traffic loads in order to sustain system stability is necessary. The method of identifying point of state transition is considered by mean of an alarm packet which contains the number of error bits more than that was bounded. When an alarm packet is detected, system can decide the process to protect or moderate the effect of degradation. The total number of error bits in a packet may or may not exceed "t" bit errors which can be completely corrected by a FEC code.

2. Characterization of SSA Channel

In this section, we consider channel characteristics of SSA scheme under impaired environment, as depicted in Fig.1.

In satellite mobile system, line-of-sight signal become a dominant component since the propagation environment is less hostile than that in the terrestrial link, unless the system is operated under the circumstance close to zero elevation angle. Such circumstance is normally treated as an exceptional area for usage because it requires more link margin for reparation to high shadowing, propagation loss and interference caused by other users. It is also important to state that channel is assumed to operate in frequency non-selective channel and multipath characteristics do not change the correlation properties of spreading sequences.

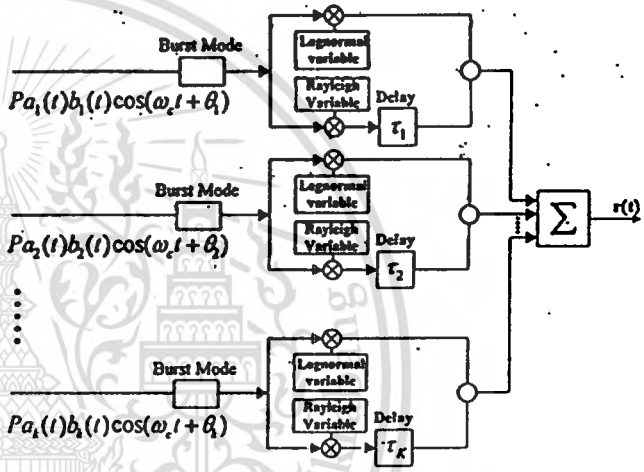

Fig. 1 Basic SSA Channel

A. System Performance : Bound on error Probability.

To simplify the analysis, we assume tracking error results of signal and phase can be neglected. We also define burst(slot) mode at each users is constantly synchronized to satellite channel slot. Following Pursley[1], Assume that K users occupies simultaneously a satellite timeslot and each transmits a signal :

$$s_k(t) = P_t b_k(t) a_k(t) \cos(\omega_c t + \theta_k) \qquad (1)$$

where P_t is transmitted signal amplitude, $b_k(t) \in \{+1,-1\}$ is user binary sequence, $a_k(t) \in \{+1,-1\}$ is spectral-spread PN sequence which is generated at a period of N chips and θ_k is carrier phase. If the desired user is user 1, after sequence correlation and coherent demodulation, we have signal at the receiver output :

$$\begin{aligned} r_1(t) = & \sum_{n=1}^{N} b_1(t) P_{11} \cos\phi_{11} \\ & + \sum_{k=2}^{K} P_{1k} (b_k^{-1} . R_{1,k}(\tau_{1k}) + b_k^0 . \hat{R}_{1,k}(\tau_{1k})) \cos\phi_{1k} \\ & + \sum_{k=2}^{K} \sum_{m=2}^{M} P_{mk} (b_k^{-1} . R_{1,k}(\tau_{mk}) + b_k^0 . \hat{R}_{1,k}(\tau_{mk})) \cos\phi_{mk} \\ & + \eta_n \end{aligned} \qquad (2)$$

Here τ, ϕ and P are time delays, phase shift and signal amplitude respectively. If T_c is chip duration of PN sequence, NT_c represents one period of user data bit(T_b). Random variable η_n is Gaussian

Copyright© by Chiang Mai University
All rights reserved
This document is provided for educational use only, not allowed for commercial use.

noise with mean equal to zero and variance σ_n^2. $b_{mk}(t) \in \{+1,-1\}$ is user data sequence and $a_{mk}(t) \in \{+1,-1\}$ is code sequence. where k and m denote the user who transmits this signal and its propagation path, respectively. The relation of equation (2) is computed with respect to the independent random variables P, τ, ϕ, $a(k)$ and $b(k)$. The second and third term of the right-hand side of (2) state the events of direct and multipath components, respectively. b_k^{-1} and b_k^0 are previous and current user data bits, and $R_{1,k}$ and $\hat{R}_{1,k}$ [1] are partial cross-correlation function defined by:

$$R_{1,k}(\tau) = \int_0^{\tau} a_k(t-\tau)a_1(t)dt$$

$$\hat{R}_{1,k}(\tau) = \int_{\tau}^{T_b} a_k(t-\tau)a_1(t)dt$$

For simplicity, we assume $\tau_{11} = 0$, $\phi_{11} = 0$, equal received power for all signals traveling in direct(line-of-sight) link which free from shadowing, and let interference caused by multipath signals which are inadvertently produced by desired user be characterized as Gaussian random variable and included in η_o. We also assume ϕ_{mk} is uniformly distributed on the interval $[0,2\pi]$ and τ_{mk} is uniformly distributed on the interval $[0,T_b]$. As stated in Pursley[2], the maximum value of the term $[(b_k^{-1}.R_{1,k}(\tau) + b_k^0.\hat{R}_{1,k}(\tau))\cos\phi]$ in equation (2) is achieved when τ is an integer multiple of T_C and when ϕ=0. Thus equation (2) can be rewritten in the form

$$r_1(t) = Nb_1 + \sum_{m=2}^{N} b_k^0 \psi_c \cos\phi_{11} + \sum_{m=2}^{M} \rho\psi_a \mu \cos\varphi_{m1} + \sum_{k=2}^{K}\sum_{m=2}^{M} \psi_{max}\Delta_{mk}\cos\phi_{1k} + \eta_o \quad (3)$$

where Δ_{mk} symbolizes amplitude of multipath components which are normalized with received amplitude level of the first path. ψ_c is the maximum periodic cross-correlation magnitude over all k, and $\hat{\psi}_c$ is the maximum of odd cross-correlation magnitude[2].

In some practical purpose, not only average or estimate results obtained from statistical evaluation of the experiment, but also the upper bound values are required to optimize appropriate parameters. We adopt Chernoff bounds technique described in Viterbi[3] to analyze the upper bound of error probability. Assuming the occurrence of data bits -1 and 1 are equiprobable, we obtain simple expression of bit error probability :

$$P_{E,up} = \Pr\{r_{out} > 0 \mid b_1 = -1\} < E\{\exp[\rho r_{out}]\} \quad (4)$$

Given real number $\rho > 0$.

By using the expression, we have in place of (2),

$$P_{E,up} < \exp[-\rho N].\prod_{k=2}^{K} E[\exp(\rho\psi_c b_k^0 \cos\phi_{1k})] \cdot \prod_{k=2}^{K}\prod_{m=2}^{M} E[\frac{1}{2}\exp(\pm\rho\psi_{1k}\Delta_{mk}\cos\phi_{mk}) + \frac{1}{2}\exp(\pm\rho\hat{\psi}_{1k}\Delta_{mk}\cos\phi_{mk})] \cdot \prod_{m=2}^{M} E[\exp(\rho\psi_a\mu\cos\phi_{m1})] \cdot E[\exp(\rho\eta_o)] \quad (5)$$

Since the 3rd term of the right-hand side is depend on multipath components from relative propagation paths, each arriving signals will have Rayleigh distributed gain and uniformly distributed phase. Then

$$= \prod_{k=2}^{K}\prod_{m=2}^{M} \frac{\Delta_{mk}}{\alpha}\int_0^{\infty}\exp(\frac{-\Delta_{mk}^2}{\alpha}).[I_0(\rho\psi_c\Delta_{mk}) + I_0(\rho\hat{\psi}_c\Delta_{mk})]d\Delta$$

$$= \prod_{k=2}^{K}\prod_{m=2}^{M}[\exp(\psi_c) + \exp(\hat{\psi}_c)]^{\frac{\rho^2\alpha}{4}} \quad (6)$$

where $I_0(x) = \frac{1}{2\pi}\int_0^{2\pi}\exp(x\cos\theta)d\theta$

and

$$E[\exp(\rho\eta_o)] = \int_{-\infty}^{\infty}\frac{1}{\sqrt{\pi\alpha_\eta}}\exp(\frac{2\rho\eta_o - \eta_o^2}{\alpha_\eta})d\eta = \exp(\frac{1}{4}\alpha_\eta\rho^2) \quad (7)$$

Thus

$$P_{E,up} < \exp[-\rho N].\prod_{k=2}^{K} I_0(\rho\psi_c).\prod_{m=2}^{M} I_0(\rho\psi_a\mu) \cdot \prod_{k=2}^{K}\prod_{m=2}^{M}[\exp(\psi_{1k}) + \exp(\hat{\psi}_{1k})]^{\frac{\rho^2\alpha}{4}} .\exp(\frac{1}{4}\alpha_\eta\rho^2) \quad (8)$$

B. System Performance : Guassian approximation.

Let us start by considering signal at the receiver output with respect to chip duration(T_C). We have

$$y_n = P_{11}a_{11}(t) + n_c \quad (9)$$

Note that Gaussian noise n_c is different from η_o identified in (2) since it comprises system noise plus multiple-access interference defined from correlator output[1][4]. Multiple-access interference will be modeled as a Guassian random variable with the distribution specified by means and variance. Assuming the data bits are equiprobable and following the concept of discrete aperiodic and continuous-time partial cross-correlation functions described in [2] [3]. From the correlator output, we reorganized noise variance as

$$\sigma_{out}^2 = \frac{1}{2T_b}\{\sum_{k=2}^{K}(E[P_{1k}^2].\sum_{l=0}^{N-1}(R_{1,k}^2(\tau_0) + \hat{R}_{1,k}^2(\tau_0)))) + \sum_{k=2}^{K}\sum_{m=2}^{M}(E[P_{mk}^2].\sum_{l=0}^{N-1}\int_{l_{T_c}}^{(l+1)T_c} R_{1,k}^2(\tau_{mk})$$

This material is reserved for educational use only, not allowed for commercial use.
Forbidden to modify the content, and cite the document when use.

$$+\hat{R}_{l,k}^2(\tau_{mk})d\tau)\}+\frac{N_o T_b}{4} \quad (10)$$

where M is multipath components and $0 \le lT_c \le T_b$.

After some algebraic manipulations, we have r.m.s noise

$$n_c = \{(k-1)\psi_c^2[\frac{3\mu_L^2 \exp(\sigma_L^2)+4\sigma_R^2}{6N} + \frac{N_0 T_b}{4}\}^{1/2} \quad (11)$$

Where σ_L^2 and μ_L are variance and mean of long-term (lognormal) fading. σ_R^2 and T_b are mean signal power of multipath components and data period ,respectively.

C. State Probability

To moderate the effect of long-term fading, a margin is assigned to users when they are passing fading region. This can be achieved by recorded data related to satellite angle which has been kept in on-board processor. We consider the case when a signal X dBm oscillating by W dB around area mean of fading, M dBm (users are assigned M-dB margin when moving into a specific area), $X = M + W$, while area mean W dB is the combined result of short-term(Rayleigh variables) and long-term fading (Lognormal variables) around its local mean, $W = y + \beta_w$. We use the general concepts that the cumulative distribution for a random variable $z = x + y$ is given by

$$P(z) = \int_{-\infty}^{\infty} P(z-y)p(y)dy$$

Thus, the probability that the envelope level does not cross a specified level W dB below long-term margin is:

$$P_w = \int_{-\infty}^{\infty} \frac{\exp(-w^2/2\sigma_L^2).\exp(10^{0.1\beta_w})dw}{\sqrt{2\pi}\sigma_L} \quad (12)$$

Let β_w be defined as fade depth factor.

This equation bases on the assumption that short-term fluctuation variables and slowly varying variables are statistically independent[5][6].

C. Average Fade Duration(AFD)

According to Castro[7], AFD is defined by the equation

$$AFD = \frac{1}{N_w(w)} \int_0^{r_b} f_w(w)dw - \frac{P_w}{N_w(w)} \quad (13)$$

where $N_w(w)$ is the level crossing rate defined as the expected rate at which the envelope crosses a specific signal envelope with the negative slope(downward LCR), and P_w is the cumulative distribution function given in (12)

3. Numerical Results

This section presents some numerical and simulation results for channel performance under a number of different conditions. Since β_w depends strongly on shadow characteristic as well as long-term margin, we will treat β_w as the key parameter. To evaluate channel behavior in different circumstance, we have four environment conditions obtained from the experiment results recorded in Lutz[8] and rearranged in Table I.

Table I Channel Parameters

Case	$\mu_L(dB)$	$\sigma_L(dB)$	$\sigma_R(dB)$
1	-12.9	5	11.9
2	-11.8	4.0	9.3
3	-8.8	3.8	11.7
4	-7.7	6	11.9

Fig. 2 illustrates the upper bound or guaranteed probability of bit error as a function of received signal variance under short-term fading. With regard to the condition that each user has been assigned margin to compensate long-term fading, we fix mean signal gain(μ_L) equal to 0 and -3 dB, optimum factor(ρ)=0.115, the number of user K=10, and M=5 for each user. Since signal gain -3 dB below threshold causes small effect on channel performance, variance(σ_R^2) related to short-term variation can be viewed as a major factor. We obtained from Fig.2 the maximum probability of bit error in case of clear sky and impaired link. With reference to Fig.3, results of E_b/I_0 versus β_w with channel parameter according to Table I show the relation between signal gain due to fading E_b/I_0. Parameters use in the experiment are K=10, M=5 and N=127. The curve indicated that σ_R^2 is likely to dominate the SNR while μ_L has the least effect. According to Fig.2, σ_R^2 can be used as an indicator of the channel behavior. If statistic information of each region was known, we would have important parameter such as average fade duration(AFD) as a reference data in associate with the specified threshold envelope.

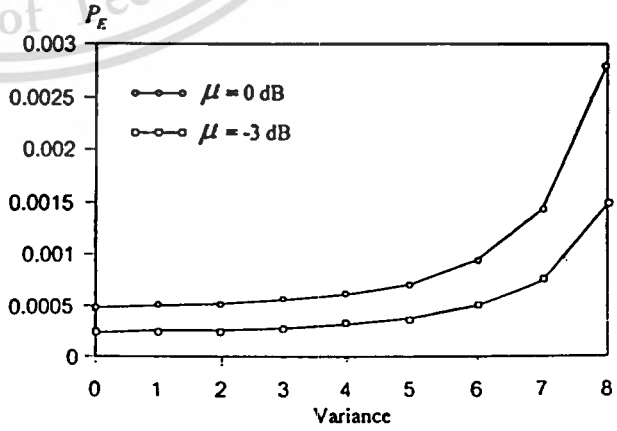

Fig. 2 Upper bound process : P_E versus received signal Variance for $\mu_L = 0$ dB and $\mu_L = -3$ dB

This material is reserved for educational use only, not allowed for commercial use.
Forbidden to modify the content, and cite the document when use.

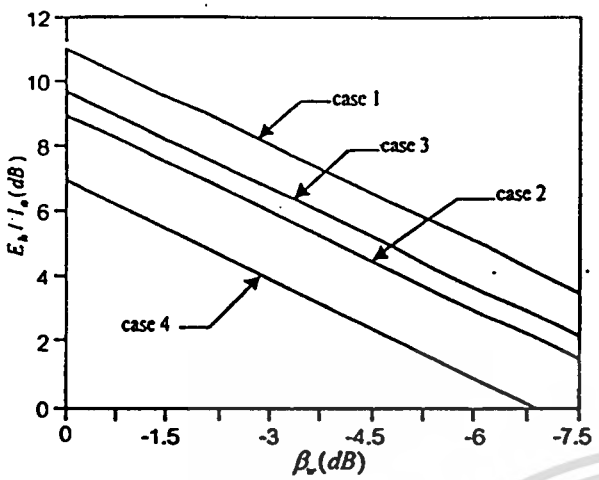

Fig. 3 E_b/I_O versus β_w for channel parameter case 1 to 4.

This can be done when momentary fade duration is assumed to exceed two consecutive packets.

In case we select transition threshold at lower values of fade depth factor(higher values of E_b/I_O), probability that signal fluctuation will be kept within threshold level and probability of bit error(derived from Gaussian approximation method) are increased, as shown in Fig.4 and Fig.5, but duration of fade is also extended. Long fade duration tend to obscure the received information and higher order of FEC is required to improve system performance in this state. The results obtained from Fig.2 to Fig. 5 can be concluded by following iteration route

$$\ldots - P_E - \beta_w - P_w - E_b/I_O - P_E - \beta_w - P_w \ldots E_b/I_O - \ldots$$

which are bounded by P_E derived from equation (8).

When bit error probability(P_E) is known, the simplest method to derive packet error probability is by following equation

$$P_{packet} = \sum_{i=0}^{x} \left(\frac{L}{i}\right)(P_E)^i(1-P_E)^{L-i}$$

where L is the number of bits in a packet.

Based on above diagram, designer can design point of alarm based on "x" error bits within a received packet in accordance with AFD. Range of both x and AFD are limited by means of upper-bounded P_E.

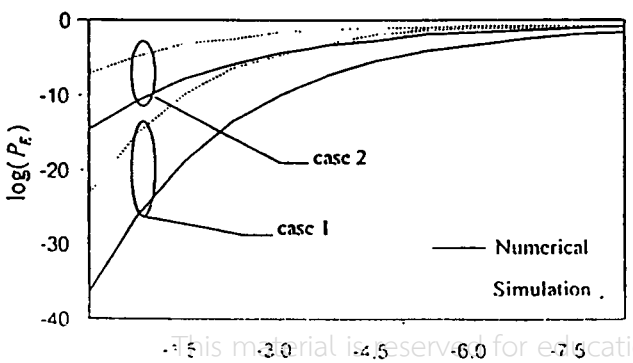

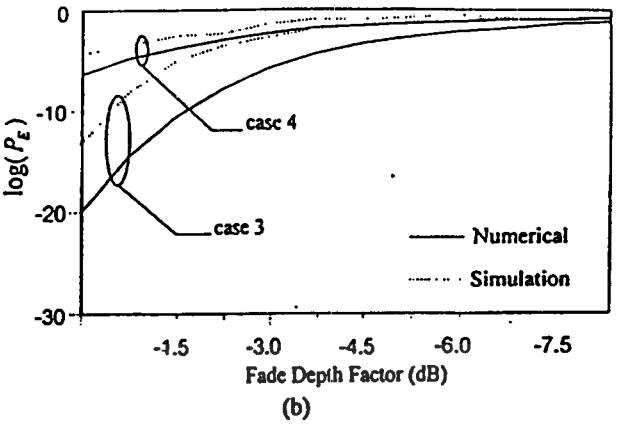

Fig. 4 P_E versus fade depth factor(β_w) for channel parameter (a) case 1 and 2, (b) case 3 and 4.

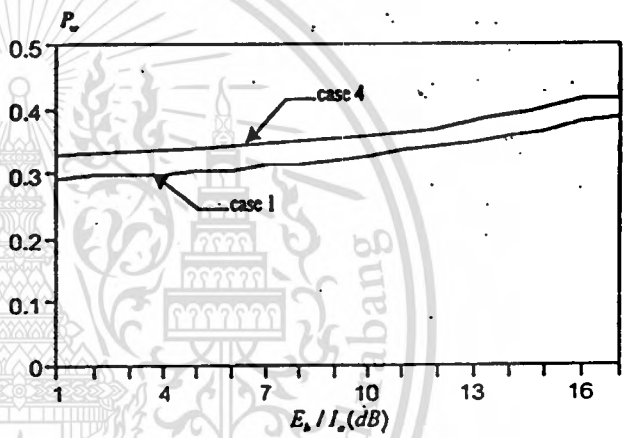

Fig. 5 P_w versus E_b/I_O for channel parameter case 1 and 4.

References

[1] Michael Pursley, "Performance evaluation for phase-coded spread-spectrum multiple-access communication -Part I: System Analysis," *IEEE Trans. Commun.*, August 1977.

[2] Michael Pursley, "Performance evaluation for phase-coded spread-spectrum multiple-access communication-Part II: Code Sequence Analysis," *IEEE Trans. Commun.*, August 1977.

[3] Andrew J. Viterbi, "Principles of spread spectrum communication," *Addison-Wesley*, 1995.

[4] S.O.Rice, "Statistical properties of a sine wave plus random noise," *Bell Syst.., vol. 27*, Jan 1948

[5] Petr Beckmann, "Probability in communication engineering," *Harcourt, Brace&World* 1967.

[6] Michel D. Yacoub, "Foundation of mobile radio Engineering," *CRC Press*, 1993

[7] Jonathan P. Castro, "Statistic observation of data transmission over Land Mobile Satellite Channels," *IEEE J. Select Area Comm.* October 1992.

[8] E.Lutz,D. Cygan, M. Dippold, F. Dolainsky,W. Papke, "The land mobile satellite Communication Channel-Recording, statistics, and Channel Model," *IEEE Trans. on Vehicular, vol.40*, May 1991.

This material is reserved for educational use only, not allowed for commercial use.
Forbidden to modify the content, and cite the document when use.

IEEE

IEEE
APCCAS
1998

NECTEC

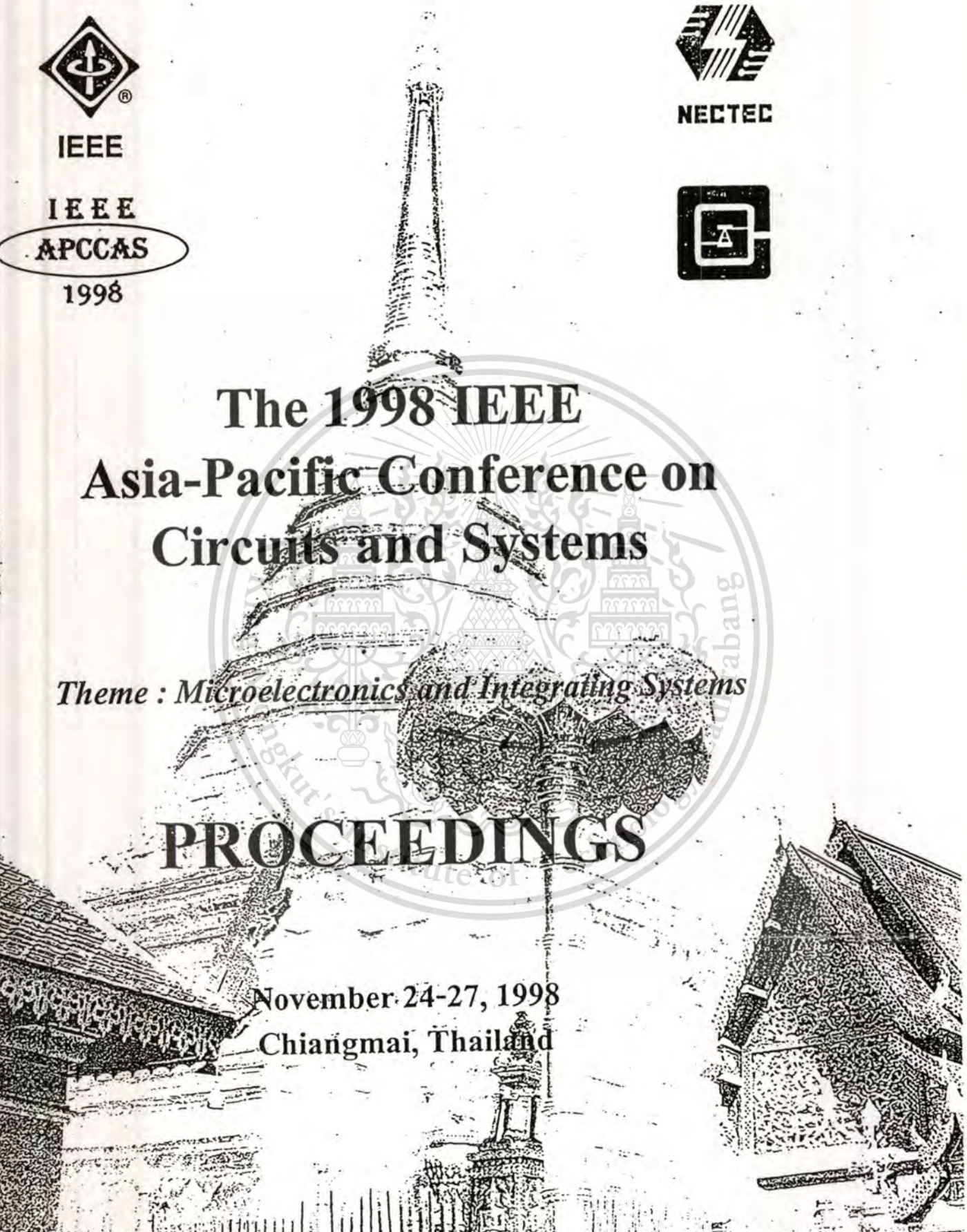

The 1998 IEEE Asia-Pacific Conference on Circuits and Systems

Theme : Microelectronics and Integrating Systems

PROCEEDINGS

November 24-27, 1998
Chiangmai, Thailand

IEEE Catalog Number : 98EX242

Some General Approaches for Performance Analysis of the ALOHA-Based Satellite Channel

Seri Assavaruk, Suvipol Sittichevapak and Ruttikorn Varakulsiripunth
Faculty of Engineering & Research Center for Communication and Information Technology
King Mongkut's Institute of Technology Ladkrabang, Bangkok 10520, Thailand
Phone : 02-3269968, Fax : 02-3269965, e-mail : kvruttik@kmitl.ac.th

Abstract

Satellite link has been employing as the minor part of data networks for many years, but it is a hard task for engineer to initially design and evaluate a network employing both terrestrial and satellite links, since the satellite scheme from each vendor has different aspects and conditions, though their basic structures are similar. This paper presents a general model of satellite channel with multiple access scheme. It employs a simple flow basis of the number of *blocked* stations to represent system behavior at equilibrium point. The model has a general and plain structure and, thus, has the benefit of: 1) easy to be conformed to different types of satellite channel which rudiment structure is random access method, especially slotted ALOHA, for inroute channel, 2) results are expressed in terms of general performance measures which could be painlessly interfaced to terrestrial network. Finally, results obtained from simulation and numerical computation are presented and compared.

1. Introduction

Currently, the existence of various satellite that has multiple access become a problem for the engineer who, at the outset, designs and selects the type of satellite links which are suitable for his network and also conforms the desirous application for operation. This paper proposes a general model of multiple access satellite channel which has basic structure as slotted ALOHA and could be easily adapted to satellite channel from different vendors. Before describing further in detail, we must first make clear that the result obtained from this model might be not as precise as that from the original elaborate analysis and detailed simulation which had been done by system owner. The primary purpose solicited here is to build a simple model which can be utilized as a primary idea for engineer who is designing and investigating the performance of the integrated media network by examining alternate conditions of satellite channel. Section 2 presents basic channel models which can be used as a general model for ALOHA based satellite channel. Section 3 demonstrates the idea of proposed model by analyzing well-known satellite channel. Section 4 describes and compares the results obtained from numerical and simulation method. Some conclusions are given in section 5.

2. Performance Analysis

A familiar generalization of the described model for slotted ALOHA channel with multiple access scheme, had been summarized in [1]. We define here the simple parameters that used to characterize the performance of an expected satellite channel. There are, 1) maximum throughput at equilibrium point, 2) average delay measured from the time that a packet is first transmitted from sender station until it was successfully received by receiver station, including time that spent for retransmission(s) and waiting in buffers in case of overlapping of subframes, 3) channel capacity and input load, 4) optimum and stability point of system performance.

2.1 Throughput Consideration

Behavior of satellite channel (or state) depends upon a number of factors such as the number of *thinking* or *idle* stations, *blocked* stations, retransmission algorithm, the methodology of the particular algorithm intended to gain more efficiency of network parameters for different types of application, input rate of terminal, etc. However, our principle concern in this paper is the number of *blocked* station (terminals in retransmission mode). It should be obvious that the state of slotted ALOHA channel can be described by the transition of blocked stations[2]. To reduce the complexity of computation, system behavior will be evaluated at the equilibrium point. Thus we can first define a simple formula for slotted ALOHA based channel as :

$$Q_{in}(1-P_n) = Q_{out}P_n \qquad (1)$$

where

- Q_{in} and Q_{out} denote respectively the number of packets arrived at the system and packets successfully transmitted in a period of time.
- P_n is the probability that a newly generated packet and retransmitted packet will be successfully transmitted.

We will use "Q_{in}" as a key parameter to contain the channel event occurred in each condition for those different types of satellite channel as previously mentioned. We shall demonstrate this further in section 3.

2.2 Delay Analysis

The expected average time from when a packet is generated until it is successfully received, in case that the positive acknowledgment is not required, can be simply expressed as the sum of average delay time occurred in each possible condition (assumed independent to each others) weighted by probability of the occurrence of event in that condition. With this definition, the total delay time can be written as :

$$T_{tot} = p_1(T_{s1} + T_{r1}) + p_2(T_{s2} + T_{r2}) + \ldots + \ldots + p_n(T_{sn} + T_{rn}) \qquad (2)$$

where p_n is the probability of n-th conditioned event.

In writing this delay formula, we take advantage of the fact that, in slotted ALOHA multiple access system, there are only two possible delay encountered by a terminal after it had transmitted a packet. One is the delay time occurred in case of successfully transmission, T_s, and the other is delay time

This material is reserved for educational use only, not allowed for commercial use.
Forbidden to modify the content and cite the document when use.

caused by collision, T_r,. Noted that, generally, the first part of the delay encountered by a message when it arrives at a station is the delay in the queue before it is conformably divided into satellite packets. The evaluation of this delay is complicated by the fact that the time spent in the queue depends on the number of messages coming from other stations, though the stations in that system has been defined to be independence between each others. This corresponds to the behavior of the whole system and is important for designation of the integrated network previously mentioned, thus, it will be left to concerning topic and not included here.

3. Example of Numerical Analysis

For example, let us demonstrate the utilization of the above model by analyzing a well-known satellite reservation access scheme proposed in [3][4]. The computation will be made by using *frame* structure categorized as shown in Fig.1, and by using channel conditions and processes which had been defined in [3][4].

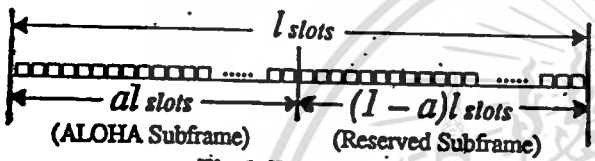

Fig. 1. Frame structure

3.1 Throughput Analysis (: S)

Based on above definition, each remote station in the *thinking* state generates new packets (packets contain one short message or first part of long message) with a Poisson rate of λ_a packets per frame. The terminal which encounters a collision at the channel and have to process retransmission by following retransmission algorithm is said to be "*blocked*", and terminals in this state are called "*blocked stations* : n_{rtx} ". Each packet suffering collision must delay for r slots (assumed exponentially distribution and conforms to next ALOHA parts) before retransmission. When a packet occurs, the station have to calculate whether its transmitted packet will arrive ALOHA part or reservation part. By observation with respect to the frame, the arrival of new packets can be identified as follows:

1) If the station transmits that packet, it will arrive at the reservation part. This case is prohibited, thus station has to wait until next frame. Assume that $0 < \lambda_a \le 1$, we can estimate the number of packets generated during a frame period by:

$$(N - n_{rtx}).\lambda_a \qquad (3)$$

Since the events are independent, the average number of stations in this state are simply :

$$n_{rsv} = \mathrm{int}\left[(N - n_{rtx}).\lambda_a.(1-a)\right] \qquad (4)$$

where int[..] is minimum positive integer. Assume that stations are defined to transmit the packets to next ALOHA parts with independent random process, thus packets from n_{rsv} which will access to any slots in the next ALOHA part and follow uniform distribution are n_{rsv}/al.

2) In ALOHA part, a packet arrived at the station's transmission buffer is transmitted immediately with rate λ_a packets per frame.

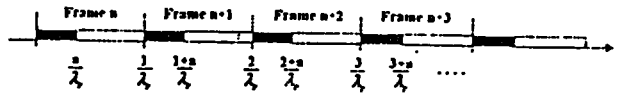

Fig. 2. Interval of the retransmission probability

In reference to (1), the quantity of packets (per slot) that flow into the system can be derived as

$$Q_{in} = (N - n_{rtx} - n_{rsv}).\lambda_a.a + (n_{rsv}/al) \qquad (5)$$

After learning that a collision has taken place, the station transits to *blocked* state and retransmits with uniform probability anywhere in next ALOHA parts and on the average λ_r packets/frame. Fig.2 Illustrates the probability range of packet randomly retransmitted from *blocked* station, following definition of channel division. Let p_{rtx} denote the probability that *blocked* stations will transmit to any slots in the ALOHA part of next frames. We have :

$$p_{rtx} = \frac{1 - \exp(-a\lambda_r)}{1 - \exp(-\lambda_r)} \qquad (6)$$

Thus the number of packets represented *blocked* stations trying to flow out of the system are simply as :

$$Q_{out} = n_{rtx}\lambda_r p_{rtx} \qquad (7)$$

Consider the probability that a packet is successfully transmitted, P_n,[4] which is equal to $\exp(-G_s)$,where:

$$G_s = (N - n_{rtx} - n_{rsv}).a.\lambda_a + (n_{rsv}/al) + (n_{rtx}\lambda_r p_{rtx}) \qquad (8)$$

From (1), (5), (7), we can now derive n_{rtx} at the equilibrium point, and average throughput (S_n) can also be obtained from the following well-known formula :

$$S_n = [(N - n_{rtx} - n_{rsv}).a.\lambda_a + (n_{rsv}/al)].\exp(-G_s) \qquad (9)$$

At the equilibrium point, the average numbers of the first packet of long message which are successfully transmitted in each frame is given by:

$$W_q = al(1 - l_L)G_s P_n \qquad (10)$$

When l_L:l_S is assumed to be the ratio of the first packet of long message and short message (single packet), Consider reservation part which is limited at $(1-a)l$ slots, if the quantity of reserved packets exceeds the limited number, they will be suspended and would try to reserve again in future frames. Assume that each station's queue is independent, and

This material is reserved for educational use only, not allowed for commercial use.
Forbidden to modify the co[illegible]nd cite the document when use.

filled up by following exponential process and FCFS queuing discipline, we now compare such event to the event that at least r outcomes had occured during interval [0,x]. Suppose that the probability of event is $P(N_x \geq r)$, then we have :

$1 - P(N_x < r)$ = 1-Pr[at least r queues have contained total packets equal to x].

Thus the probability that at least r queues have contained x packets is equal to :

$$= \sum_{i=0}^{x} \frac{\exp^{-\frac{x}{w}}.(\frac{x}{w})^i}{i!} \quad (11)$$

where, w represents average number of packets per queue. Since we define Poisson process for newly generated packets, we have i queues from i stations derived by a probability function

$$= \frac{\exp^{-W_q}.(W_q)^i}{i!}$$

If $x = (1-a)l$, we have the probability that the queue will not suspended, p_{sum}, as :

$$p_{sum} = \sum_{i=0}^{(1-a)l} \frac{\exp(-W_q - \frac{(1-a)l}{w}).(\frac{(1-a)l}{w})^i.W_q^{\,i}}{(i!)^2} \quad (12)$$

Then the average throughput of reservation part is $W_q p_{sum} w$.

3.2 Delay Analysis (: D)

Consider T_{tot}, the response time after a packet had been transmitted. It is the sum of propagation delay(R), processing time(T_{proc}), retransmission delay and delay according to each particular condition. Let us classify delay time due to both parts of the frame, ALOHA and reservation. When a packet is generated during ALOHA part, it is sent immediately. Following this event, there will be two possible delay according to transmission results, delay in case of successful transmission given by [4]:

$$T_{s1} = 1.5 + 2R + 2T_{proc} \quad (13)$$

and delay in case of collision given by:

$$T_{r1} = 1.5 + 2R + 2T_{proc} + E[r](D_r) \quad (14)$$

where, $E[r]$ is the average number of retransmission given by $1 - P_n / P_n p_{rtx}$. By definition that *blocked* station must retransmit to ALOHA part only, we have :

$$D_r = \frac{l}{\lambda_r} + 2R + 2T_{proc} \quad (15)$$

For the case when a packet is generated during reservation part, it can also be divided into two types of delay. One is in case of successful transmission given by :

$$T_{s2} = \frac{(1-a)l}{2} + \frac{al}{2} + 2R + 2T_{proc} \quad (16)$$

and the other is in case of collision given by :

$$T_{r2} = \frac{(1-a)l}{2} + \frac{al}{2} + 2R + 2T_{proc} + E[r]D_r \quad (17)$$

Queue which is suspended will be sent once again in future frames. Then the average response time of the system is:

$$T_{tot} = l_S(D_1) + (1-l_S)[(p_{sum}D_1) + ((1-p_{sum}).(D_1 + (1-a)l))] \quad (18)$$

where,

$$D_1 = \exp(-G_s)[aT_{s1} + (1-a)T_{s2}] + (1-\exp(-G_s))[aT_{r1} + (1-a)T_{r2}]$$

4. Numerical Analysis Results

In this section we present both numerical and simulation results showing system performance parameters versus λ_g. To analyze system performance, a number of states have to be considered and in order to cover possible characteristics of the system, but we will present here only to justify in the case of practical interest at the parameter value: w=3, l=24, R=6, l_r= 0.54, λ_r =0.5. The algorithm of the software model used for simulation was constructed based on realistic events with simulation time 20,000 slots. In Fig.4-5 (a),(b) and (c), the average throughput and mean delay are depicted as a function of input load(λ_g) at 75, 100 and 125 stations respectively. Slot size in the satellite channel is chosen to be 0.0416 sec. Note that the scale of input load is stepped in three intervals for clarity purpose. To obtain the moderate optimization between throughput and delay curve, we select the length of ALOHA part with respect to the distribution of average packets in queue at a=0.5(see Fig.3). The mean throughput given by (9) is a global measure of the packets transmitted by the idle stations in every inbound channel conditions. The results exhibits unstable behavior as shown by [5] and [2]. In Fig. 5, mean delay given by(18) is rapidly increase when it is close to saturated point.

5. Conclusion

We do not develop here any new treatment of feasibility but rather limit ourselves to the simplicity of that how to deal with the complexity of satellite channel in case of designing integrated media system. Finally, our results indicate, 1) for each value of station N, there is a critical value of load that causes the system saturate. As general examine method, we can use this throughput-delay relationship to design or select the acceptable point of operation, 2) the comparison of the results obtained from simulation and analytic model exhibits the conformity. Thus both method can be employed to find the optimal value of system parameter, 3) the results obtained from the model described through this papers are based on the fundamental architecture with independent property of each station and each channel condition, thus they are easily adapted

This material is reserved for educational use only, not allowed for commercial use.
Forbidden to modify the content and cite the document when use.

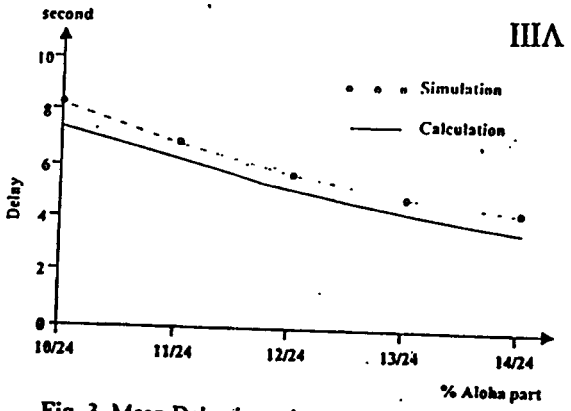

Fig. 3. Mean Delay in various ratio of subframe

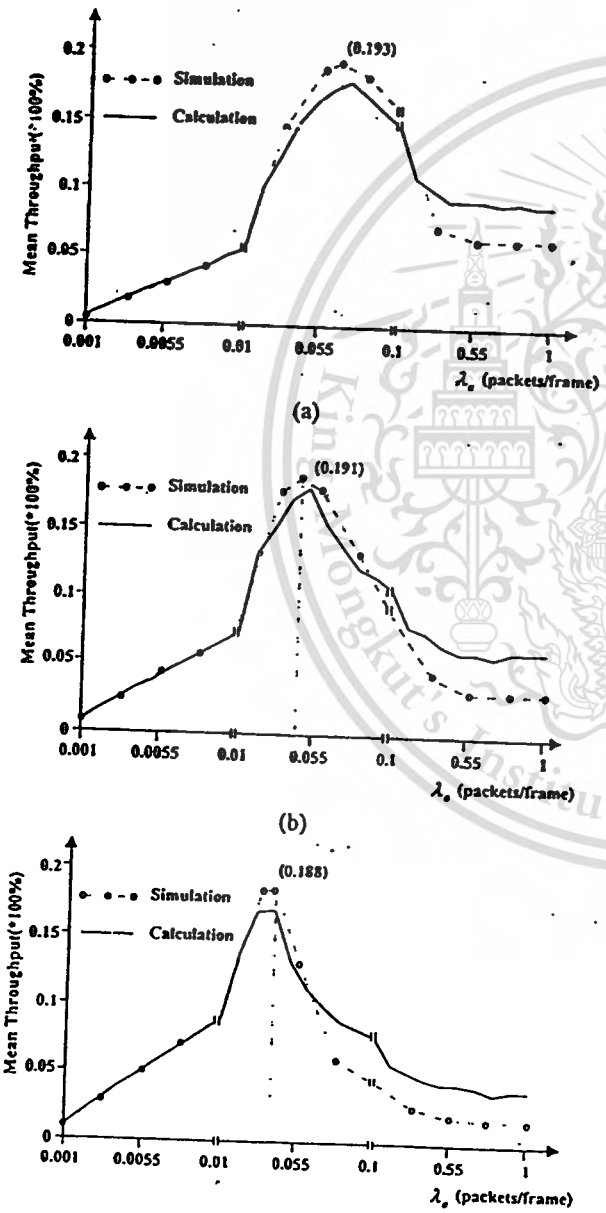

Fig. 4. Mean Throughput vs. Input Loads for three value of N: (a)=75, (b)=100 and (c)=125

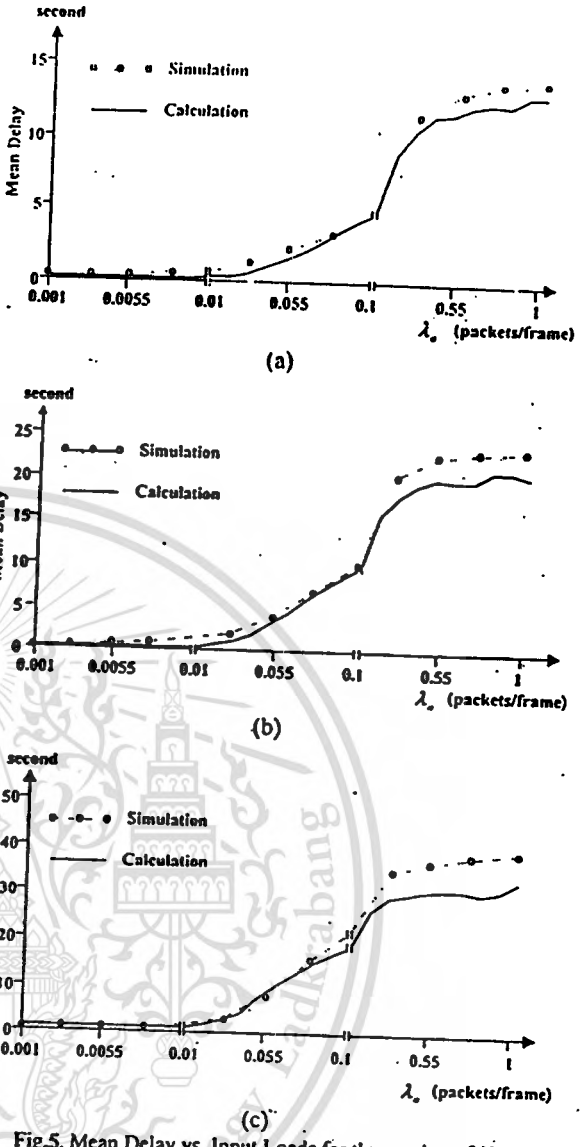

Fig.5. Mean Delay vs. Input Loads for three value of N: (a)=75, (b)=100 and (c)=125

in accordance with conventional model of computer network which used only land-line media.

Reference

[1] T. T. Ha,"Digital Satellite Communication," *McGraw-Hill*, 1990.

[2] D. Raychaudhuri, "Dynamic performance of ALOHA-type VSAT channel: A simulation study," *IEEE Trans. Commun.*, February 1990.

[3] Y. Onozato, et. all.,"Performance Analysis of a Combined Random Reservation Access Scheme," *IEEE Trans. Commun.*, April 1991.

[4] Fujii, and Matsumoto, "AA/TDMA adaptive satellite access method for mini-earth station network," in *Conf. Rec. Proc. GLOBECOM'86*, pp. 1464-1499, Texas, December 1986.

[5] Leonard Kleinrock and Simon S. Lam, "Packet-Switching in a slotted satellite channel," *NCC'73* pp. 703-710, 1973.

This material is reserved for educational use only, not allowed for commercial use.
Forbidden to modify the content, and cite the document when use.

IEICE The Institute of Electronics.Information and Communication Engineers

he Current Status of the Review Process

ACK

Paper Number: **2003EBP3301**

Your Associate Editor: **Dr. Yoshinori Arimoto** arimoto@nict.go.jp

Processing Status: **The Final Evaluation Result has been mailed** << Meaning of Each Term >>

Volume: **Vol.E88-B,No.6,pp.-,Jun. 2005.**

< The Final Review Process >> Received: **2004/06/13**

Reviewer	Review requested	Report received	Status
A	2004/06/14	2004/07/05	Review completed
B	2004/06/14	2004/09/17	Review completed

Result of the Final Evaluation: **Accepted** Evaluation Date: **2004/11/19**

<< The 1st Review Process >> Received: **2003/06/23**

Reviewer	Review requested	Report received	Status
A	2003/10/28	2003/11/18	Review completed
B	2003/10/28	2004/03/18	Review completed

Result of the 1st Evaluation: **Conditional Acceptance** Evaluation Date: **2004/04/12**

Note: For authors of the Transactions on "Communications", the notification of acceptance will be made

This material is reserved for educational ... for commercial use.
Forbidden to modify the content, and cite the document when use.

IEICE TRANS. INF. & SYST., VOL.E87–D, NO.10 OCTOBER 2004

PAPER

Performance Analysis on the Controllable Slotted DS-CDMA with an Allocating Buffer for Collided Traffic

Seri ASAVARUK†, Suvipol SITTICHEVAPAK††, Ruttikorn VARAKULSIRIPUNTH†, *Nonmembers*, Yasushi KATO†††, *Member*, *and* Norio SHIRATORI††††, *Fellow*

SUMMARY This paper presents an analysis of the Slotted DS-CDMA system with modified node components in order to construct a load control structure in which the service rates of each node can be dynamically adapted without using feedback information. In contrast to the traditional Slotted DS-CDMA which is widely represented with single queue, prior emphasis of the approach is laid on the usage of an additional queue which is applied to manage the collided packet traffic while its queue size is also used as a load control parameter. Semi-Markov process is applied to describe the statistic behavior of the system in steady state. Trade-offs between two major performance parameters, i.e., delay and throughput, are presented and compared with those of the traditional system. Results obtained from the simulation and numerical analysis using queuing concept are compared. With these results, an advantage performance for group packets is shown, and we finally extend the concept based on the obtained results to describe a simple algorithm using one way control message as the tool to alleviate the stability problem.

key words: Slotted DS-CDMA, collision-resolved queue, system throughput, message delay.

1. Introduction

In certain applications, user information is sent in the form of variable-sized messages that need to be segmented into smaller packets. The length of the packet is assumed to be equal to the size of the channel time slot. When these packet segments are sent across the large propagation network such as satellite system, the delay incurred by the propagation, multiple access and time spent in the terminal's queues may cause upper protocol layer to assume some of them as lost events, despite correctly receiving, and possibly retransmitted them needlessly. These disadvantages will significantly limit the channel performance and capacity. Main factor that also makes the system susceptible to the delay figures is the backlogged condition which is considered necessary for stabilizing channel reliability and also for keeping the packets in the correct sequence when arriving at the receiver [1],[2]. Although the corresponding results achieve the required performance when considering individual packet, the scheme has a potential problem of increasing the waiting time within the internal queue, resulting in throughput constraint and high message delay when input traffic is the messages carrying one or more packet(s)[3],[4]. To mitigate this disadvantage, we apply the concept of freely transmitting the packets in order to reduce time spent in the terminal's queues. When a terminal has the new packet(s) in its first buffer, it immediately sends those packets to the next time slot. In the proposed system, the terminal can send the new packets up to the limited window size, and the terminal whose packet was collided can also sends new packets at the original rate, and simultaneously manages the retransmission. The rest of this paper is organized as follows. Section 2 introduces and explains the model of the proposed system. Section 3 study analytical models for deriving the throughput and delay. Numerical and simulated results are analyzed and compared in section 4. Control architecture and its simulation results are also given in this section. Finally, discussion and conclusions are provided in Section 5 and 6, respectively.

2. Modeling

The system illustrated in Fig.1 consists of N terminals, each of which is assigned a different spreading code. New traffic is assumed to be in the form of message carrying one or more packet(s), and will be unconditionally sent out in order to reduce the time spending in the queue. Each terminal is represented with three queues. The first queue (Q_1) deals with newly arrival packets, while the second queue (collision-resolved queue : Q_2) is used to store and manage the sequence of packets that are declared as collided traffic. The third queue (Q_3) is used as the output queue which is assumed to operate in First-In-First-Out order. P_s and P_e are defined as unconditional successful and unsuccessful transmission probabilities, with P_s=1-P_e.

In traditional Slotted DS-CDMA system, the collision is not declared unless the number of packets in

Manuscript received August 25, 2002.
Manuscript revised December 19, 2004.
Final manuscript received July ..., 2004.

†The authors are with Faculty of Engineering & Research Center for Communications and Information Technology, King Mongkut's Institute of Technology Ladkrabang, Bangkok 10520, Thailand.
††The author is with Faculty of Engineering, King Mongkut's Institute of Technology Ladkrabang, Bangkok 10520, Thailand.
†††The author is with Sendai National College of Technology. Japan.
††††The author is with Research Institute of Electrical Communication, Tohoku University. Japan.

This material is reserved for personal use only and is prohibited for commercial use.
Forbidden to modify the content, and cite the document when use.

2

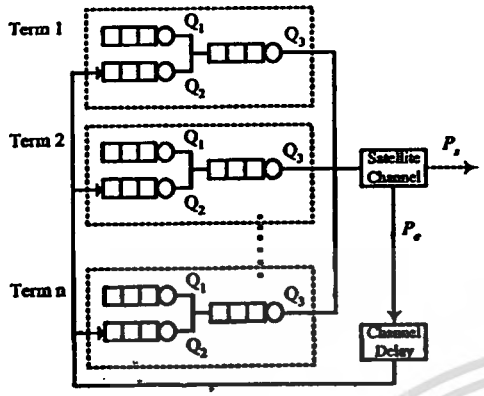

Fig. 1 System Model

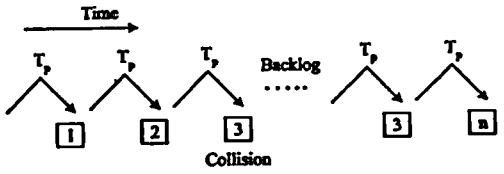

Fig. 2 Timing diagram of Traditional system

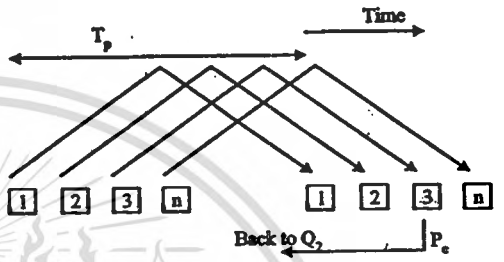

Fig. 3 Timing diagram of Traditional system

a slot exceeds the limitation. The terminals with unsuccessfully transmitted packets will be called backlog, and backlogged terminals will attempt to retransmit their packets until they are successful as shown by timing diagram in Fig. 2. The diagram in Fig.3 shows the timing process of the proposed approach starting at the time when a message is sent out from Q_1. The shaded box represents the collided packet which will be acknowledged as a failure to the source.

If we denote the average number of packets arriving at the channel during one slot duration by the offered load, it will consists of new and retransmission traffic. New traffic arriving at the terminal is assumed to be the variable-sized messages which can be divided into one or more packets. These messages will be transferred to Q_1. When their first segments(packets) reach the head of the queue and ready for service, without backlogged condition, they are orderly sent out to Q_3 with exponential rate of μ_1 packet per slot. After transmission, the terminal sends the replica of the transmitted packets to Q_2, and waiting for individual acknowledgements. When receiving the successful acknowledgements, the terminal discards the success packets out of Q_2. It will starts the retransmission process with Poisson parameter μ_2 packet per slot if collision acknowledgements are received. This collision-resolved process will be repeated until each collided packet is successfully received. We assume a terminal can process the new transmissions and retransmissions individually and independently. Terminals also assume to operate in two states defined by the status of Q_2. It generates traffic with rate μ_1 when Q_2 is idle and with rate $\mu_1+\mu_2$ when Q_2 is busy.

With the concept of unconditional transmission, it frequently results in increasing the sending rate of terminals based on the active Q_2. This requires a simple control approach which can adjust the burstiness of the offered load to obtain overall system availability while maintaining individual user's performances. More detail of the control approach is explained in section 5.

3. System Analysis

3.1 Throughput Analysis

In this section, the channel throughput *(S)* is used as a measure to evaluate the system performance. Here, S is defined as the average number of successfully received packets per time slot, and is given[5],[6] by

$$S = \sum_{k=1}^{N} k P_k P_s(k) \tag{1}$$

where N is the number of terminals, P_k is the probability that a packet is transmitted simultaneously with other *k-1* packets, $P_s(k)$ is the conditional successful transmission probability of a packet and given by $P_s(k) = [1 - Q_b(k)]^{L_b}$. Here, L_b is the number of data bit per packet, and $Q_b(k)$ is the bit error probability given in [7] as follows

$$Q_b(k) = Q([\frac{k-1}{2n_c} + \frac{\eta_o}{2E_b}]^{-1/2}) \tag{2}$$

where $Q(.)$ is the integral Gaussian function, $\frac{E_b}{\eta_o}$ is the ratio of energy per bit and spectral density of noise power, k is the total number of simultaneously transmitted packet(s)in the slot, and n_c is the spreading sequence length. The modulation scheme used in the system is BPSK(the results are also valid for QPSK)[7],[8]. We assume that the long spreading code sequences and perfect power control are employed. Approximate expression of $Q_b(k)$ will be derived based on the same manner of channel environment originally described in [7]. Systems are also assumed to be ideal, and all imperfections such as multi-path fading is not considered.

The dominant cause of unsuccessful transmission

Copyright © 2004 The Institute of Electronics, Information and Communication Engineers
Forbidden to modify the content, and cite the document when use.

in a slot is the multiple-access interference(MAI). Note that all spread interference appeared to the channel including MAI, is approximated as a Gaussian random variable (Gaussian approximation). Thus P_k is mainly based on the present number of terminals that have its second queue(Q_2) in busy condition(busy-Q_2).

Consider a slotted time queuing system with N statistical independent traffic sources. Let p_{ij} be a state transition probability that the number of terminals having busy-Q_2 changing from i to j $(0 \le i \le N, 0 \le j \le N)$ at slot time t and $t+1$, respectively. p_{ij} can be obtained in according to the following conditions.

Case 1: when $i < j$

$$p_{ij} = \Sigma_{a=0}^{min(N-j,i)} C_{j-i+a}^{N-i} \tau_1^{j-i+a}(1-\tau_1)^{N-j-a} .C_a^i \tau_o^a (1-\tau_o)^{j-a} \quad (3)$$

Case 2: when $i > j$

$$p_{ij} = \Sigma_{a=0}^{min(N-i,j)} C_a^{N-i} \tau_1^a (1-\tau_1)^{N-i-a} .C_{j-a}^i \tau_o^{i-j+a}(1-\tau_o)^{j-a} \quad (4)$$

Case 3: when $i = j$

$$p_{ij} = \Sigma_{a=0}^{min(N-i,i)} C_a^{N-i} \tau_1^a (1-\tau_1)^{N-i-a} .C_a^i \tau_o^a (1-\tau_o)^{i-a} \quad (5)$$

where $C_b^a = \frac{a!}{(a-b)!b!}$. and τ_o and τ_1 are the Busy-to-Idle and Idle-to-Busy transition probabilities of Q_2. Both events are assumed not to occur at the same given time slot. Let U_n be the steady state probability denoting there are n terminals having busy-Q_2 during a time slot, and P be the state transition matrix of p_{ij}(i.e., $P = [p_{ij}], (N+1)*(N+1) matrix$) that can be obtained from equations (3), (4) and (5). Then, we can derive U_n by using the following $N+1$ equations [3].

$$U^T = U^T P \quad (6)$$

where, $U^T = [U_0, U_1, U_2, ..., U_N]$ and $\Sigma_{n=0}^{N} U_n = 1$. Thus, the average number of terminals having busy-Q_2, i.e., N_{av}, can be obtained as follows

$$N_{av} = \Sigma_{n=0}^{N} n U_n \quad (7)$$

To derive the value of τ_o and τ_1, it is necessary to study the queuing behavior of each terminal, especially that of Q_2. With the component shown in Fig.3, let us rewrite it by folding all the components, except Q_2, into one box as illustrated in Fig. 4. In diagram,μ_1 and μ_2 are the generate rates of new and retransmitted packets presented to the X box, respectively. λ_{q3} is the packet departure rate of the X box and P_s is the unconditional packet success probability. Now, let x and y be the number of packet(s) in X box (including one being serve). and in Q_2, respectively. By using the concept of birth-death process, we create the state-transition-rate diagram for the system as shown in Fig.5.

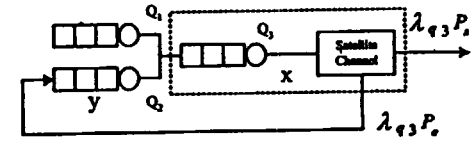

Fig. 4 Functional Diagram

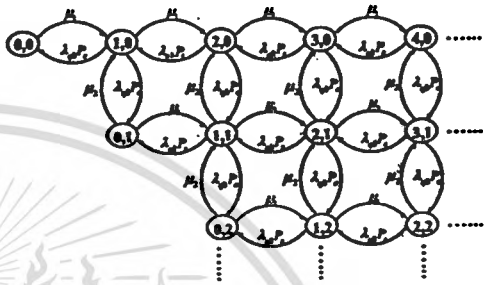

Fig. 5 State-Transition Diagram

Let $p_{x,y}$ denotes the equilibrium probability that the X box and Q_2 contains x and y packets respectively. Using the property of the double z-transform, we obtain a set of state balance equations as:

Case 1: when $x = 0, y = 0$

$$\mu_1 p_{0,0} = \lambda_{q3} P_s p_{1,0} \quad (8)$$

Case 2: when $x > 0, y = 0$

$$\sum_{x=1}^{\infty} \mu_1 p_{x,0} z_1^x + \sum_{x=1}^{\infty} \lambda_{q3} p_{x,0} z_1^x = \sum_{x=1}^{\infty} \mu_1 p_{x-1,0} z_1^x + \sum_{x=1}^{\infty} \lambda_{q3} P_s p_{x+1,0} z_1^x + \sum_{x=1}^{\infty} \mu_2 p_{x-1,1} z_1^x \quad (9)$$

Case 3: when $x = 0, y > 0$

$$\sum_{y=1}^{\infty} \mu_1 p_{0,y} z_2^y + \sum_{y=1}^{\infty} \mu_2 p_{0,y} z_2^y = \sum_{y=1}^{\infty} \lambda_{q3} P_s p_{1,y} z_2^y + \sum_{y=1}^{\infty} \lambda_{q3} P_e p_{1,y-1} z_2^y \quad (10)$$

Case 4: when $x > 0, y > 0$

$$\sum_{x=1}^{\infty}\sum_{y=1}^{\infty} (\mu_1 + \lambda_{q3} + \mu_2) p_{x,y} z_1^x z_2^y = \sum_{x=1}^{\infty}\sum_{y=1}^{\infty} \lambda_{q3} P_s p_{x+1,y} z_1^x z_2^y + \sum_{x=1}^{\infty}\sum_{y=1}^{\infty} \mu_1 p_{x-1,y} z_1^x z_2^y + \sum_{x=1}^{\infty}\sum_{y=1}^{\infty} \mu_2 p_{x-1,y-1} z_1^x z_2^y$$

This material is reserved for educational use only. Not approved for commercial use.
Forbidden to modify the content, and cite the document when use.

4

$$+\sum_{x=1}^{\infty}\sum_{y=1}^{\infty}\lambda_{q3}P_e p_{x+1,y-1}z_1^x z_2^y \quad (11)$$

Then summing both sides of all cases and identifying,

$$P(z_1,z_2)=\sum_{x=0}^{\infty}\sum_{y=0}^{\infty}p_{x,y}z_1^x z_2^y$$

to obtain

$$\mu_1 P(z_1,z_2)+\lambda_{q3}[P(z_1,z_2)-\sum_{y=0}^{\infty}p_{0,y}z_2^y]$$
$$+\mu_2[P(z_1,z_2)-\sum_{x=0}^{\infty}p_{x,0}z_1^x]$$
$$=\mu_1 z_1 P(z_1,z_2)+\frac{\lambda_{q3}P_s}{z_1}[P(z_1,z_2)-\sum_{y=0}^{\infty}p_{0,y}z_2^y]$$
$$+\frac{\lambda_{q3}P_e z_2}{z_1}[P(z_1,z_2)-\sum_{y=0}^{\infty}p_{0,y}z_2^y]$$
$$+\frac{\mu_2 z_1}{z_2}[P(z_1,z_2)-\sum_{x=0}^{\infty}p_{x,0}z_1^x] \quad (12)$$

Given $\sum_{i=0}^{\infty}p_{i,0}z_1^i = P(0,z_2)$ and $\sum_{j=0}^{\infty}p_{0,j}z_2^j = P(z_1,0)$ and substituting $z_1=z_2=z$ into (12), we obtain

$$\mu_1 P(z_1,z_2)+\lambda_{q3}[P(z,z)-P(0,z)]$$
$$+\mu_2[P(z,z)-P(z,0)]$$
$$=\mu_1 zP(z,z)+\frac{\lambda_{q3}P_s}{z}[P(z,z)-P(0,z)]$$
$$+\lambda_{q3}P_e[P(z,z)-P(0,z)]$$
$$+\mu_2[P(z,z)-P(z,0)]$$

with some manipulations, we obtain

$$\mu_1 zP(z,z)+\lambda_{q3}P_s[P(z,z)-P(0,z)] \quad (13)$$

given z=1, we obtain

$$P(0,1)=\frac{\lambda_{q3}P_s-\mu_1}{\lambda_{q3}P_s} \quad (14)$$

and

$$P(1,0)=1-\frac{\mu_1 P_e}{\mu_2 P_s} \quad (15)$$

Here, $P(1,0)$ and $P(0,1)$ represent the probability that there is no packet in the X box and in Q2, respectively. With the description of τ_o and τ_1 given earlier, we now obtain $\tau_o=\mu_2 P_s\sum_{x=0}^{\infty}p_{x,1}$ and $\tau_1=\mu_1 P_e P(1,0)$. Let the ratio between the average number of terminals having busy-$Q_2(n_{av})$ and the number (N) of total terminals be v_w, we approximate the total offered traffic appeared to the channel as:

$$\mu_{w0}=(1-v_w)N\mu_1+v_w N(\mu_1+\mu_2) \quad (16)$$

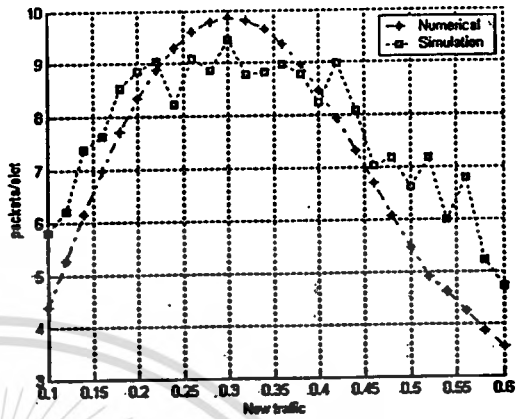

Fig. 6 Throughput results with μ_2=0.3

If the assumption of Poisson environment for μ_1 and μ_2 exists, then μ_{w0} can also be assumed as Poisson process. In considering the equilibrium probability, we need the long-term unconditional value of P_s. Instead of evaluating the average, we analyze the system behavior by selecting P_s corresponding to the system at the condition between average and unstable area.

Let $P_{[k/n]}$ be the probability of having k attempted transmissions(packet arrivals) in a time slot, when the system is in state n, denoted by

$$P_{[k/n]}=\Sigma_{i=max[k-n,0]}^{min[k,N-n]}C_i^{N-n}\mu_1^i(1-\mu_1)^{N-n-i}$$
$$.C_{k-i}^{n}(\mu_1+\mu_2)^{k-i}(1-\mu_1-\mu_2)^{n-k+i} \quad (17)$$

Thus the successful transmission probability for a packet at a given time slot is [8]

$$P_s=\Sigma_{j=1}^{N}[j\Sigma_{k=j}^{N}\frac{1}{k}C_j^k P_s^j(k)$$
$$(1-P_s(k))^{k-j}P_{[k/n]}] \quad (18)$$

Now the throughput can be obtained from (1), (18) and $P_s(k)$. We verify the accuracy of our analysis by comparing numerical results with the simulations running by OPNET software as shown in Fig. 6 and Fig. 7. Simulations are performed based on the same system configuration and environment previously defined for numerical analysis. The simulation period is 3600 seconds for every experiment. We fix $N=35$,$\mu_2=0.3$ in Fig.6 and $N=35$,$\mu_2=0.5$ in Fig.7, and define $\frac{E_b}{\eta_o}=15$,$n_c=127$,$L_b=1000$ for the CDMA channel. Curves illustrate the generated rates(μ_1) of the new traffic as a function of throughput (packet per time slot). We select the relevant parameters of P_s at the area where the traffic generated to the channel becomes heavy. We remark that the results obtained by numerical analysis show higher throughput than the simulation around the maximum area.

In Fig. 8, the average number of terminals having

This material is reserved for educational use. It is not allowed for commercial use.
Forbidden to modify the content, and cite the document when use.

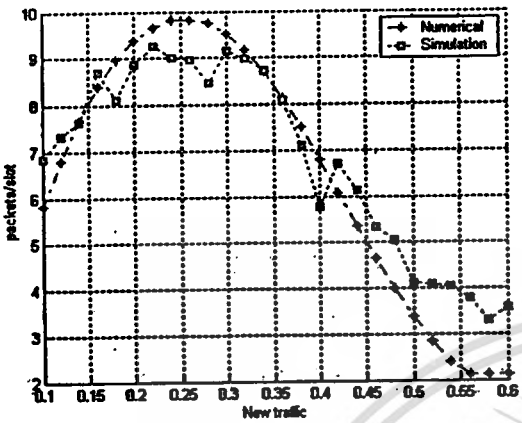

Fig. 7 Throughput results with μ_2=0.5

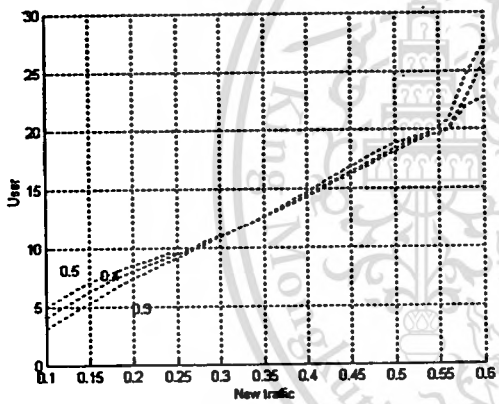

Fig. 8 n_{av} versus μ_1, when N=35

busy-Q_2 is plotted as a function of μ_1 with N=35. The results suggest that the critical area starts up at $\mu_1 \approx 0.22$. In solving the queuing behavior of each terminal, v_w should be kept lower than 10 for N=35 in order to stabilize the channel.

3.2 Delay Analysis

In this section we evaluate the message delay by means of numerical approximation. As mentioned in the preceding sections, all queuing components are assumed to operate independently, and the waiting time plus service time in all queues is taken into account through the total message delay. Let us define the total message delay, W_{tot}, over the satellite link in terms of the sum of fixed transmission delay, processing time and average queuing delay as follows

$$W_{tot} = T_1 + T_3 + T_p + \overline{b_{e,t}} + (\overline{g}T_{pc}) \quad (19)$$

In the above equation, T_1 and T_3 are the expected delay time spent by each message in Q_1 and Q_3 respectively, $\overline{g}$ is the average message size(packets), T_{pc} is the processing time of central HUB, T_p is the propagation delay, and $\overline{b_{e,t}}$ is the mean delay of the retransmission events. When all message segments are successfully received, the total message delay is

$$T_1 + T_3 + 2T_p + (\overline{g}T_{pc})$$

The analysis of W_{tot} can be carried out using the timing sequence shown in Fig.9.

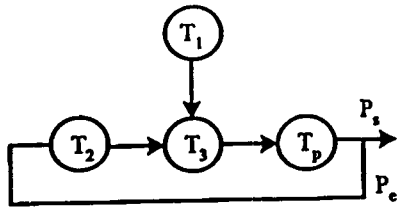

Fig. 9 Timing Diagram

3.2.1 Delay on Q_1

We describe the process of Q_1 with the Bulk arrival M/G/1 queuing system. A delay measure of Q_1 is the average waiting time for a message denoted by W_{q1}. To derive the value, the first and second moment of service time of a message denoted by $t_m^{(1)}$ and $t_m^{(2)}$ are required.

Let $T_m^*(s)$ be the Laplace transform of the density function of message service time defined as $T_m^*(s) = G(B_{q1}^*(s))$, $G(z) = \sum_{i=1}^{\infty} g_i z^i$ be the distribution of the message size, g_i be the probability that a message carrying i packets. Given the service time distribution of an individual packet, $B_{q1}^*(s)$, we have

$$T_m^{*(1)}(s) = G^{(1)}(B_{q1}^*(s))B_{q1}^{*(1)}(s) \quad (20)$$

and

$$T_m^{*(2)}(s) = G^{(1)}(B_{q1}^*(s))B_{q1}^{*(2)}(s) + (B_{q1}^{*(1)}(s))^2 G^{(2)}(B_{q1}^*(s)) \quad (21)$$

where $T_m^{*(1)}(s)$ and $T_m^{*(2)}(s)$ are the first and second derivative of $T_m^*(s)$. These values will be used to calculate $t_m^{(1)}$ and $t_m^{(2)}$. Letting s=0 in (21) and applying Little's result, we have the average waiting time in Q_1 for a message[9]:

$$W_{q1} = \frac{\lambda_g(\overline{g}t_m^{(1)})^2}{2(1-\rho_{q1})}[1 + C_g^2 + \frac{C_t^2}{\overline{g}}] \quad (22)$$

where C_g^2 and C_t^2 are the squared coefficient of variation for message size and message service time, respectively. λ_g is the message arrival rate per slot. ρ_{q1} is the utilization factor of Q_1. Given the average message size, $\overline{g}$, we obtain

$$T_1 = (\frac{\overline{g}}{\mu_1}) + W_{q1} \quad (23)$$

This material is protected by copyright. Personal use only. Not allowed for commercial use.
Forbidden to modify the content, and cite the document when use.

3.2.2 Extended Delay on Q_2 and Q_3

Q_2 and Q_2 are assumed to generate interdeparture traffic with Poisson process. The combined traffic which is also in the form of Poisson process becomes the input to Q_3. We use the expression of M/D/1 to evaluate average waiting time of Q_3. Since its constant service time is equal to the satellite time slot, the average waiting time for Q_3 is given[9] by

$$W_{q3} = \frac{\lambda_{q3} t_{slot}^2}{2(1-\rho_{q3})} \tag{24}$$

Applying this value and an average message segments, we obtain

$$T_3 = \overline{g}(W_{q3} + t_{slot}) \tag{25}$$

where t_{slot} is the slot time of satellite channel, ρ_{q3} and ρ_{q3} is the utilization factor of Q_3. Note that the first packet from a message segment that arrives at Q_3 could reach the head of the queue and gets service before the complete arriving of the whole message segment. When Q_3 sends out a packet, it could be still in busy state, or becomes empty. Given ρ_{q3}, the distribution of the interdeparture time can be obtained by

$$B_{q3}^*(s) = (1-\rho_{q3}) A_{q3}^*(s) D_{q3}^*(s) + \rho_{q3} D_{q3}^*(s) \tag{26}$$

where $A_s^* = \frac{\lambda_{q3}}{s+\lambda_{q3}}$ is the interarrival time distribution of Q_3. $\lambda_{q3} = \mu_1 + \rho_{q2}\mu_2$. ρ_{q2} is the utilization factor of Q_2. Since service time of Q_3, $d_{q3}(x)$, is deterministic with value t_{slot}, we have $d_{q3}(x) = U_0(x - t_{slot})$ and $D_{q3}^*(s) = exp(-st_{slot})$. Applying these parameters to (26) and taking out the Laplace transform, we finally get the departure time density:

$$b_{q3}(t) = (1-\rho_{q3})\lambda_{q3} exp(-\lambda_{q3}(t - t_{slot}))\delta(t - t_{slot}) + \rho_{q3} U_0(t - t_{slot}) \tag{27}$$

If $\rho_{q3} << 1$(the service time is very short compared to the arrival rate), we expect the effect of Q_3 is insignificant, and its interdeparture traffic is close to λ_{q3}. When the packets arrive at the central HUB, they must spend some time in the HUB to be considered a success or failure before leaving to the higher protocol layer or returning to the sender. We make use of this definition to model Q_2 as a discrete time queue with general arrival process and Poisson distributed service rate with parameter $P_e\lambda_{q3}$ and μ_2, respectively. Given the upper bound on average waiting time of G/M/1 by [10], we have

$$W_{q2} = \frac{(1+C_b^2)\rho_{q2}^2}{1+C_b^2\rho_{q2}^2}\left[\frac{(\sigma_t^2+\sigma_b^2)P_e\lambda_{q3}}{2(1-\rho_{q2}^2)}\right] \tag{28}$$

where C_b^2 is the squared coefficient of variation of service time. σ_t^2 and σ_b^2 are the variance of interarrival time and variance of service time. Since a packet may circulate more than one time, the remaining priority factor is the mean delay of the retransmission event,$\overline{b_{e,t}}$.

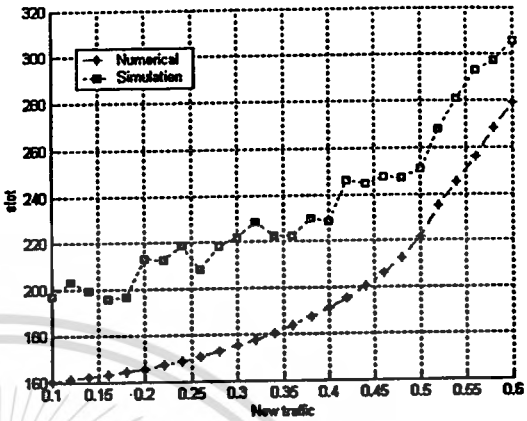

Fig. 10 Delay result, with $\mu_2 = 0.3$

Let $B_{e,t}^*(s)$ be the Laplace transform of service time of Q_2, $B_{e,e}^*(s)$ be the Laplace transform for delay time of the unsuccessful attempt, and $B_{e,s}^*(s)$ be the Laplace transform for delay time of the successful attempt after retransmitting n times. Thus

$$\begin{aligned} B_{e,t}^*(s) &= \sum_{n=0}^{\infty}[(P_e B_{e,e}^*(s))^n (P_s B_{e,s}^*(s))] \\ &= \frac{(P_s B_{e,s}^*(s))}{1-(P_e B_{e,e}^*(s))} \end{aligned} \tag{29}$$

Differentiate and let s=0, we get

$$\overline{b_{e,t}} = \frac{P_s B_{e,s}^{(1)}(0) - P_s P_e (B_{e,s}^{(1)}(0) - B_{e,e}^{(1)}(0))}{(1-P_e)^2} \tag{30}$$

where P_s is the unconditional packet success probability obtained from (18), $P_e = 1 - P_s$, and

$$B_{e,e}^{(1)}(0) = \overline{b_{e,e}} = 2T_p + \overline{g}P_e(W_{q2} + W_{q3} + t_{slot}) \tag{31}$$

$$B_{e,s}^{(1)}(0) = \overline{b_{e,s}} = \overline{b_{e,e}} + T_{pc} \tag{32}$$

We are now able to derive by using (23), (25) and (30).

The correctness of the mathematical model is verified by comparing with simulation results given in Fig. 10 and Fig. 11. Regarding the message segments presented at Q_1, we define λ_g= 1, $\overline{g}$ = 8 and $\sigma_g^2 = 144.2$. With the same environment as in the last section, curves show analytic and simulation results obtained for average delay of an individual message with fixed values of μ_2= 0.3 and 0.5. One of the main impacts that makes the difference between the results obtained by the simulation and numerical analysis is the effect of gap size between channel slots. This gap size helps the simulation program to identify two slots in a roll. If we select the value too high it will results

Copyright © 2004 The Institute of Electronics, Information and Communication Engineers
Forbidden to modify the content, and cite the document when use.

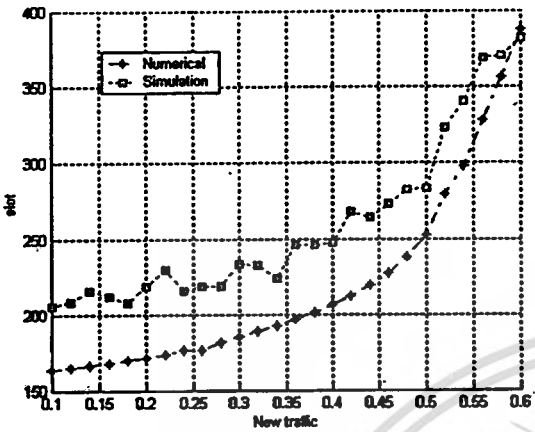

Fig. 11 Delay result, with $\mu_2 = 0.5$

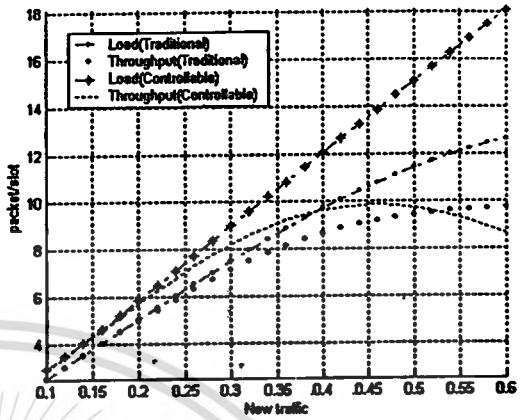

Fig. 12 Throughput-Load comparison, with $\mu_2 = 0.3$ and $N=25$

in losing throughput, but gain more success probability and lower delay. In this paper, we concentrate on the results obtained from two systems (traditional and proposed one) at the same channel environment. Thus, we select the gap size that causes the lowest value of the packet error. This results in losing around 7 percent in throughput, but gain the reduction in success probability and system delay by factor of 13 percent.

4. System Comparison

In this section, we evaluate the performance of the controllable scheme by means of numerical results, and compared them with that of traditional scheme. We assume that both techniques are equivalent for which the offered loads are generated with the same manner and have the same pattern of throughput. Thus, μ_2 of the controllable system and average retransmission rate of traditional system can be considered as a common parameter.

4.1 Throughput Comparison

Computing the throughput S as a function of μ_1 using (1) and (18) results in the plots of Fig. 12 - 15. In the figures, the throughput is plotted against the offered load for various values of μ_1 with μ_2 qual to 0.3 and 0.5 with N equal to 25 and 35. The new traffic generated with rate μ_1 is assumed to be an average departure rate of Q_1 of all terminals. Compared with the traditional scheme, we define μ_1 as the transmission rate for the terminal in ready mode, while μ_2 is compared with retransmission rate for the terminal in backlogged mode.

The plots are made with transmission rate μ_1(new traffic) as a parameter while retransmission rate, μ_2, is kept constant. We do not use the transmission rate more than 0.6, since it may be too large for the Markov chain to provide the correct values of the steady state

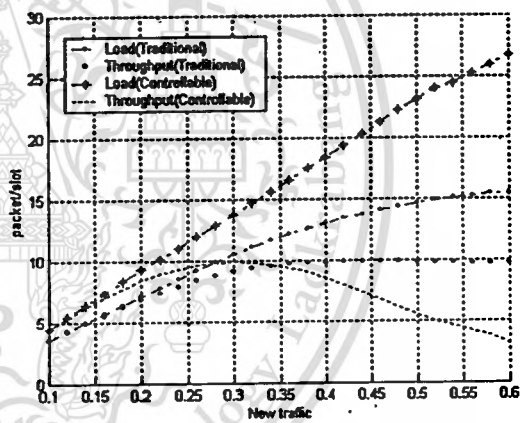

Fig. 13 Throughput-Load comparison, with $\mu_2 = 0.3$ and $N=35$

distribution. When the control method is applied, each terminal will try to adjust its resources to keep the channel operating below this point. By simulation, we found that varying μ_2 doesn't result much in adjusting the performance. A parameter that is more appropriate for this purpose is μ_1.

4.2 Delay Comparison

We present in this subsection the mean message delay results assuming infinite terminal's queue size. Let us reconfigure the equation (19) into two components as $T_1 + T_{cir}$. T_1 is the message waiting time which occur on the terminal's first queue, while T_{cir} is the delay since the first segment of the message was sent out from the terminal's first queue (input queue) until all the message segments is successfully received. Fig. 16 - Fig. 18 illustrate the results of delay comparison, with the parameters of N=25, 30 and 35, and μ_1=0.3-0.5.

Forbidden to modify the content, and cite the document when use.

8

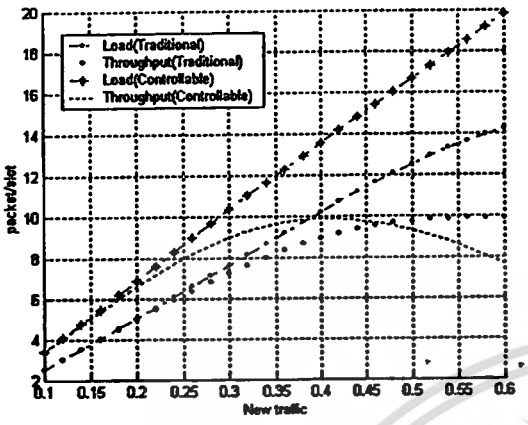

Fig. 14 Throughput-Load comparison, with $\mu_2 = 0.5$ and $N=25$

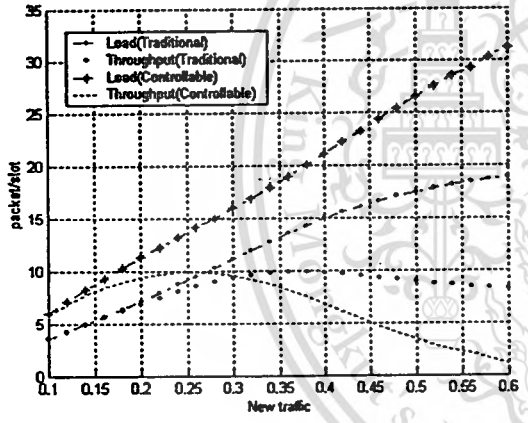

Fig. 15 Throughput-Load comparison, with $\mu_2 = 0.5$ and $N=35$

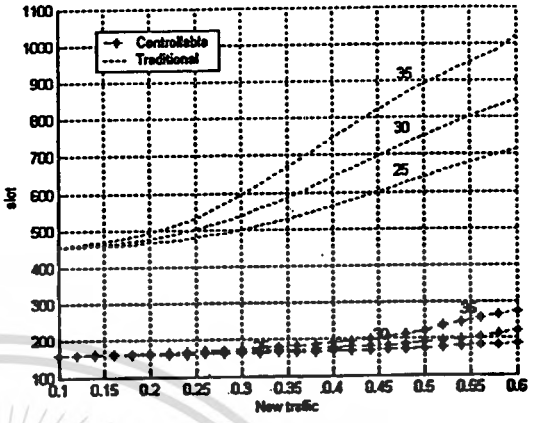

Fig. 16 Delay comparison, with $\mu_2 = 0.3$

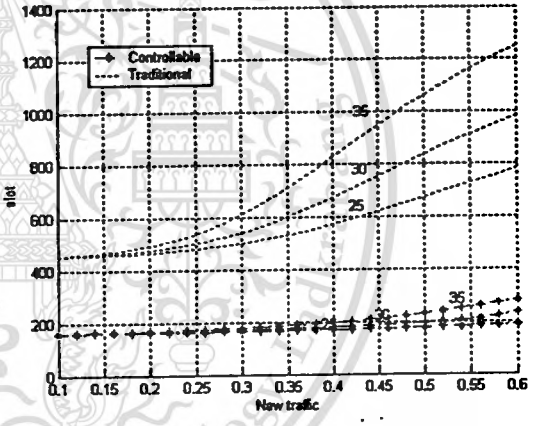

Fig. 17 Delay comparison, with $\mu_2 = 0.4$

Since both schemes are operated based on time interval of channel slot, the results are shown in the unit of slot.

As an illustration of the results, the controllable technique is more sensitive to the offered loads than the traditional ones. This is because we assume two individual queues contained in a terminal. When the channel status becomes worse by the result of heavy traffic, the number of terminals that have active-Q_2 rapidly increases, and the throughput reaches the saturated point faster than that of traditional one. On the contrary, it can be seen that the total message delay obtained from the controllable system is far better, since the terminal is allowed to freely send out the packets in their input queues and let Q_2 take care all the collided packets. This makes a message deal with only one propagation delay plus the waiting time in queue, multiplied by the number of segments contained in that message in case of no collision occurring. Packets are also kept waiting in the buffer for a shorter duration in the Q_1 and Q_2.

4.3 Control Architecture

The flowchart of the control approach is given in Fig.19 Since Q_2 is used to store and manage the sequence of packets that are declared as collision, we simply use its queue size associated with ACK messages as the parameters for determining the current status of the system and also for specifying the sending rate at which Q_1 should be performed.

The cycle of the control process start when terminals receive the acknowledgement (ACK). In case that ACK is negative, terminal stores the packet at the tail of Q_2, and checks whether its queue size reach the threshold. By adjusting the output rate of Q_1 based on pre-assigned threshold, we can control the total offer loads presented to the satellite channel. For simplicity of the simulation, we assign single control step at each terminal. For example, given the fixed value of

This material is reserved for personal use. Unauthorized use is prohibited.
Forbidden to modify the content, and cite the document when use.

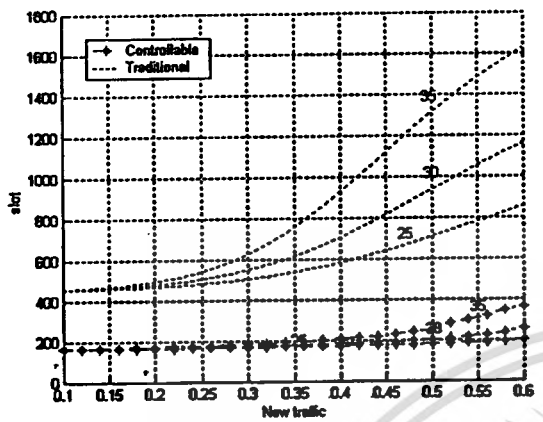

Fig. 18 Delay comparison, with $\mu_2 = 0.5$

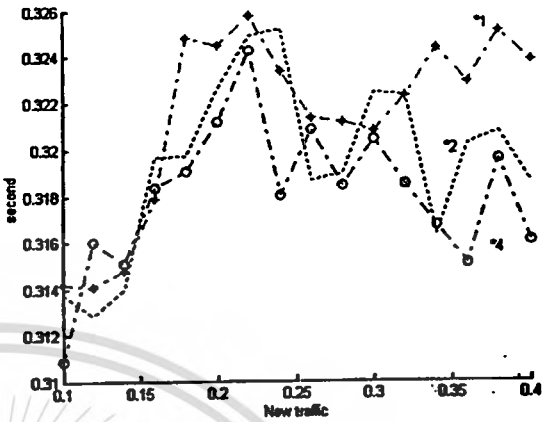

Fig. 20 System with control approach under normal condition

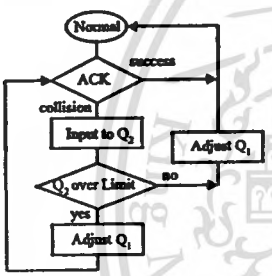

Fig. 19 Flowchart of control approach

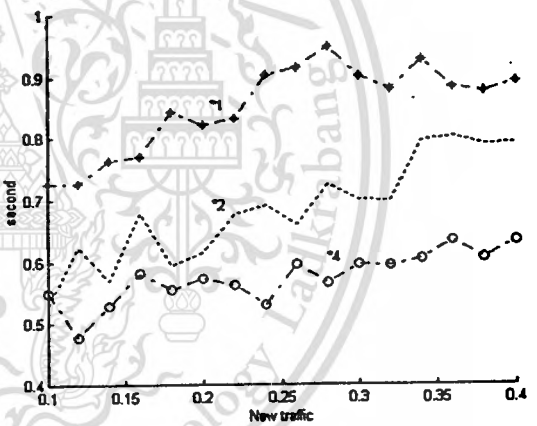

Fig. 21 System with control approach under impaired condition

$\mu_2 = 0.4$, the service time of Q_1 is $\frac{1}{\mu_1}$ when its queue size < 8, and is $\frac{2}{\mu_1}$ or $\frac{4}{\mu_1}$ when its queue size > 8 (including the one being serviced). Fig. 20 provides the results of message delay in unit of second under normal condition. It can be noticed that the results obtained from the systems with and without control conditions become close to each others, since the channel is stable and the queue size of Q_2 is always lower than threshold. Fig. 21 shows the results when the channel suffer with degradations(Eb/No lower than 5 dBm). In this range, the lower μ_1 becomes, the better the total message delay is. This is because the packets are kept within Q_2 instead of letting the terminal attempt to transmit packets over the acceptable traffic level. This event is not last if the arrival messages rate of Q_1 keep increasing. It is confirmed by the results illustrated in Fig. 22. The plots show the average time duration of turning the terminal state from stable to unstable (start) and from unstable to stable (stop).

5. Discussion

In Fig. 12-18. we see that the controllable scheme drives the system into saturation point faster, but gives the better delay results. For a particular load offered to the channel. we wish to determine if the throughput at this point is still below the saturation point and the delay can be accepted by the application. In considering these questions, we use power factor (i.e., throughput/message delay) as a parameter to justify the performance of our system, and the results shown in Fig.23. As seen form the plots, it is evident that the controllable scheme still works well if the offered load presented in the area mask of 30 percent below the saturation point, although the performance of the controllable technique degrades very rapidly as the offered traffic increases. To keep the system in the workable area, we need a control policy for each remote terminal. Since the propagation delay is high not only in the satellite environment, but possibly also in other wireless media, it is not appropriate for the remote terminal to depend strictly on the response messages sent form the centralized or main HUB to control the output traffic.

This material is presented for personal use only. Unauthorized commercial use.
Forbidden to modify the content, and cite the document when use.

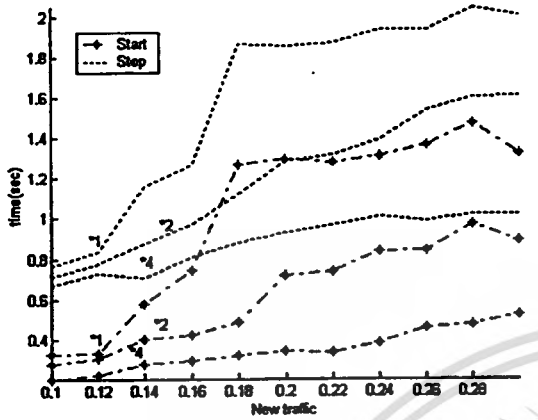

Fig. 22 System stability

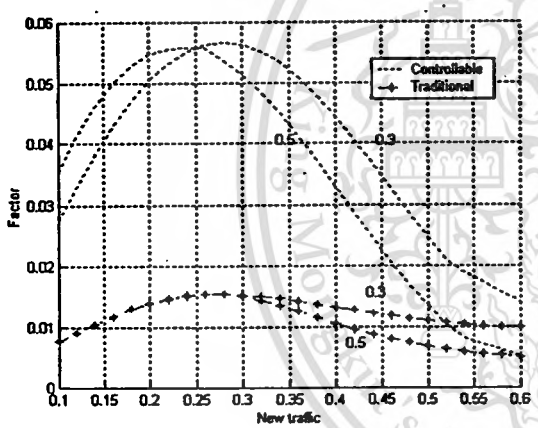

Fig. 23 Power Factor versus new traffic,with $\mu_2 = 0.3$

6. Conclusions

In this paper, we concentrate on the structure of the ground terminals. By allocating an additional buffer as Q_2 for resolving problem packets, the terminal can manage two types of traffic independently. Furthermore, the terminal can sense the channel status by evaluating the size of this queue. We found that the number of active terminal does not change much when varying the average departure rate assumed to be used in all terminals when we consider the number of terminals who have their second queue active as the parameter of system status. The results of analytical and simulation show that the approach is capable to change the traffic intensity and, consequently, keep the system stable for longer period. Thus, to stabilize the whole system status, each terminal is designed to control its service rate based on the behavior of Q_2.

References

[1] F.A. Tobagi, "Multiple access Protocols in Packet Communication systems," IEEE Trans Commun., Vol. COM-28, No.4, April 1980.
[2] T. Saadawi and A. Ephremides, "Analysis, Stability and Optimization of Slotted ALOHA with a Finite Number of Buffered Users," IEEE Trans on Automated Control, June 1981.
[3] R. Al-Naami, "Queuing analysis of slotted ALOHA with finite buffer capacity," IEEE Globecom'93, pp.1139-43, 1993.
[4] X. X. Yao and O. W. Yang, "A queuing analysis of slotted ALOHA system," IEEE CCECE'93, pp.1234-38, 1993.
[5] D. Makrakis and K. M. Sundara Murthy, "Spread Slotted ALOHA Techniques for Mobile and Personal Satellite Communication Systems," IEEE J. Select. Areas Commun., vol. 10, no.6, Aug. 1992.
[6] Richard D. J. van Nee and R.N. van Wolfswinkel, "Slotted ALOHA and Code Division Multiple Access Techniques for Land-Mobile Satellite Personal Communications," IEEE Trans Commun., Vol. COM-13, No.2, Feb 1995.
[7] Micheal B. Pursley, "Performance Evaluation for Phase-Coded Spread-Spectrum Multiple-Access Communication Part I: System Analysis," IEEE Trans Commun, Vol. COM-25, No.8, August 1977.
[8] P.W. de Graaf and J. S. Lehnert, "Performance Comparison of a Slotted ALOHA DS/SSMA network and a Multichannel Narrow-Band Slotted ALOHA Network," IEEE Trans Commun., Vol. COM-46, No.4, April 1998.
[9] L. Kleinrock, "Queuing Systems, Vol.I: Theory." John Wiley and Sons, New York.
[10] L. Kleinrock, "Queuing Systems, Vol.II: Computer Application." John Wiley and Sons, New York.

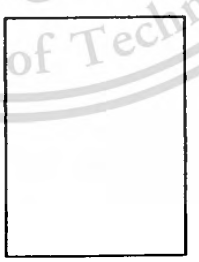

Seri Asavaruk received the B.Sc. degree in Engineering from King Mongkut's Institute of Technology Ladkrabang, Thailand in 1991, the M.Eng. degree in Electrical Engineering from King Mongkut's Institute of Technology Ladkrabang (KMITL), Bangkok, Thailand. He is now an engineer in the Information System and Quality Assurance Division, Computer Research and Service Center, KMITL. He is currently working toward the D.Eng degree at Faculty of Engineering, KMITL. His current research interests are computer communication network and wireless communications.

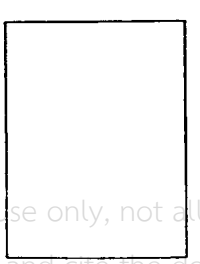

Suvepon Sittichevapak received the B.E.(first class Hons,) degree in 1982 from King Mongkut's Institute of Technology Ladkrabang, the M.E. degree from Osaka University in 1987 and Ph.D degree in System Science from Kobe University in 1991. Since 1991, he has been with Telecommunication Engineering department, Faculty of Engineering, King

All rights reserved. Permitted for educational use only, not allowed for commercial use.
Forbidden to modify the content, and cite the document when use.

Mongkut's Institute of Technology Ladkrabang, where he is now Associate Professor. His current interests are in high speed optical networks and wireless network.

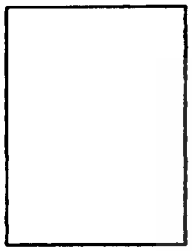

Ruttikorn Varakulsiripunth received the B.E. degree in Electrical and Electronics from Kyoto University, Kyoto, Japan in 1978. He obtained his M.E. and Ph.D. degrees in Electrical and Communication Engineering from Tohoku University, Sendai, Japan in 1983 and 1986, respectively. He is now an associate professor in the Department of Electronics, Faculty of Engineering, King Mongkut's Institute of Technology Ladkrabang, Bangkok, Thailand. His current research interests are concerned with computer communication network including switching system, queueing analysis, flow and congestion control, multimedia communication, wireless communication, image processing and natural language processing.

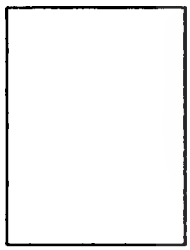

Yasushi Kato is currently a professor and the chairman in the Department of Information Engineering, Sendai National College of Technology. His research interests include concurrent systems design, Semantic Web, multi-agent system, micro-ITRON based embedded system and education method for digital technology. He received the Ph.D. degree in Electrical and Communication Engineering from Tohoku University, Sendai in 1978. He had been a visiting researcher at Twente University, the Netherlands from 1995 to 1996 and had engaged in the research on formal description techniques. He received the achievements award of JSEE (Japanese Society for Engineering Education) in 1994. He is a member of IPSJ (Information Processing Society of Japan) and JSEE. He is also a senior visiting advisor of Miyagi, Fukushima and Iwate Prefectural Institute of Technologies.

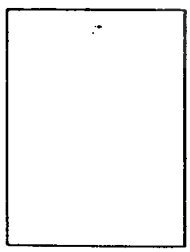

Norio Shiratori was born in Miyagi Prefecture, Japan, on May 11, 1946. He received the B.E. degree from Tokai University, Tokyo, in 1972, and the M.E. and Ph.D. degrees in Electrical and Communication Engineering from Tohoku University, Sendai, in 1974 and 1977, respectively. He has joined RIEC (Research Institute of Electrical Communication), Tohoku University, Sendai, since 1977, and he is now a Professor of Computer Science at RIEC of Tohoku University. He is internationally known for his numerous contributions to the field of computer communication networks. One of his earlier contributions was applications of Artifical Intelligence technology to a newly emerging field, an intelligent distributed system and its software design support environment. His current research interests include Flexible computing and its application to Post modern distributed system and symbiosis cyberspace of human and computers. Professor Norio Shiratori received the 25^{th} Anniversary of IPSJ Memorial Prize-Winning Paper Award in 1985, the 6^{th} Telecommunications Advancement Foundation Incorporation Award in 1991, the JWCC-8 Best Presentation Award in 1993, the Best Paper Award of ICOIN-9, ICOIN-11 and ICOIN-12 in 1994, 1997 and 1998, respectively, IEICE Information Network Research Award in 1997, and the IPSJ Best Paper Award in 1997. He has been named a Fellow of the IEEE for his contributions to the field of computer communication networks since 1998. He has also received the IPSJ Fellow since 2000.

King Mongkut's Institute of Technology Ladkrabang

Personal use only, not allowed for commercial use.

Forbidden to modify the content, and cite the document when use.

Biography

Seri Asvaruk received the B.Sc. degree in Engineering from King Mongkut's Institute of Technology Ladkrabang, Thailand in 1991, the M.Eng. degree in Electrical Engineering from King Mongkut's Institute of Technology Ladkrabang (KMITL), Bangkok, Thailand. He is now an engineer in the Information System and Quality Assurance Division, Computer Research and Service Center, KMITL. His current research interests are computer communication network and wireless communications.

This material is reserved for educational use only, not allowed for commercial use.
Forbidden to modify the content, and cite the document when use.